

Chapter 2

ARRAYS

In case of arrays the wave directional spectrum is estimated from the simultaneous time series measurements of wave elevation at a number of gauges placed either in linear or polygonal arrays.

Two examples of linear arrays are given in Figure 2.1. The first example shown in Figure 2.1 is the 6-gauge linear array of Hasselmann et al. [1973] comprising of two 4-gauge sub-arrays each having a spacing of ratio D , $4D$ and $6D$, the sub-array having $D = 7m$, being tuned for the wavelength band 10m-150m, and the sub-array having $D = 28m$ being tuned for the wavelength band 40m-600m. The second example shown in Figure 2.1 is the 4-gauge linear array of Pawka [1974] having a spacing of D , $3D$ and $4D$, with $D = 30.5m$. A make-shift polygonal array comprising of 10 alongshore gauges and five intersecting cross shore gauge located at $8m$, at the Coastal Engineering Research Center's (CERC) Field Research Facility at Duck, North Carolina, USA, is shown in Figure 2.2. Measured data at this $8m$ array at Duck was procured for the purpose of the present study. An excellently designed 25-gauge polygonal array, which has been used by Elgar et al. [1992], Elgar et al. [1994] and Herbers et al. [1995], also located at Duck, but at $13m$ depth is shown in Figure 2.3. The five gauge polygonal array of Esteva [1976] and Esteva [1977], which has been discussed elaborately in this thesis is shown in Figure 2.4. The 14-gauge polygonal array in the form of a cross used by Donelan et al. [1985] for studying wave directionality in case of waves of period less than $4s$ is shown in Figure 2.5.

The gauges comprising an array may be surface piercing capacitance gauges or bottom mounted pressure gauges. Arrays are generally located in shallow water depths of around 7–13m. At larger depths it is not feasible to install capacitance gauges unless they are pile driven or mounted on spar buoys. Also at larger depths, the wave signal at the bottom mounted pressure gauges is attenuated as a function of wave period (frequency), the attenuation being greater for smaller periods, so that the shorter waves may not be sensed at all. At depths shallower than 7m wave breaking takes place so that linear wave theory, on which all the techniques for determining the wave directional

Figure 2.1 Examples of Linear arrays — (a) 6-gauge array of Hasselmann et al. [1973] and (b) the 4-gauge array of Pawka [1974]

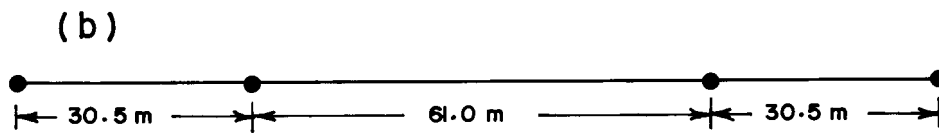
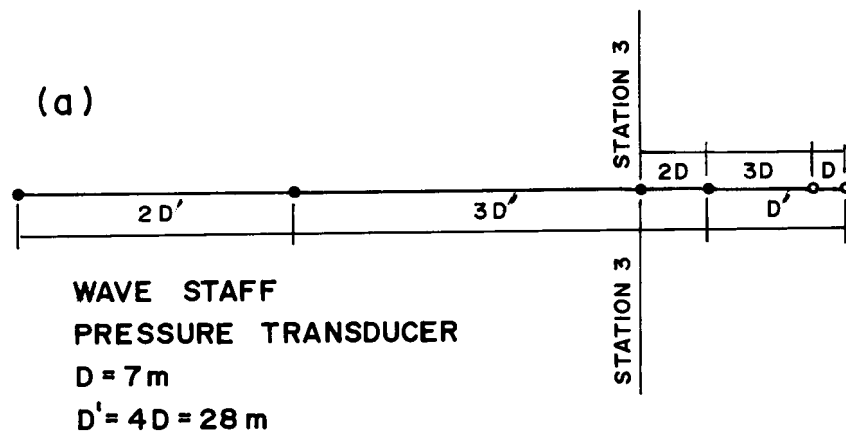


Figure 2.2 15-gauge polygonal array at the CERC's Field Research Facility at Duck, North Carolina, USA, located at 8m depth. The 10 longshore gauges are operational since March 1987. The 5 cross-shore gauges were added in 1990. This is the array, the measurements at which are analysed and discussed in this thesis

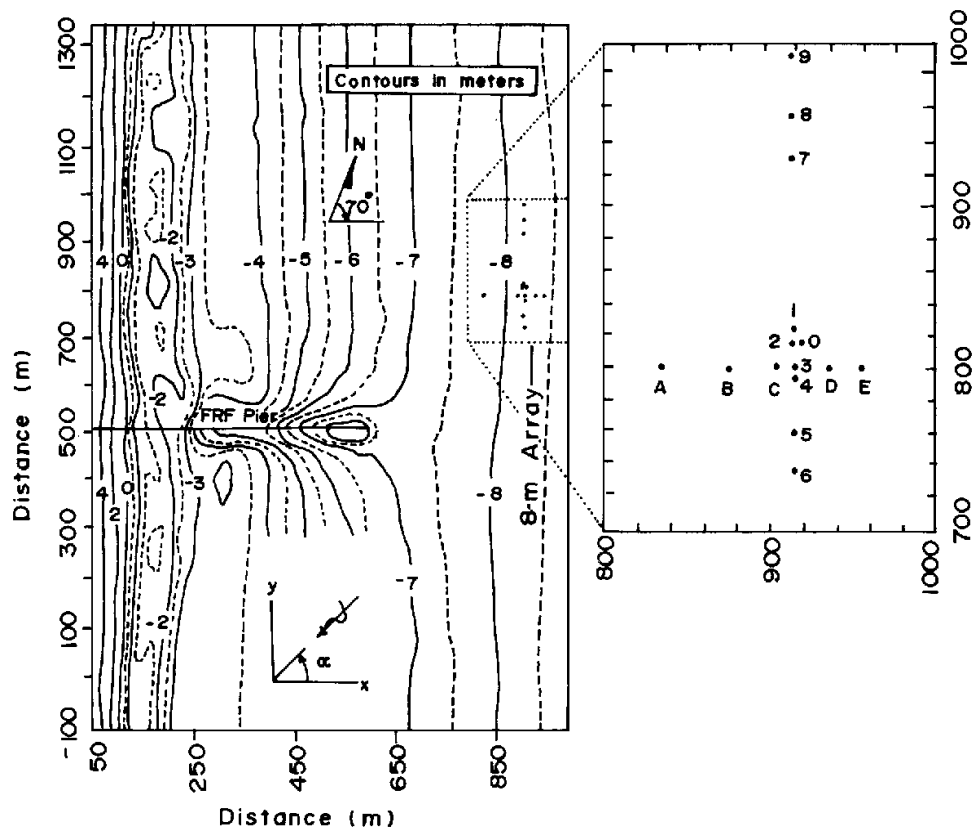


Figure 2.3 25-gauge polygonal array at the CERC's Field Research Facility at Duck, North Carolina, USA, located at 13m depth. This is a very excellently designed array, which has been used by the group composed of Guza, Herbers, Steve Elgar to study wave directionality, principally of surf beat

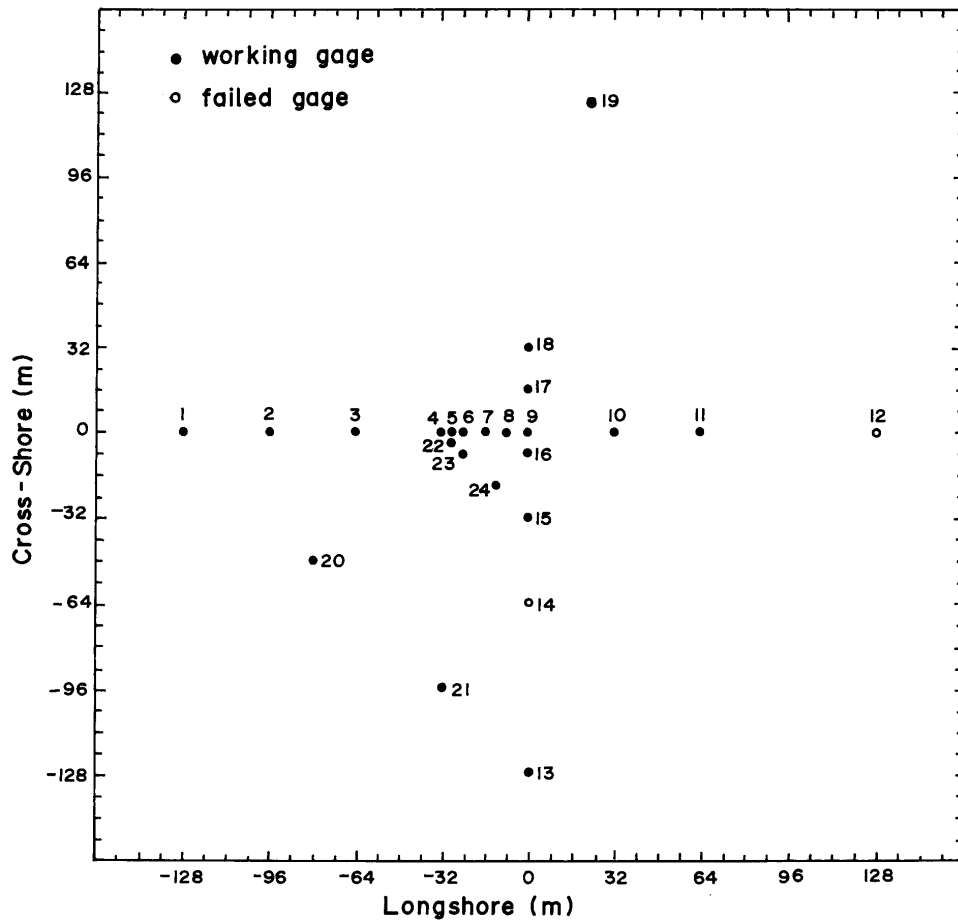


Figure 2.4 The 5-gauge array of Esteva [1977] located at Pt. Mugu California at 9.14m depth, where swell of 8s and 16s was observed. Esteva was successful in correctly determining the direction of the 16s swell, but failed in determining correctly the direction of 8s swell, in case of both measured as well as computer simulated data, although the array was designed for the range 7 – 25s by L. E. Borgman

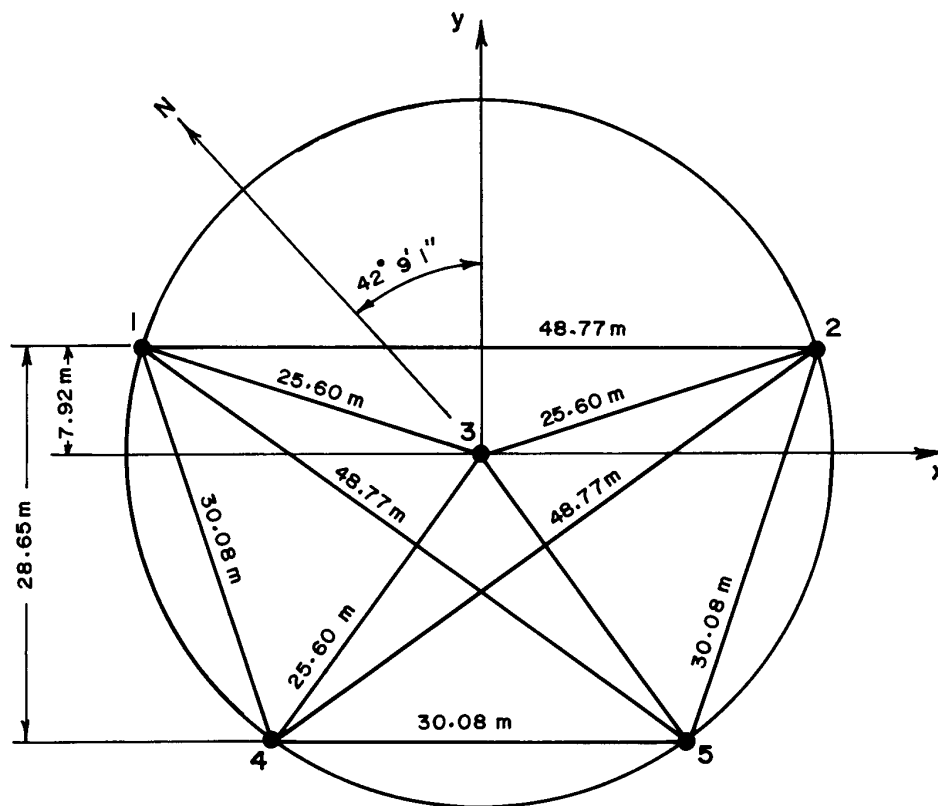
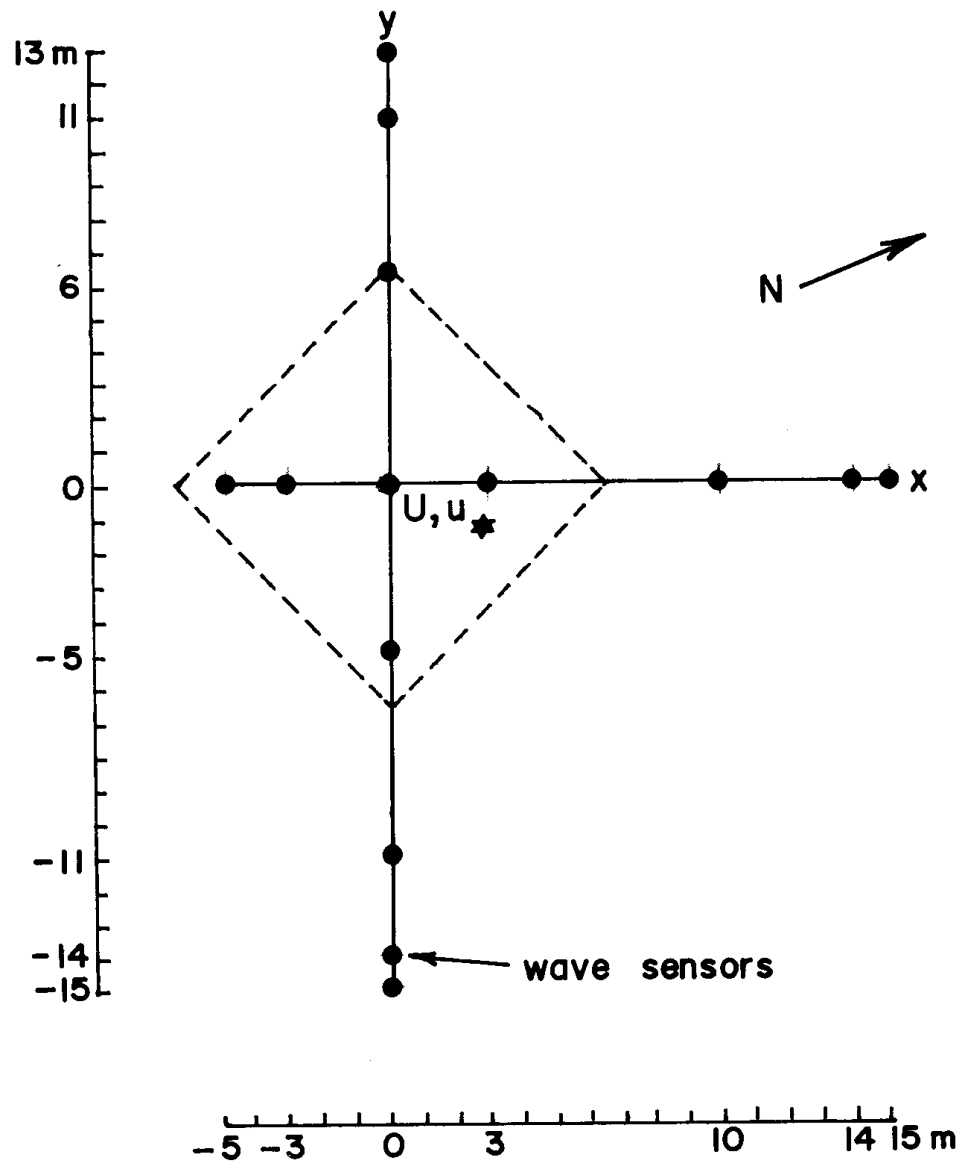


Figure 2.5 The 14-gauge array of Donelan et al. [1985] used to study wave directionality for waves of period less than 4s in Lake Ontario at 10m depth



spectrum are based, no longer holds.

Linear arrays are unable to distinguish between waves arriving at the array at the same angle but from opposite sides, i.e., linear arrays suffer from an ambiguity within a mirror symmetry. Linear arrays can resolve directions well only when waves approach nearly normal to the array. On the other hand polygonal arrays can determine wave direction unambiguously. The major drawback of arrays is that they cannot be installed in deep water. Precision in the determination of the coordinates of the gauges, i.e., the knowledge of its exact location, which is a prerequisite for accurate determination of wave direction, is difficult as the gauges are underwater.

There are two approaches for the determination of wave direction from array measurements. In the first approach pioneered by Barber [1963], at each spectral frequency band energy is evaluated as a function of direction, wherefrom the mean wave direction is determined from the location of the energy peak. This approach allows for the possibility of waves approaching from more than one direction at each frequency and is the traditional approach. Refinements of this approach are the Maximum Likelihood Estimation Method of Regier [1975], Regier and Davis [1977] and Davis and Regier [1977]; and the Iterative Maximum Likelihood Estimation method of Pawka [1982] and Pawka [1983]. Other refinements to the method of Barber [1963] are the variational method of Long and Hasselmann [1979] and the modified Barber method of Donelan et al. [1985]. Almost all the literature on the directional spectrum deals with this approach, which is used for both array as well as buoy measurements.

The traditional approach in dealing with wave direction assumes that the sea surface is composed of a large number of sinusoidal waves of varying frequency and direction, as is exemplified by Pierson et al. [1955] who proposed the frequency direction spectrum:

$$E(f, \alpha) = \rho(f) (2\pi)^{-1} g(\alpha), \text{ where}$$

$$g(\alpha) = \begin{cases} \cos^2\alpha, & \text{if } -\pi/2 < \alpha < \pi/2 \\ 0 & \text{otherwise} \end{cases}$$

Such unimodal bell-shaped directional spreading function with the peak of the bell generally in the direction of the wind has been observed by Longuet-Higgins et al. [1963] from the measurements of a floating buoy; by Tyler et al. [1974] from synthetic radar observations of radio scatter; and by Donelan et al. [1985] from the measurement of wave elevation at a multi-element array. Since the directional spreading function has been found to be unimodal, the computation of the “mean” wave direction as a function of frequency is both meaningful and useful and is routinely performed in case of commercially available wave directional buoys fabricated by EN-DECO, WAVEC and NEREIDES.

In the other approach “mean” wave direction is computed as a function of frequency directly using phase/time/path difference (PTPD) concepts. Fernandes et al. [1988] have aptly named the methods based on PTPD concepts as PTPD methods. The mathematical model on which PTPD methods are based make two assumptions, viz., (i) that the sea surface is the result of a small number of narrow banded wave trains consisting of long-crested waves travelling in well defined directions, and (ii) that only one wave train is present with a particular period. These assumptions may be restated in terms of spectral analysis, as saying that in a particular frequency band the waves can approach from a single direction – the direction may be different for different frequency bands. As evidence in support of this approach and the underlying assumptions, Esteva [1977] cited photographs of the sea surface, radar images of the sea, “redundancy”, “expediency” and the work of Thompson [1974], Fujinawa [1974] and Fujinawa [1975].

There are two reasons why PTPD methods for determining wave direction from array measurements have not become popular, the first being the insufficient documentation of Borgman [1974] in case of linear arrays; and the second being the failure of Esteva [1976] and Esteva [1977] in determining wave direction correctly over the design range 25–7 sec of her 5-gauge polygonal array at Pt. Mugu, California.

In the method of Borgman just 2 gauges are sufficient for determining wave direction, i.e. the analysis is done in units of gauge pairs with the different gauge pairs possible in the linear array giving redundant estimates of wave direction. By the method of Borgman, as we shall see in Chapter 2.4, wave direction is estimated as a function of frequency, from the distance between the gauges and the phase difference, ϕ_{12} between the two gauges, which is computed as a function of frequency by cross spectrum analysis.

In the method of Esteva just 3 non-collinear gauges are sufficient for determining wave direction, i.e the analysis is done in units of 3 gauges, i.e., gauge triads, with the different gauge triads possible in the polygonal array giving redundant estimates of wave direction. By the method of Esteva, as we shall see in Chapter 2.5, wave direction is estimated as a function of frequency, from the coordinates of the three non-collinear gauges, ijk , say, and the phase differences, ϕ_j and ϕ_{ik} between the gauges ij and ik , which are computed as a function of frequency by cross spectrum analysis.

At the Pt. Mugu site of Esteva’s 5-gauge polygonal array, designed by Leon E. Borgman, swell of 16s and 8s was observed. Since Esteva’s array had five gauges, ${}^5C_3 = 10$ different combinations of gauge triads are possible giving 10 independent estimates of wave direction. Esteva, using “consistency” within these 10 redundant estimates of wave direction as a criterion for accuracy, reported success in determining the direction of swell of 16s and failure in case of swell of 8s; and on the basis of computer simulation studies concluded that (i) gauge triads which are nearly equilateral have greater direction discernability (this idea was first propounded by Barber [1963]).

(ii) the analysis gives correct directions only for waves coming from certain directions. (iii) that at the Pt. Mugu site, directional information provided by the array adds little to the information that could be obtained from wave refraction studies, and thus seems hardly cost-effective.

Fernandes et al. [1986] and Fernandes et al. [1988] provided the necessary documentation in case of linear arrays and repeating the computer simulations of Esteva for her polygonal array, were successful in consistently, accurately and unambiguously determining the direction of both 16s swell as well as 8s swell. Their success was due to their adroit use of the criterion of Barber and Doyle [1956] which stipulates, that for ensuring correct directions, the distances between the gauges used for determining phase/time/path difference through cross spectrum analyses, should be less than half a wavelength for the particular wave period (spectral frequency band) for which wave direction is determined; and demonstrated that all the above three conclusions of Esteva were erroneous.

Thus Fernandes et al. [1988] established that the method of Esteva for determining wave direction from polygonal arrays works in case of computer simulated data. The present study is principally aimed at establishing that the method of Esteva works in case of measured data also, and presents detailed documentation of work carried out towards determination of wave direction from linear and polygonal arrays using the PTPD methods of Borgman and Esteva respectively in case of measured data.

It may be interesting to first give additional details about the results of Esteva [1977] and then discuss the reason behind her failure to determine wave direction correctly for the observed swell of 8s.

From measured data at the 5-gauge array at Pt. Mugu, California, Esteva [1977] obtained ten redundant estimates of wave direction for each frequency band 0.01 Hz wide between approximately 30 and 3s. These redundant estimates of wave direction displayed discrepancies of the order of 20° for those bands with central periods above 10s and of 180° for those with shorter central periods. It had been expected that the array would yield direction to better than 20° for periods between 25 and 7s.

In order to isolate problems associated with the calculations from measured data, Esteva simulated the propagation of narrow-banded wave trains across the array in a computer, and from high resolution spectra (1/1024 Hz), recovered the assigned directions within 1° for 16s waves when the frequencies of the spectral components in the wave train differed by 0.003 Hz or more, and the directions were spread within a 5° arc. The recovery of the assigned directions in case of 8s waves was a total failure, which Esteva reported as “meaningless”.

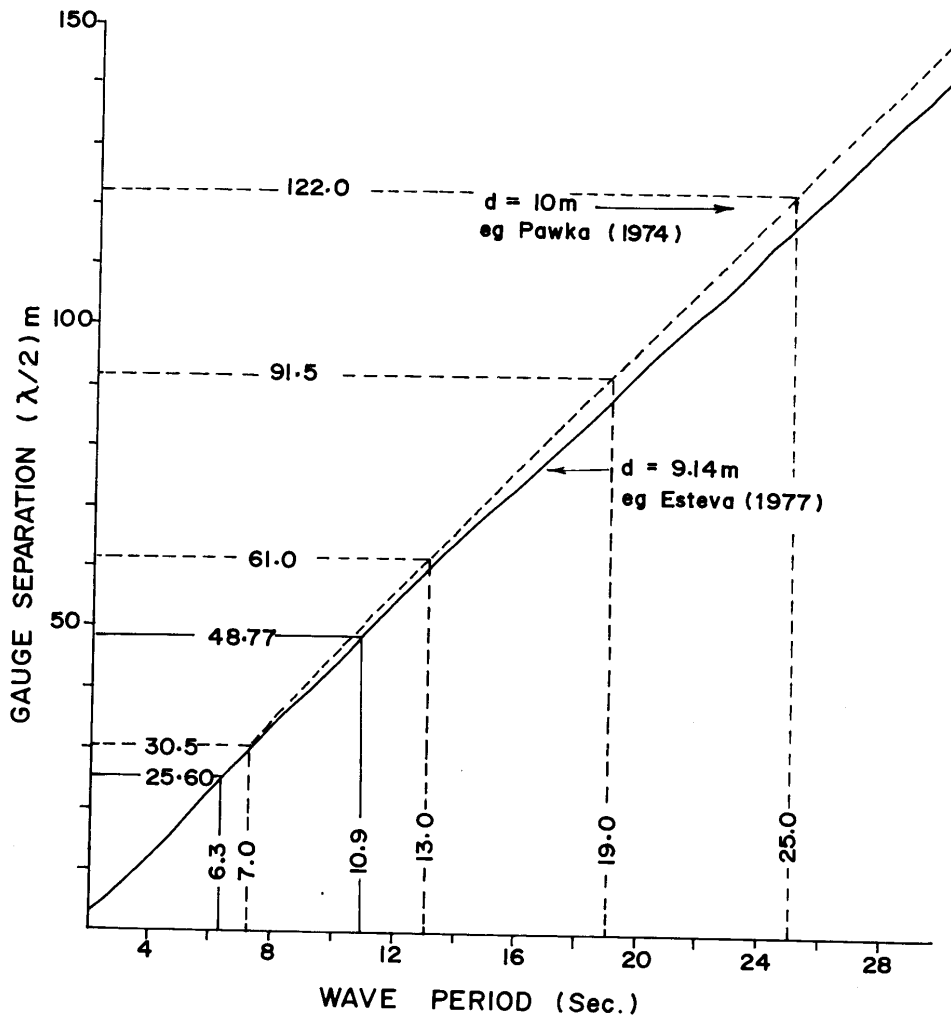
For determining wave direction as a function of frequency using the PTPD methods of Borgman and Esteva in case of linear and polygonal arrays respectively, as mentioned above, knowledge of the phase difference between the gauges is required. Phase differences computed from cross spec-

trum analysis, are generally reported in the range $(-\pi, \pi)$ to allow for both phase lags and phase leads. This rendition of the phase difference in the interval $(-\pi, \pi)$ generally does not faithfully represent the physical situation, so that the wave directions computed from phase differences in this rendition may be erroneous. Let me elaborate. The key assumption in the above rendition of phase difference is that the angles θ and $\pm 2n\pi + \theta$, are equivalent, where n is an integer and θ is any arbitrary angle, here measuring phase difference. Consider, for example a sinusoidal long-crested wave of period T seconds approaching two gauges located at points A and B. A phase difference of 30° may be defined to mean that a wave crest will arrive at B, $T/12$ seconds *after* it crosses A. By this definition a phase difference of -330° signifies that the wave crest arrives at B, $(11T/12)$ seconds *before* it crosses A. Thus the phase differences 30° and -330° , are equivalent by the above assumption as $30 = 360 - 330$, but represent two distinct, entirely different situations physically. Thus if the phase difference in the actual physical situation, i.e., the *true* phase difference is -330° , cross spectrum analysis will erroneously report the phase difference as 30° . It therefore stands to reason that that the phase difference (at a particular central period) determined by cross spectrum analysis in the range $(-\pi, \pi)$, which may be termed as the *apparent* phase difference, will faithfully represent the physical situation only if we are able to restrict the phase difference in the physical situation, i.e., the *true* phase difference also to the range $(-\pi, \pi)$. This is obviously ensured by restricting the distance D between the points A and B to to less than half a wavelength, i.e., $D < \lambda/2$, which is the criterion of Barber and Doyle [1956]. Whenever the criterion of Barber and Doyle [1956] is violated, i.e., the distance between the gauges is greater than half a wavelength, the phase difference between the gauges in the physical situation, i.e., the *true* phase difference will lie beyond the range $(-\pi, \pi)$ if the wave direction is along or close to the line joining the gauges. **Thus it may be concluded that the wave directions determined from *apparent* phase differences in the range $(-\pi, \pi)$, will definitely be correct if and only if the criterion of Barber and Doyle [1956] holds.**

Esteva's 5-gauge array is shown in Figure 2.4. It may be seen that the distances between the gauges is limited to three values only, viz., 25.60, 30.08 and 48.77m; and that the nearly equilateral gauge triads (triangles), viz., 134, 345 and 235, which Esteva surmised had greater direction discernability have 30.08m as the maximum distance between the gauges. From Figure 2.6, which depicts the relation between the wave period and the wavelength (actually half the wavelength!), it may be noted that when the largest arm in the triangle formed by a gauge triad is 30.08m, the criterion of Barber and Doyle [1956] is satisfied for all periods above 7.1s. Therefore wave directions in case of swell of 8s as well as 16s, both of which are above 7.1s, will be computed correctly from the *apparent* phase differences in case of the gauge triads 314, 345 and 325, which only incidentally happen to be nearly equilateral triangles. Fernandes et al. [1988], in their successful attempt in recovering the assigned direction of both 8s as well as 16s swell, have classified

the above three gauge triads as belonging to the class “ALWAYS”, indicating that the computed wave direction using these three gauge triads will *always* be correct for swell of both 8s as well as 16s.

Figure 2.6 Criterion for true phase to lie within $(-\pi, \pi)$ — $D \leq \lambda/2$



As mentioned above, from measured data, Esteva [1977] reported consistency within the 10 redundant estimates of wave direction as a function of frequency for wave periods above 10s. This result may be explained with the help of Figure 2.6, which shows that for the maximum distance between Esteva’s gauges, viz., 48.77m, the criterion of Barber and Doyle [1956] is satisfied for all wave periods above 10.9s, which is spectrally very close to the value 10s reported by Esteva. This

argument explains the reason behind Esteva's success in case of 16s swell and her failure in case of 8s swell both arising from the use of the *apparent* phase differences.

Fernandes et al. [1988] grouped Esteva's 10 redundant combinations of gauge triads or triangles into the following three distinct classes for the purpose of determining wave direction at a specified spectral frequency: (i) Class "ALWAYS", composed of gauge triads all of whose gauge separations are within half a wavelength at the specified frequency, thereby *always* giving correct directions; (ii) Class "IF", composed of those gauge triads that contain a single gauge separation, i.e., one arm of the triangle, which exceeds half the wavelength at the specified frequency, thereby giving correct directions *if* we do not use that particular arm in the computation of phase differences. This can easily be done; (iii) Class "NEVER", composed of those gauge triads that contain at least two arms of the triangle that exceed half a wavelength. In this case computed wave directions can be correct by chance only!

Since as seen above, for a gauge triad belonging to class "IF", the choice of gauge pairs used for determining phase differences is crucial to the analysis, we use the following convention: A gauge triad is considered as a semi-ordered sequence of gauges ijk for which we compute the phase differences ϕ_{ij} , ϕ_{ik} , where the order of the first gauge i , which is the pivot is important; and the triads ijk and ikj are equivalent.

In case of 16s swell, all the 10 gauge triads of Esteva, viz., (123, 124, 125, 134, 135, 145, 234, 235, 245, 345), fall into the class "ALWAYS", as a consequence of which all these gauge triads ought to, and as reported by Esteva [1977] do yield correct directions.

In case of swell of swell of 8s; the following three gauge triads belong to the "ALWAYS", (134, 235, 345), and therefore *always* yield correct directions; the following five gauge triads of Esteva belong to the class "IF", (123, 135, 145, 234, 245), and will yield correct directions only *if* the following semi-ordered gauge triads are used, (312, 315, 415, 324, 524), indicating that Esteva's ordering of all the five gauge triads in this class happened to be wrongly chosen, so that the computed wave directions will not be correct; the following two gauge triads belong to the class "NEVER", (124, 125), and will yield incorrect wave directions. Therefore out of total 10 gauge triads of Esteva, in case of 7 gauge triads comprising of the classes "IF" and "NEVER" her computations just could not yield the correct directions — whence her failure.

The above strategy can be used in case of measured data also, but it is wasteful, as it treats perfectly good signal at the the higher frequencies as noise and discards it. The two innovations that have been adopted in this thesis for determining wave direction as a function of frequency using the PTPD methods of Esteva [1977] and Borgman [1974], from actual measurements, in case of "swell", "sea" and "surf beat", are (i) the use of *true* phase differences instead of the *apparent* phase differences (ii) and the use of the concept of "coherence" between the gauges. These two innovations are used to unravel the signal at the higher frequencies, so that no "signal" is lost.

The above two methods incorporating the two innovations are referred herein as the ‘modified Borgman method’ and the ‘modified Esteva method’.

2.1 DATA

The measured wave data used in this study comes from a 15-gauge polygonal array of bottom mounted pressure gauges operational at the Coastal Engineering Research Center’s (CERC), Field Research Facility (FRF) at Duck, North Carolina, USA. The array comprises of 10 alongshore gauges (operational since March 1987) and 5 intersecting cross-shore gauges (added in 1990) placed at ≈ 8 m depth (7.44 – –8.13m, see Figure 2.2). The gauges are placed ≈ 0.5 m above the sea bed.

Code names and FRF identification numbers (the latter in braces) for the 15 gauges are as follows: 1(111); 2(121); 3(131); 4(141); 5(151); 6(161); 7(171); 8(181); 9(191); 0(101); A(211); B(221); C(231); D(241) and E(251). Gauge coordinates, mean water depth at the gauge location, the height of the pressure sensor above the bottom, and the distances between the different gauges are given in Table 2.1.

Long and Oltman-Shay [1991], who discuss the directional characteristics of the waves at the FRF at Duck using the then 10-gauge linear array, present detailed information about the pressure sensors used, data collection procedure, coastline characteristics, wind and wave climate etc.. The coastline in the vicinity of the FRF is nearly straight and the depth contours are nearly parallel. The coastline is oriented such that the seaward shore normal makes an angle of 70° with true North. According to Leffler et al. [1989] wind and wave climate at FRF can be classified into four basic types. The first is low wind situations, characterised by low frequency swell arriving from the east to the south east and the most common wave generating winds are *Northeasters*.

Table 2.1 Distance between the gauges (in metres) comprising the 8m polygonal array at Duck, Nort Carolina, USA. x,y are the co-ordinates of the gauges in metres; d is the mean depth at the gauge in metres; and b is the height of the gauge above the bottom in metres

Gauge	1	2	3	4	5	6	7	8	9	0	A	B	C	D	E	x	y	d	b
1	.00	9.61	25.20	30.40	64.80	90.30	105.00	130.40	164.50	10.74	83.71	47.12	32.56	32.56	47.22	914.50	825.70	7.90	.40
2	9.61	.00	15.62	20.80	55.20	80.70	114.60	140.00	174.10	5.00	80.94	42.28	26.14	26.14	43.27	914.10	816.10	7.90	.40
3	25.20	15.62	.00	5.22	39.61	65.10	130.20	155.60	189.70	16.06	80.20	39.90	20.10	20.10	39.60	914.90	800.50	7.90	.34
4	30.40	20.80	5.22	.00	34.40	59.90	135.40	160.80	194.90	21.20	79.96	39.78	21.12	21.12	40.35	914.50	795.30	7.90	.43
5	64.80	55.20	39.61	34.40	.00	25.50	169.80	195.20	229.30	55.34	88.59	55.23	44.74	44.74	56.71	914.00	760.90	7.90	.50
6	90.30	80.70	65.10	59.90	25.50	.00	195.30	220.70	254.80	80.75	102.69	75.56	68.25	68.25	76.65	914.20	735.40	7.90	.48
7	105.00	114.60	130.20	135.40	169.80	195.30	.00	25.40	59.51	114.80	152.69	136.48	131.93	131.93	136.17	914.30	930.70	7.90	.24
8	130.40	140.00	160.80	160.80	195.20	220.70	25.40	.00	34.11	140.18	174.87	160.97	157.07	157.07	160.61	914.30	956.10	7.90	.40
9	164.50	174.10	189.70	194.90	229.30	254.80	114.80	140.18	.00	174.24	206.17	194.40	190.83	190.83	193.63	915.20	990.20	7.90	.40
0	10.74	5.00	16.06	21.20	55.34	80.75	114.80	140.18	174.24	.00	206.17	194.40	190.83	190.83	193.63	915.20	990.20	7.90	.40
A	83.71	47.12	39.90	39.78	55.23	75.56	68.25	68.25	76.65	85.83	.00	40.30	100.30	100.30	119.80	834.70	800.00	7.44	.46
B	47.12	.00	15.62	20.80	55.20	80.70	114.60	140.00	174.10	5.00	80.94	42.28	26.14	26.14	43.27	914.10	816.10	7.90	.40
C	32.56	26.14	20.10	21.12	44.74	44.74	56.71	56.71	76.65	85.83	.00	40.30	100.30	100.30	119.80	834.70	800.00	7.65	.49
D	32.56	26.14	20.10	21.12	44.74	44.74	56.71	56.71	76.65	85.83	.00	40.30	100.30	100.30	119.80	834.70	800.00	7.65	.49
E	47.22	43.27	39.60	40.35	56.71	76.65	136.17	160.61	193.63	38.60	119.80	79.50	19.50	19.50	.00	954.50	800.60	8.13	.52

The data used consisted of 47 three hourly records of time series of wave elevation measured at the 15 wave gauges during 1-6 February, 1994. Simultaneous time series, of wind speed and direction measured at the pier end, and of barometric pressure were also available. At each gauge the time series consisted of 5 X 4096 points sampled at 2Hz, i.e., 0.5s sampling interval and was ≈ 2.84 hours long. Starting times of the records were 01, 04, 07, 10, 13, 16, 19, and 22 hours of each day. The record at 10 hours on 1 February was not available. The data was kindly supplied by Dr. Charles E. Long of the CERC on two 150Mb cartridge tapes. Earlier Dr. Long had supplied 2 day's data (2-3 February, 1994) on a 1/2" magnetic tape along with plots of frequency-direction spectra for the same using the Iterative Maximum Likelihood Estimation (IMLE) method of Pawka [1983] in case of both the full 15-gauge array as well the 10-gauge linear part of the array. Fernandes et al. [1995] have presented a preliminary analysis of part of the data on the 1/2" magnetic tape spanning 27 hours, using the phase/time/path difference methods of Esteva [1977] and Borgman [1974] in case of polygonal and linear arrays respectively. An analysis of the full six day data is briefly given in Fernandes et al. [1996]. A more elaborate analysis of the full six day data is given in Fernandes et al. [2000].

Sources of error in the determination of wave direction are: (A) Error in the measurement of the location of the gauges, which at Duck is within $\pm 0.15m$, (B) Coarseness of the time series sampling interval – this is significant at very high frequencies, and (C) Non uniform depth at the gauges in the array and the presence of astronomical tide – at Duck, omitting gauge A, which we have not used, the depth changes by $< 0.5m$ over the array and the tidal range ($\approx 1.0m$) is small, so that the assumption of a constant depth of 8m at the gauges, that we have made, should not introduce too much error. The errors are diminished substantially, essentially due to the long record length and the large number of gauges, available at Duck, which permit a great deal of “averaging” to be carried out. Experiments with computer simulated wave trains, show that the error in estimation of wave direction at Duck from a single determination is much less than ± 3 even in presence of random noise.

2.2 CROSS-SPECTRUM ANALYSIS

Cross-spectrum analysis means the computation of two parameters, viz. phase and coherence between two time series, as a function of frequency (phase spectrum and coherence spectrum).

The phase function gives the average phase difference (lead/lag) between the two series. The coherence is a measure of the consistency or stability of the relative phase difference between the two series, and like the regression coefficient is defined in the range (0,1). A coherence of zero indicates that the phase difference has a large variance (see Halpern [1973]), so that the average phase difference does not make any physical sense.

The following operations are performed in the computing scheme used. In step (i) ensembles are defined. Steps (ii)-(v) are performed for each ensemble. In steps (vi)-(viii) the essential results of the cross-spectrum analyses are computed.

(i) Divide the two time series into M ensembles, each ensemble having N points, where N may be chosen for convenience to be a power of 2, i.e. $N = 2^a$, where a is a positive integer. The total number of points in each series is clearly, NM . Let $x_k^m, y_k^m, k = 0, 1, \dots, N - 1; 1 \leq m \leq M$, represent the m th ensemble of the time series of surface elevation simultaneously measured at two gauges. Let the sampling interval be h , so that each ensemble is of duration $Nh = T$ (say).

Table 2.2 Characteristics of five different windows used in cross spectrum analysis. s^\dagger is the inverse of the factor by which spectral densities have to be scaled up to compensate for energy loss due to windowing. W^\ddagger is the half power frequency band width, and T is the record length

Window	Coefficients				
	α	β	γ	s^\dagger	W^\ddagger
Rectangular	1.00	0.00	0.00	1.0000	0.88/T
Hanning	0.50	0.50	0.00	0.3750	1.44/T
Hamming	0.54	0.46	0.00	0.3974	1.33/T
Blackman	0.42	0.50	0.08	0.3030	1.64/T
Cosine Taper	0.50	0.50	0.00	0.8750	1.03/T

(ii) Apply a window in time domain to the two time series so as to redefine them as follows:

$$x_k^m = x_k^m \cdot b_k$$

$$y_k^m = y_k^m \cdot b_k, \text{ where.}$$

$$b_k = \alpha + \beta \cos\left[\frac{2\pi}{N}\left(k - \frac{N}{2}\right)\right] + \gamma \cos\left[\frac{4\pi}{N}\left(k - \frac{N}{2}\right)\right] \quad (2.1)$$

and α, β, γ are coefficients which depend on the particular window that is being used. Table 2.2 constructed after LeBlanc et al. [1975] gives the coefficients α, β, γ for five different windows, viz. Rectangular or Box-car, Hanning, Hamming, Blackman and Cosine Taper. In case of Cosine Taper, below given is the window in time domain in analytic form as it is somewhat different from the general type given in (2.1).

$$w(t) = \begin{cases} \frac{1}{2}\left(1 - \cos \frac{10\pi t}{T}\right) & \text{for } \frac{2T}{5} < |t| \leq \frac{T}{2} \\ 1.0 & \text{for } 0 < |t| \leq \frac{2T}{5} \\ 0 & \text{for } |t| > \frac{T}{2} \end{cases}$$

(iii) Define a complex time series z_k^m as follows:

$$z_k^m = x_k^m + iy_k^m$$

(iv) Compute the Fourier Transform Z_k^m of z_k^m as follows:

$$Z_k^m = \sum_{n=0}^{N-1} z_n^m \exp\left(\frac{-2\pi i k n}{N}\right), \text{ where } i = \sqrt{-1}$$

(v) Compute the Fourier Transforms X_k^m of x_k^m and Y_k^m of y_k^m as follows ([Bendat and Pier-sol, 1971]):

$$X_k^m = \{Z_k^m + [Z_{N-k}^m]^*\} / 2$$

$$Y_k^m = \{Z_k^m - [Z_{N-k}^m]^*\} / (2i)$$

where the asterisk indicates the complex conjugate.

(vi) Compute the mean power spectral densities (energy), \tilde{G}_x , \tilde{G}_y of the two series correspond-ing to the frequencies f_k

$$f_k = k/(Nh), k = 0, 1, \dots, N/2 \quad (2.2)$$

$$\tilde{G}_x(f_k) = \frac{2h}{N_s} p_k^2 \sum_{m=1}^M |X_k^m|^2 / M \quad (2.3)$$

$$\tilde{G}_y(f_k) = \frac{2h}{N_s} \hat{p}_k^2 \sum_{m=1}^M |Y_k^m|^2 / M \quad (2.4)$$

where s is the inverse of the factor by which the spectral densities are scaled to compensate for energy loss due to windowing, and depends on the window used (see Table 2.2); \mathcal{R} , \hat{p}_k are wave attenuation correction factors, which are functions of frequency (wave number), water depth at the gauge location, and height of the pressure sensor above the bottom. If the water depth and the height of the gauge above the bottom are the same for the two gauges, then $\mathcal{R} = \hat{p}_k$. The spectral densities have units of $L^2 T$. Sometimes for convenience spectral densities are given in units of amplitude squared, i.e. L^2 as follows, for example in the case of \tilde{G}_x

$$\tilde{G}_x(f_k) = \frac{4}{N^2 s} p_k^2 \sum_{m=1}^M |Y_k^m|^2 / M \quad (2.5)$$

From (2.2) we see that spectral densities are available at frequency intervals of $1/T$, ($T=Nh$), from zero frequency to the high frequency limit $1/(2h)$, which is called the Nyquist frequency. The half-power band-width frequency resolution is given by W/T , where W which is given in Table 2.2 depends on the window used. The number of degrees of freedom is $2*M$.

(vii) Following Thompson [1979], the coherence squared, $c^2(f_k)$ for all frequencies defined by (2.2). is computed as follows:

$$c^2(f_k) = \frac{|\sum_{m=1}^M [X_k^m]^* \cdot Y_k^m|^2}{\sum_{m=1}^M [X_k^m]^2 \cdot \sum_{m=1}^M [Y_k^m]^2} \quad (2.6)$$

Sometimes instead of $c^2(f_k)$ its square root, viz., $c(f_k)$ called coherence is used. Table 2.3 gives the threshold values of c^2 and c which are significant at 0.05 and 0.01 significance level. The thresholds are computed using the following formula

$$c^2 = 1 - \psi^{1/(M-1)} \quad (2.7)$$

where $\psi = 0.05$ or 0.01 and M is the total number of ensembles in each time series. For 80 ensembles the threshold value of coherence squared at 0.01 significance level is 0.057, indicating that if the observed coherence squared is larger than 0.057, then in just one case out of 100 the two time series are likely to be not coherent.

(viii) Let $\sum_{m=1}^M [X_k^m]^* Y_k^m = a_k + i b_k$

The real part a_k and the imaginary part b_k are known as the co-incident spectrum/co-spectrum and quadrature/quad-spectrum respectively. The phase spectrum $\phi(f)$ for all frequencies defined by (2.2) is then uniquely defined in the interval $(-\pi, \pi)$ by taking into consideration the signs in the numerator and denominator in the formula given below

$$\phi(f_k) = \arctan(-b_k/a_k) = \phi \text{ (say)} \quad (2.8)$$

The phase spectrum defined in this fashion gives the phase lead of the time series x over the time series y . Assume that the two time series are coherent at frequency f . We emphasize that (2.8) determines the apparent phase difference ϕ in the interval $(-\pi, \pi)$. Owing to the circular nature of the angular scale the true phase difference in the actual physical situation is just one of the infinite number of possible phase differences $\phi + 2j\pi$, where j is an integer that has to be determined.

One strategy is to ensure that $j = 0$, so that the phase ϕ computed by (2.8) is a true representation of the actual physical situation, i.e. is the true phase. This can be done by insisting that

Table 2.3 Threshold values of coherence and coherence squared, which are significant at 0.05 and 0.01 significance level, for different number of ensembles M

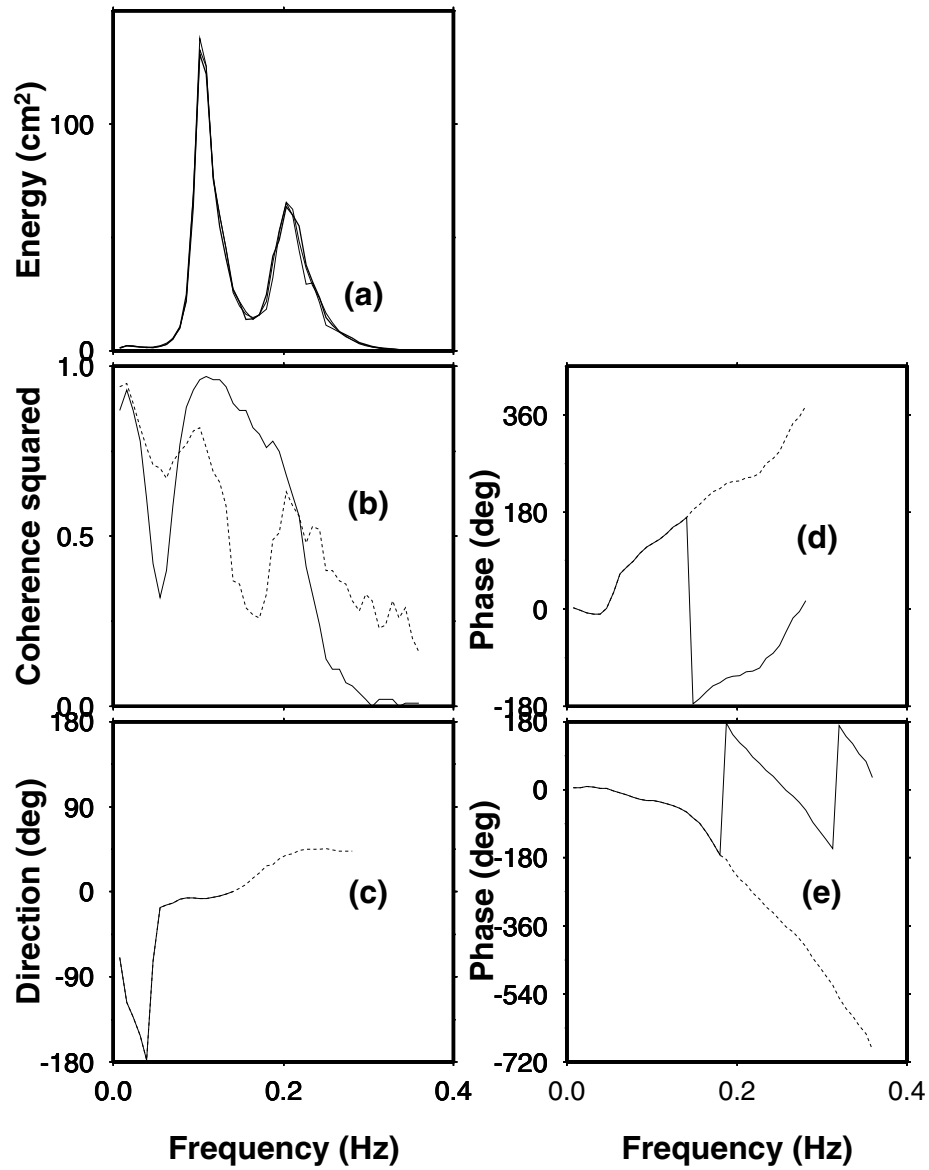
No.	M	Coherence		Coherence squared	
		(0.05)	(0.01)	(0.05)	(0.01)
1	3	.881	.949	.776	.900
2	4	.795	.886	.632	.785
3	5	.726	.827	.527	.684
4	6	.671	.776	.451	.602
5	7	.627	.732	.393	.536
6	8	.590	.694	.348	.482
7	9	.559	.662	.312	.438
8	10	.532	.633	.283	.401
9	11	.509	.607	.259	.369
10	12	.488	.585	.238	.342
11	13	.470	.565	.221	.319
12	14	.454	.546	.206	.298
13	15	.439	.529	.193	.280
14	16	.425	.514	.181	.264
15	17	.413	.500	.171	.250
16	18	.402	.487	.162	.237
17	19	.392	.475	.153	.226
18	20	.382	.464	.146	.215
19	25	.343	.418	.117	.175
20	30	.313	.383	.098	.147
21	35	.290	.356	.084	.127
22	40	.272	.334	.074	.111
23	45	.257	.315	.066	.099
24	50	.244	.300	.059	.090
25	55	.232	.286	.054	.082
26	60	.223	.274	.050	.075
27	65	.214	.263	.046	.069
28	70	.206	.254	.042	.065
29	75	.199	.246	.040	.060
30	80	.193	.238	.037	.057

the distance between the gauges is less than half a wavelength so that the phase difference in the actual situation is restricted to the interval $(-\pi, \pi)$. Fernandes et al. [1986] and Fernandes et al. [1988] used this strategy in their successful attempt at determining wave direction from computer simulated time series of wave elevation at gauges arranged in both linear and polygonal arrays. This strategy may be used in case of measured data also, but it is wasteful, as it treats perfectly good signal at the higher frequencies as noise and discards it. An inspection of cross-spectra from measured data suggests an alternative strategy to determine the true phase $\phi + 2j\pi$ from the apparent phase ϕ . Generally when the distance between the gauges is $\approx 30m$, the gauges are coherent for all frequencies less than about 0.25 Hz and the phase spectrum in the above frequency range is a continuous function of frequency evolving from zero phase at zero frequency, except for a few jumps (generally a maximum of two jumps) across the $(-\pi, \pi)$ pseudo-discontinuity arising due to the circular nature of the angular scale. Such phase spectra have either positive jumps or negative jumps as shown in Figure 2.7, from which it is clear that the true phase at a particular frequency, f_k is obtained from the apparent phase ϕ by adding $+2j\pi$, where the integer j indicates the last jump number prior to be frequency f_k . At frequency zero Hz, as there is no prior jump, the jump number is reckoned as zero. For negative jumps j is negative and for positive jumps j is positive. For example for all frequencies between the first and second positive jumps, the jump number $j = +1$. Similarly for all frequencies between the second and third negative jump the jump number $j = -2$ Figure 2.7 shows both the apparent phase ϕ as well as the true phase $\phi + 2j\pi$. The true phase spectra are terminated at the high frequency end of the spectrum at the frequency where the gauges are statistically no longer coherent, i.e. the coherence squared falls below the threshold given by (2.7). Thus the true phase is determined from the apparent phase by taking into consideration the jump number. **We may summarize by saying that, subject to the gauges being statistically coherent as discussed above, the *true* phase is determined from the *apparent* phase by adding $+/-2\pi$ for every positive/negative jump respectively. By using the *true* phase we ensure that wave directions *will* be correct and we also increase the high frequency limit at which the waves can be correctly determined.**

2.3 ATTENUATION CORRECTION

When wave elevation is measured with a bottom mounted pressure gauge, the observed waves are attenuated in height. The attenuation increases with increasing frequency. To compensate for attenuation, wave amplitudes have to be scaled by a factor $p(\kappa)$ derived using Linear Wave Theory (see Shore Protection Manual, Vol 1):

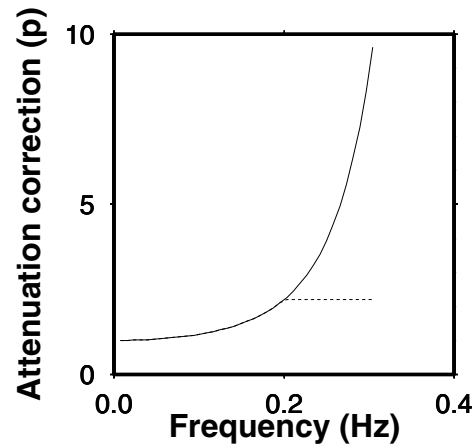
Figure 2.7 Examples of positive and negative jumps: Wave directional spectrum using the method of Esteva [1977] for the gauge triad CB1 on 2 February 1994 at 04 hours. Note that the estimates of wave direction are available even when the criterion $|D \sin \alpha| < \lambda/2$, is not valid



$$p(\kappa) = \frac{\cosh(\kappa d)}{\cosh(\kappa b)} \quad (2.9)$$

where κ is the wave number, d is the water depth at the location of the gauge, and b is the height of the gauge above the bottom. The attenuation correction as a function of frequency is shown in Figure 2.8. To avoid amplification of noise at higher frequencies, the attenuation correction for frequencies above 0.2 Hz (say) may be reckoned as equal the attenuation correction for 0.2 Hz. (It may be mentioned that since we perform only ensemble averaging [frequency averaging is not done!], our wave direction estimates are independent of attenuation correction.)

Figure 2.8 Attenuation correction from linear wave theory (solid line) for gauge 0 at the 8m array at Duck, North Carolina, USA. For frequencies above 0.2Hz, we have assumed the same attenuation correction as for 0.2Hz (dashed line)



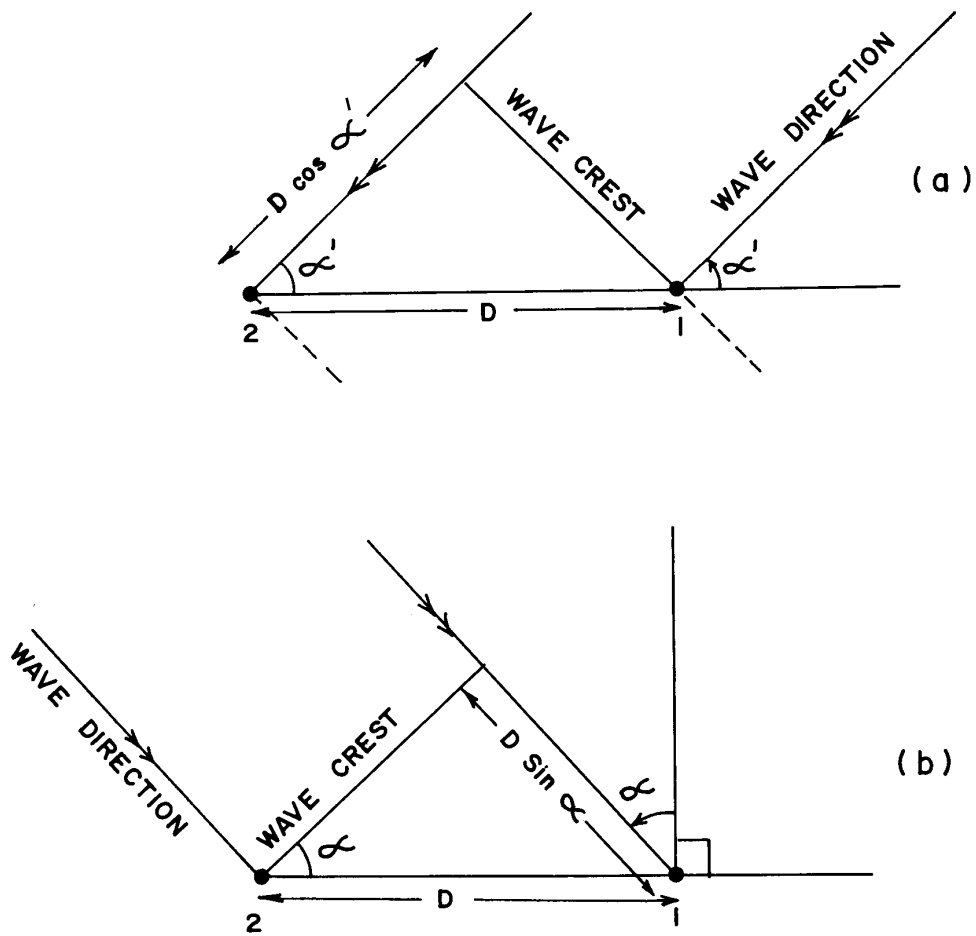
2.4 BORGMAN'S METHOD FOR LINEAR ARRAYS

Consider a sinusoidal long crested wave of frequency f (wave period T , $T = 1/f$) approaching gauges 12, separated by distance D , at an angle α' measured with respect to the line joining the gauges (see Figure 2.9).

By convention wave direction is the direction *from* which waves approach. Equating two definitions of path difference we obtain (see [Borgman, 1974]):

$$D \cos \alpha' = C \tau \quad (2.10)$$

Figure 2.9 The method of Borgman [1974] for determining wave direction as a function of frequency in case of linear 2-gauge arrays



where the wave celerity C is a function of f alone; the time difference τ between the arrival of a wave crest at the two gauges is related to the corresponding phase difference ϕ as follows:

$$\tau = \phi T / (2\pi) \quad (2.11)$$

The phase difference ϕ between the arrival of a wave crest at the two gauges is computed as a function of frequency by cross-spectrum analysis using (2.8).

To evaluate the celerity C , the wave number κ , corresponding to the frequency f is first determined from the following dispersion relationship by the method of iteration:

$$(2\pi f)^2 = \kappa g \tanh(\kappa d) \quad (2.12)$$

where d is the mean water depth at the gauge sites. The wavelength λ ($\lambda = 2\pi/\kappa$) can then be determined and the celerity, C ($= \lambda/T = \lambda f$) evaluated.

In (2.10) the only unknown is α' . Thus wave direction as a function of frequency is easily computed in the interval $(0, \pi)$. As in the case of the 15-gauge array at Duck, North Carolina (see Figure 2.2), with the linear part of the array being parallel to the shore, wave direction α is sometimes measured with respect to the seaward normal to the shore. This can be done by simply adding $-\pi/2$ to the wave direction α' computed by (2.10). Sometimes the axis for measuring wave direction does not coincide with the line passing through the two gauges for which a suitable correction, δ computed from the coordinates of the gauges has to be applied.

Thus $\alpha = \alpha' - \pi/2 + \delta$ gives the wave direction, with respect to the normal to the shore, as function of frequency, computed from the *apparent* phase differences.

This is called as PASS = 0 of the analysis, which is exactly equivalent to the analysis of Borgman [1974]. In this case if the criterion, $|D \cos \alpha| < \lambda/2$, is violated, the computed directions will be incorrect, as the true phase is not restricted to the interval $(-\pi, \pi)$. In measured data, the smallest frequency at which the above criterion is violated is immediately recognised from the phase spectrum by the first jump across the $(-\pi, \pi)$ pseudo discontinuity. (In case of computer simulated data instead of the above criterion, because there is no gradual evolution of phase difference with increasing frequency, the more stringent criterion of $D < \lambda/2$ must necessarily be used).

Therefore in what is called PASS = 1 of the analysis, wave directions α are given a value of 9999.99 for all frequencies above f_a , where f_a is the smallest frequency at which either the first jump across the $(-\pi, \pi)$ discontinuity occurs or the coherence falls below the threshold given by (2.7). Thus PASS = 1 is superior to the analysis of Borgman [1974] in that in PASS=1 incorrect wave directions are flagged with the value 9999.99 as the wave direction.

In PASS = 2 of the analysis, for frequencies above the first phase jump across the $(-\pi, \pi)$ discontinuity, the true phase is determined from the apparent phase computed by (2.8) by taking into consideration the jump number as explained in the section on cross spectrum analysis, and directions are computed from the true phase difference. In PASS = 2, directions are given a value of 9999.99 for all frequencies above f_b , $f_b \geq f_a$, where f_b is the smallest frequency at which the coherence falls below the threshold given by (2.7) and f_a is the same as defined above. Thus PASS = 2 of our analysis, which is superior to both PASS = 0 (the Borgman analysis!), and PASS = 1, makes full use of the **signal** in the measured data. PASS = 2 is also superior to the analysis of Munk et al. [1963], who directly compute the wave direction α , without the intermediate computation of α' .

In PASS = 0 as well as PASS = 1, the apparent phase is used in (2.11), whereas in PASS = 2, the true phase is used. PASS=2 is herein referred as the ‘Modified Borgman Method’.

The true phase is determined from the apparent phase by taking into consideration the jump number discussed in Chapter 2.2. The jumps occur when the path difference between the arrival of a wave crest at the two gauges satisfies the relationship

$$D \cos \alpha' = D \sin \alpha = (2n + 1) \lambda/2$$

where D is the distance between the gauges, the wave direction is given by α' or α , λ is the wavelength, n is any integer (positive, zero or negative) and the jump number j is given by

$$j = \begin{cases} n + 1 & \text{for } n \geq 0 \\ n & \text{for } n < 0 \end{cases}$$

Thus two gauges are sufficient to determine wave direction as a function of frequency. If more 2-gauge combinations (i.e. gauge pairs) are available redundant estimates of wave direction are possible. We have made 10 redundant estimates of wave direction for each of the 47 data files of measured data at North Carolina. The following 10 gauge pairs: 43, 21, 32, 42, 65, 78, 89, 31, 01 and 54; satisfying $D < \lambda/2$ for wave periods above 9s, were chosen with the help of a figure similar to Figure 2.6. Two gauge pairs with small gauge separation, viz, 43 and 21 satisfied the same criterion for periods above 3.5s.

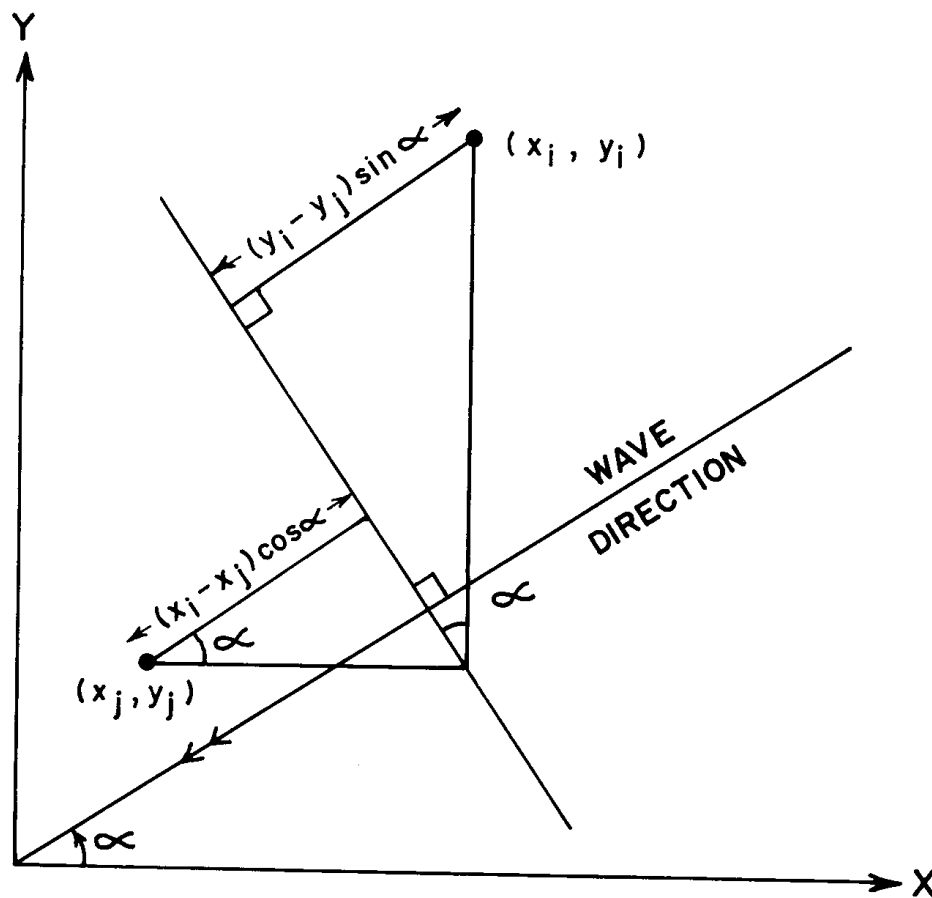
Linear (2-gauge) arrays are unable to distinguish between waves arriving at the gauges at the same angle but from opposite sides, i.e. at angles α' and $-\alpha'$, or in terms of α , at angles α and $\pi - \alpha$, as the phase difference for either case is the same. However, oftentimes it may be possible to assume that waves come from just one side, viz., the seaward side, e.g. swell at a long coastline, so that linear array can be used to advantage.

2.5 ESTEVA'S METHOD FOR POLYGONAL ARRAYS

More often than not it is wrong to assume that waves come from just one side as has to be done in case of linear arrays. In such cases polygonal arrays are used to unambiguously determine wave direction.

Let (x_i, y_i) and (x_j, y_j) be the coordinates of two gauges. Let α be the wave direction (see Figure 2.10) measured anti-clockwise positive with respect to the x-axis, By convention wave direction is the direction *from* which waves are approaching.

Figure 2.10 Method of Esteva [1977] for determining wave direction as a function of frequency from polygonal 3-gauge arrays



For length λ , the phase difference is 2π . Therefore for length $(x_i - x_j) \cos \alpha + (y_i - y_j) \sin \alpha$, the corresponding phase difference is

$$\begin{aligned}\phi_{ij} &= (2\pi/\lambda) [(x_i - x_j) \cos \alpha + (y_i - y_j) \sin \alpha] \\ &= \kappa [(x_i - x_j) \cos \alpha + (y_i - y_j) \sin \alpha]\end{aligned}$$

In particular,

$$\phi_{12} = \kappa [(x_1 - x_2) \cos \alpha + (y_1 - y_2) \sin \alpha] \quad (2.13)$$

$$\phi_{13} = \kappa [(x_1 - x_3) \cos \alpha + (y_1 - y_3) \sin \alpha] \quad (2.14)$$

From (2.13) and (2.14) it is clear that

$$\begin{aligned}\sin \alpha &= [(x_1 - x_2) \phi_{13} + (x_1 - x_3) \phi_{12}] / P \\ \cos \alpha &= [(y_1 - y_3) \phi_{12} - (y_1 - y_2) \phi_{13}] / P\end{aligned}$$

where, $P = \kappa [(x_1 - x_2)(y_1 - y_3) - (x_1 - x_3)(y_1 - y_2)]$, does not vanish for nonlinear arrays.

Then α is uniquely determined in the range $(-\pi, \pi)$ from the following equation by considering the signs of the numerator and the denominator:

$$\alpha = \arctan \frac{[(x_1 - x_2) \phi_{13} + (x_1 - x_3) \phi_{12}] \text{Sgn } P}{[(y_1 - y_3) \phi_{12} - (y_1 - y_2) \phi_{13}] \text{Sgn } P} \quad (2.15)$$

where $\text{Sgn } P = 1$, for $P > 0$ and $\text{Sgn } P = -1$, for $P < 0$

ϕ_{12} and ϕ_{13} can be determined as a function of frequency from the cross-spectrum between gauges 12 and 13 respectively by using (2.8). Thus from (2.15) wave direction is determined as a function of frequency. This is called as PASS = 0 of the analysis, which is equivalent to the analysis of Esteva [1977]. In this case wave directions will be incorrect for all frequencies above $f_a = \min(f_{12}, f_{13})$, where f_{ij} are the smallest frequency at which either the phase ϕ_j jumps across the $(-\pi, \pi)$ pseudo-discontinuity or the coherence squared \hat{c}_j^2 falls below the threshold given by (2.7).

Therefore in PASS = 1 of the analysis, directions for all frequencies above f_i are given the value of 9999.99, so that PASS = 1, is superior to PASS = 0, i.e., the analysis of Esteva [1977].

In PASS = 2 of the analysis, the *true* phases are determined from the *apparent* phases ϕ_2 and ϕ_{13} computed by using (2.8) by taking into consideration the jump numbers as explained in the Chapter 2.2 and directions are computed from the true phase difference. In PASS = 2, wave directions

are given a value of 9999.99 for all frequencies above f_b , $f_b \geq f_a$, where f_b , is the smallest frequency at which the coherence squared for either gauges 12 or 13 falls below the threshold given by (2.7).

It may be emphasized that in $PASS = 0$ as well as $PASS = 1$, the *apparent* phases ϕ_2 and ϕ_{13} computed from (2.8) are used in (2.15), whereas in $PASS = 2$, the *true* phase is used. $PASS=2$ is referred herein as the ‘Modified Esteva method’.

Thus three non collinear gauges are sufficient to determine wave direction unambiguously as a function of direction. If more 3-gauge combinations (i.e. gauge triads) are available, redundant estimates of wave direction are possible. We have made 15 redundant estimates of wave direction as a function of frequency for each of the 47 measured data files at North Carolina. The following 15 gauge triads: 012, 34C, DO3, D24, C1D, 4C5, DOE, CB1, CB2, CB0, DO4, DOC, 02D, 41D and C24; satisfying $D < \lambda/2$ for wave periods above 9s were chosen. Two gauge triads with small gauge separations D, viz, 012 and 34C satisfied the same criterion for periods above 3.7s.

2.6 RESULTS AND DISCUSSION

Software in FORTRAN Language, constructed on the “black-box” principle, has been developed to determine wave direction from measurements of surface elevation at the 15-gauge array at North Carolina, USA using the phase/time/path difference methods (PTPDM) of (Esteva [1976], Esteva [1977]) and Borgman [1974] in case of polygonal (3-gauge) and linear (2-gauge) arrays respectively. Before applying the software to the measured data, the software was applied to computer simulated wave fields at the 15-gauge array and was found to consistently yield directions correctly in case of both linear as well as polygonal arrays.

A sinusoidal wave can be simulated on a computer using the formula

$$\eta(t) = A \cos[2\pi ft + \delta + \kappa(x \cos \alpha + y \sin \alpha)]$$

where η is the wave elevation as a function of time t at a gauge having coordinates (x, y) ; f is the frequency of the wave; A is its amplitude; κ is the wave number; α is the wave direction measured as in Figure 2.11 and δ is an arbitrary phase at the origin.

The computer simulation of the wave fields was done by combining three sinusoidal waves with frequencies 3/1024 Hz apart, each sinusoid being assigned a specific direction, nearly equal amplitude, each frequency 0.134/1024 (= 0.00012) Hz removed from the closest spectral frequency, and having arbitrary phase at the origin in lines with Fernandes et al. [1988]. For representing ocean waves more realistically random noise within the interval $\pm 1.5cm$ was added. The simulated time series at the 15-gauge array had 1024 points sampled at 1Hz, i.e. 1s.

Figure 2.11 Simulation of wave trains in case of arrays

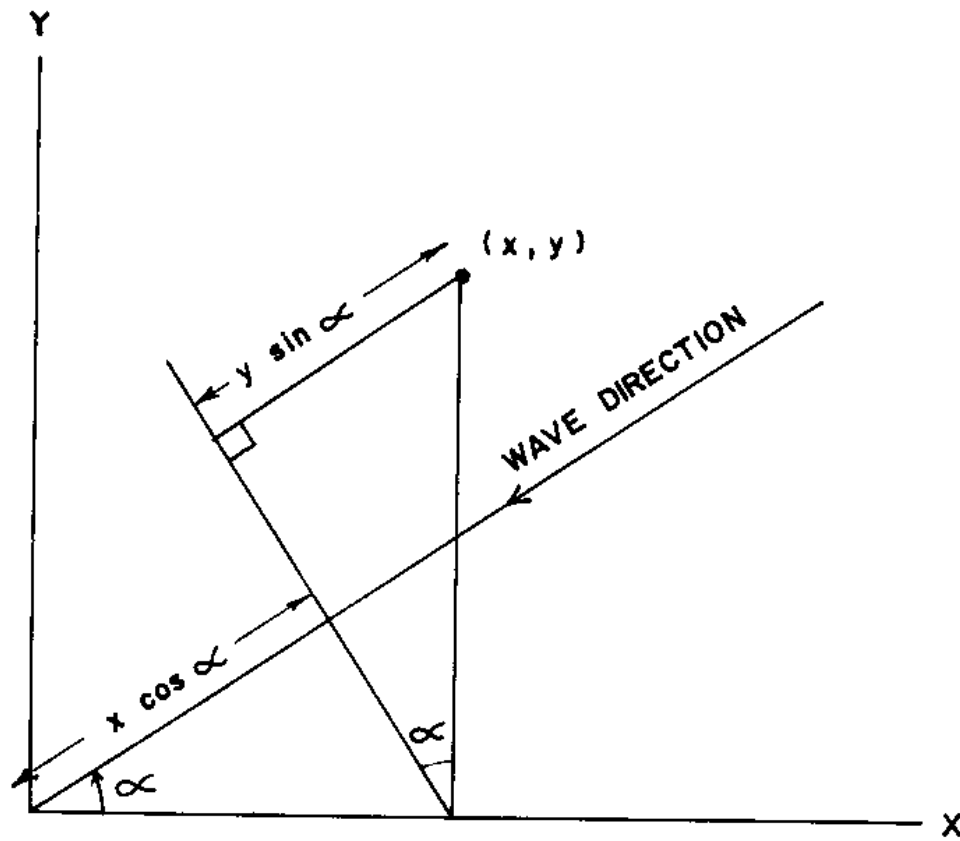


Table 2.4 presents the characteristics of one such computer simulated wave field. This wave field may be briefly described as swell of $\approx 10s$, with the three swell components having wave directions of 5° , -5° and -10° .

Table 2.4 Characteristics of a computer simulated wave field at the 15-gauge polygonal array at 8m depth at the Coastal Engineering Research Center's (CERC) Field Research facility at Duck, North Carolina, USA. [†] Indicates approximate wave period. [‡] indicates initial phase at the origin

Closest spectral		Simulated wave train			
Line (k)	Period (s)	Amplitude (cm)	Period [†] (s)	Phase [‡] (deg)	Direction (deg)
102	10.14	11.43	10.125	15	5
105	9.85	15.24	9.833	25	-5
108	9.57	11.43	9.558	20	-10

We shall be presenting an array of tables giving the wave directional spectrum in case of polygonal and linear arrays, with measured as well as computer simulated wave fields. An annotation of the specifications of the analyses performed as indicated at the top of this array of tables is given in Table 2.5.

In the spectrum and cross-spectrum analyses of the computer simulated data we used one ensemble of 1024 points sampled at 1Hz, i.e. 1s. Hanning window was used. Spectral densities are given in units of cm^2 . Spectral densities have been scaled up by a factor of 1/0.375 to compensate for loss of energy due to windowing.

Table 2.6 gives the wave directional spectrum (PASS = 0) for the computer simulated swell of $\approx 10s$ using gauge pair 89. We note that the wave directions are correctly computed for the swell of $\approx 10s$ as the swell frequencies satisfy the criterion of Barber and Doyle [1956], $D < \lambda/2$, for the gauge pair 89.

Table 2.5 Annotations of specifications in tables giving the analysis of the 15-gauge array at Duck, North Carolina, USA, using the methods of Borgman [1974] and Esteva [1977] in case of linear and polygonal arrays respectively

PAIR	- For linear arrays the analysis is done in units of gauge pairs
TRIAD	- For polygonal arrays the analysis is done in units of gauge triads
PART	= 0 , Time series is computer simulated = 6 , Time series has a total of 5 X 4096 points
PASS	= 0 , Apparent phase used for determining wave direction = 1 , Apparent phase used; incorrect wave directions flagged as 9999.99 wave directions are assumed incorrect when either coherence falls below 0.057 or phase jump across -180/+180 degrees occurs = 2 , True phase used; incorrect wave directions flagged as 9999.99 wave directions are assumed incorrect when coherence falls below 0.057
Hmo	- Significant wave height for (gauge pair 12/ gauge triad 123) computed as four times the zero th moment
NP	- Number of ensembles
SAMIN	- Sampling interval in seconds
NDF	- Number of degrees of freedom, is twice the number of ensembles
UNITS	= 1 , spectral densities in cm**2 = 2 , spectral densities in cm**2/Hz
WINDOW	= 1 , Rectangular window used = 2 , Hanning window used = 3 , Hamming window used = 4 , Blackman window used = 5 , Cosine Taper window used
ICOR	= 0 , Attenuation correction not performed = 1 , Attenuation correction performed
CUT	- Attenuation correction for frequencies above cut(-off) value are the same as for the cut(-off) value
TH, TL	- Spectral densities between periods (TH, TL) used to determine the significant wave height
DIST	- Distance between gauges 12 in case of gauge pair 12; distances between gauges 12 and 13 in case of gauge triad 123
PER	- Central period for frequency band
G1, G2	- Spectral densities for gauge pair 12
G1, G2, G3	- Spectral densities for gauge triad 123
LAM	- Wavelength corresponding to central period
PH1, COH1	- Phase and coherence respectively for gauges 12 in case of gauge pair 12; Phase and coherence respectively for gauges 12 in case of gauge triad 123
PH2, COH2	- Phase and coherence respectively for gauges 13 in case of gauge triad 123
FREQ	- Central frequency for frequency band
DIR	- Wave direction measured with respect to the seaward normal, northwards positive
QH1,QH2	- "TRUE" Phase differences, i.e., PASS=2, while PH1,PH2 are "APPARENT" phase differences, i.e., PASS=0

Table 2.6 PAIR=89 PART=0 PASS=0 00/00/00 00:00 HRS Hmo=[.63; .63] NP=1024
 SAMIN=1.0 NDF= 2 UNITS=1 WINDOW=2 ICOR=0 CUT= .20 TH=21.40 TL= 1.99 FOR-
 MAT=(8f7.2) FACTOR=1.0 DIST= 34.11

NO	PER	G1	G2	LAM	PH1	COH1	FREQ	DIR
90	11.51	.005	.005	97.80	-4.76	1.00	.0869	.66
91	11.38	.002	.002	96.59	-50.25	1.00	.0879	21.77
92	11.25	.003	.001	95.41	-57.05	1.00	.0889	24.80
93	11.13	.001	.004	94.37	-26.57	1.00	.0898	10.27
94	11.01	.004	.003	93.23	48.31	1.00	.0908	-23.03
95	10.89	.002	.001	92.12	103.79	1.00	.0918	-52.65
96	10.78	.009	.000	91.03	-64.85	1.00	.0928	27.22
97	10.67	.007	.001	89.97	-53.01	1.00	.0938	21.34
98	10.56	.000	.002	89.03	-72.27	1.00	.0947	30.08
99	10.45	.004	.001	88.00	.01	1.00	.0957	-1.52
100	10.34	.041	.022	87.00	3.56	1.00	.0967	-2.96
101	10.24	13.638	14.161	86.01	-18.41	1.00	.0977	5.90
102	10.14	85.534	86.062	85.14	-16.78	1.00	.0986	5.17
103	10.04	29.449	30.463	84.19	-17.03	1.00	.0996	5.19
104	9.94	27.749	26.949	83.26	8.79	1.00	.1006	-4.93
105	9.85	149.959	150.404	82.34	9.23	1.00	.1016	-5.06
106	9.75	56.766	57.151	81.54	9.22	1.00	.1025	-5.02
107	9.66	12.748	12.192	80.65	22.88	1.00	.1035	-10.15
108	9.57	85.925	85.796	79.79	22.30	1.00	.1045	-9.84
109	9.48	31.069	31.381	78.93	22.48	1.00	.1055	-9.82
110	9.39	.069	.081	78.18	22.23	1.00	.1064	-9.65
111	9.31	.004	.002	77.36	34.57	1.00	.1074	-14.09
112	9.23	.000	.008	76.55	-137.37	1.00	.1084	57.39
113	9.14	.004	.003	75.76	-125.51	1.00	.1094	49.23
114	9.06	.001	.002	74.97	-118.35	1.00	.1104	44.75
115	8.98	.001	.002	74.28	-152.47	1.00	.1113	65.75
116	8.90	.000	.001	73.53	-116.74	1.00	.1123	42.83
117	8.83	.001	.009	72.78	174.31	1.00	.1133	999.99
118	8.75	.002	.009	72.05	123.44	1.00	.1143	-47.92
119	8.68	.001	.003	71.40	148.91	1.00	.1152	-61.49
120	8.61	.000	.001	70.69	128.99	1.00	.1162	-49.46

Table 2.7 TRIAD=41d PART=0 PASS=0 00/00/00 00:00 HRS Hmo= [.63; .63; .63] NP=1024
 SAMIN=1.0 NDF= 2 UNITS=1 WINDOW=2 ICOR=0 CUT= .20 TH=21.40 TL= 1.99 FOR-
 MAT=(8f7.2) FACTOR=1.0 DIST= [30.40; 21.12]

NO	PER	G1	G2	G3	PH1	PH2	COH1	COH2	FREQ	DIR
90	11.51	.006	.000	.000	96.86	101.79	1.00	1.00	.0869	-142.64
91	11.38	.007	.003	.000	-136.58	144.90	1.00	1.00	.0879	151.24
92	11.25	.008	.003	.004	-152.47	70.47	1.00	1.00	.0889	133.05
93	11.13	.006	.000	.001	-171.09	48.06	1.00	1.00	.0898	123.64
94	11.01	.001	.001	.004	140.16	-136.38	1.00	1.00	.0908	-30.59
95	10.89	.003	.002	.008	146.77	-108.98	1.00	1.00	.0918	-36.53
96	10.78	.008	.000	.011	141.99	-124.88	1.00	1.00	.0928	-32.78
97	10.67	.004	.003	.009	-96.38	-146.89	1.00	1.00	.0938	26.44
98	10.56	.004	.004	.001	137.20	62.65	1.00	1.00	.0947	-113.19
99	10.45	.009	.004	.008	-79.71	-170.87	1.00	1.00	.0957	18.84
100	10.34	.012	.022	.019	17.88	-39.19	1.00	1.00	.0967	-15.95
101	10.24	14.505	13.896	13.860	-10.99	-88.77	1.00	1.00	.0977	4.87
102	10.14	86.561	85.888	84.562	-11.00	-88.51	1.00	1.00	.0986	4.89
103	10.04	31.877	30.430	31.122	-11.12	-88.77	1.00	1.00	.0996	4.93
104	9.94	26.258	26.258	26.004	11.14	-87.58	1.00	1.00	.1006	-4.80
105	9.85	153.305	150.548	151.954	11.93	-87.22	1.00	1.00	.1016	-5.15
106	9.75	54.679	55.365	55.028	11.91	-86.69	1.00	1.00	.1025	-5.17
107	9.66	14.509	14.897	15.509	22.69	-87.74	1.00	1.00	.1035	-9.49
108	9.57	83.083	85.606	84.569	22.92	-87.88	1.00	1.00	.1045	-9.56
109	9.48	31.621	31.081	31.611	22.09	-88.23	1.00	1.00	.1055	-9.20
110	9.39	.077	.023	.102	7.58	-93.54	1.00	1.00	.1064	-3.09
111	9.31	.023	.028	.002	32.26	87.79	1.00	1.00	.1074	-165.21
112	9.23	.010	.001	.009	99.58	123.85	1.00	1.00	.1084	-147.92
113	9.14	.002	.001	.001	-162.17	8.37	1.00	1.00	.1094	108.02
114	9.06	.002	.001	.002	18.89	109.17	1.00	1.00	.1104	-173.15
115	8.98	.005	.001	.001	-85.61	151.49	1.00	1.00	.1113	160.81
116	8.90	.005	.001	.002	113.41	-174.66	1.00	1.00	.1123	-21.55
117	8.83	.008	.003	.007	83.19	-172.01	1.00	1.00	.1133	-16.79
118	8.75	.003	.004	.007	102.16	-157.19	1.00	1.00	.1143	-21.56
119	8.68	.000	.001	.006	119.64	-161.94	1.00	1.00	.1152	-23.91
120	8.61	.001	.003	.001	-74.62	-143.26	1.00	1.00	.1162	21.05

Table 2.8 PAIR=78 PART=6 PASS=0 05/02/94 16:00 HRS Hmo=[.27; .27] NP= 256 SAMIN=.5 NDF=160 UNITS=1 WINDOW=4 ICOR=1 CUT= .20 TH=21.40 TL= 1.99 FORMAT=(8f5.1) FACTOR=1.0 DIST= 25.40

NO	PER	G1	G2	LAM	PH1	COH1	FREQ	DIR
2	128.00	.858	.899	1135.28	3.03	.98	.0078	-22.10
3	64.00	1.525	1.562	567.11	4.08	.99	.0156	-14.66
4	42.67	1.172	1.194	377.46	6.03	.98	.0234	-14.41
5	32.00	.428	.410	281.54	7.96	.94	.0313	-14.19
6	25.60	.265	.256	224.71	11.34	.83	.0391	-16.18
7	21.33	.434	.470	186.66	12.91	.84	.0469	-15.28
8	18.29	.816	.874	159.35	10.26	.82	.0547	-10.30
9	16.00	1.494	1.733	138.76	11.37	.82	.0625	-9.94
10	14.22	2.877	3.338	122.67	13.05	.87	.0703	-10.08
11	12.80	3.561	3.593	109.71	16.20	.85	.0781	-11.21
12	11.64	4.078	4.261	99.03	27.50	.79	.0859	-17.33
13	10.67	6.144	6.738	89.97	40.73	.79	.0938	-23.63
14	9.85	10.932	12.024	82.34	51.51	.83	.1016	-27.64
15	9.14	12.413	14.208	75.76	57.24	.84	.1094	-28.31
16	8.53	9.356	10.021	69.99	59.36	.82	.1172	-27.02
17	8.00	6.108	5.937	64.90	64.66	.81	.1250	-27.32
18	7.53	4.485	4.167	60.37	73.18	.75	.1328	-28.89
19	7.11	5.119	4.522	56.30	85.99	.77	.1406	-31.97
20	6.74	5.166	4.881	52.62	93.53	.77	.1484	-32.56
21	6.40	3.708	3.719	49.23	103.22	.72	.1563	-33.76
22	6.10	2.607	2.583	46.17	113.85	.61	.1641	-35.09
23	5.82	1.694	1.811	43.37	128.09	.59	.1719	-37.41
24	5.57	1.248	1.233	40.78	130.29	.52	.1797	-35.52
25	5.33	1.194	1.188	38.38	123.96	.55	.1875	-31.35
26	5.12	1.198	1.208	36.15	127.10	.58	.1953	-30.17
27	4.92	1.042	1.157	34.08	138.82	.55	.2031	-31.16
28	4.74	.880	.912	32.15	143.46	.54	.2109	-30.29
29	4.57	.649	.677	30.33	148.02	.42	.2188	-29.40
30	4.41	.607	.622	28.64	161.80	.40	.2266	-30.45
31	4.27	.541	.562	27.06	171.37	.34	.2344	-30.48
32	4.13	.370	.366	25.59	-160.42	.14	.2422	26.67
33	4.00	.225	.238	24.21	-144.37	.11	.2500	22.47
34	3.88	.169	.166	22.92	-119.14	.09	.2578	17.37
35	3.76	.121	.128	21.71	-97.74	.07	.2656	13.42
36	3.66	.092	.086	20.57	-72.94	.08	.2734	9.45
37	3.56	.077	.061	19.50	-20.75	.07	.2813	2.54
38	3.46	.067	.048	18.52	31.67	.08	.2891	-3.68
39	3.37	.050	.037	17.60	73.74	.15	.2969	-8.16
40	3.28	.032	.025	16.73	85.15	.08	.3047	-8.97
41	3.20	.024	.017	15.93	115.46	.04	.3125	-11.60
42	3.12	.018	.013	15.18	97.08	.11	.3203	-9.27
43	3.05	.014	.011	14.48	87.56	.09	.3281	-7.97
44	2.98	.011	.009	13.82	141.26	.00	.3359	-12.33
45	2.91	.009	.009	13.20	-109.73	.00	.3438	9.11
46	2.84	.007	.007	12.62	-8.24	.00	.3516	.65
47	2.78	.008	.006	12.08	-91.93	.01	.3594	6.98

Table 2.9 PAIR=78 PART=6 PASS=1 05/02/94 16:00 HRS Hmo=[.27; .27] NP= 256 SAMIN=.5 NDF=160 UNITS=1 WINDOW=4 ICOR=1 CUT= .20 TH=21.40 TL= 1.99 FORMAT=(8f5.1) FACTOR=1.0 DIST= 25.40

NO	PER	G1	G2	LAM	PH1	COH1	FREQ	DIR
2	128.00	.858	.899	1135.28	3.03	.98	.0078	-22.10
3	64.00	1.525	1.562	567.11	4.08	.99	.0156	-14.66
4	42.67	1.172	1.194	377.46	6.03	.98	.0234	-14.41
5	32.00	.428	.410	281.54	7.96	.94	.0313	-14.19
6	25.60	.265	.256	224.71	11.34	.83	.0391	-16.18
7	21.33	.434	.470	186.66	12.91	.84	.0469	-15.28
8	18.29	.816	.874	159.35	10.26	.82	.0547	-10.30
9	16.00	1.494	1.733	138.76	11.37	.82	.0625	-9.94
10	14.22	2.877	3.338	122.67	13.05	.87	.0703	-10.08
11	12.80	3.561	3.593	109.71	16.20	.85	.0781	-11.21
12	11.64	4.078	4.261	99.03	27.50	.79	.0859	-17.33
13	10.67	6.144	6.738	89.97	40.73	.79	.0938	-23.63
14	9.85	10.932	12.024	82.34	51.51	.83	.1016	-27.64
15	9.14	12.413	14.208	75.76	57.24	.84	.1094	-28.31
16	8.53	9.356	10.021	69.99	59.36	.82	.1172	-27.02
17	8.00	6.108	5.937	64.90	64.66	.81	.1250	-27.32
18	7.53	4.485	4.167	60.37	73.18	.75	.1328	-28.89
19	7.11	5.119	4.522	56.30	85.99	.77	.1406	-31.97
20	6.74	5.166	4.881	52.62	93.53	.77	.1484	-32.56
21	6.40	3.708	3.719	49.23	103.22	.72	.1563	-33.76
22	6.10	2.607	2.583	46.17	113.85	.61	.1641	-35.09
23	5.82	1.694	1.811	43.37	128.09	.59	.1719	-37.41
24	5.57	1.248	1.233	40.78	130.29	.52	.1797	-35.52
25	5.33	1.194	1.188	38.38	123.96	.55	.1875	-31.35
26	5.12	1.198	1.208	36.15	127.10	.58	.1953	-30.17
27	4.92	1.042	1.157	34.08	138.82	.55	.2031	-31.16
28	4.74	.880	.912	32.15	143.46	.54	.2109	-30.29
29	4.57	.649	.677	30.33	148.02	.42	.2188	-29.40
30	4.41	.607	.622	28.64	161.80	.40	.2266	-30.45
31	4.27	.541	.562	27.06	171.37	.34	.2344	-30.48
32	4.13	.370	.366	25.59	-160.42	.14	.2422	9999.99
33	4.00	.225	.238	24.21	-144.37	.11	.2500	9999.99
34	3.88	.169	.166	22.92	-119.14	.09	.2578	9999.99
35	3.76	.121	.128	21.71	-97.74	.07	.2656	9999.99
36	3.66	.092	.086	20.57	-72.94	.08	.2734	9999.99
37	3.56	.077	.061	19.50	-20.75	.07	.2813	9999.99
38	3.46	.067	.048	18.52	31.67	.08	.2891	9999.99
39	3.37	.050	.037	17.60	73.74	.15	.2969	9999.99
40	3.28	.032	.025	16.73	85.15	.08	.3047	9999.99
41	3.20	.024	.017	15.93	115.46	.04	.3125	9999.99
42	3.12	.018	.013	15.18	97.08	.11	.3203	9999.99
43	3.05	.014	.011	14.48	87.56	.09	.3281	9999.99
44	2.98	.011	.009	13.82	141.26	.00	.3359	9999.99
45	2.91	.009	.009	13.20	-109.73	.00	.3438	9999.99
46	2.84	.007	.007	12.62	-8.24	.00	.3516	9999.99
47	2.78	.008	.006	12.08	-91.93	.01	.3594	9999.99

Table 2.10 PAIR=78 PART=6 PASS=2 05/02/94 16:00 HRS Hmo=[.27; .27] NP= 256 SAMIN=.5 NDF=160 UNITS=1 WINDOW=4 ICOR=1 CUT= .20 TH=21.40 TL= 1.99 FORMAT=(8f5.1) FACTOR=1.0 DIST= 25.40

NO	PER	G1	G2	LAM	PH1	COH1	FREQ	DIR	QH1
2	128.00	.858	.899	1135.28	3.03	.98	.0078	-22.10	3.03
3	64.00	1.525	1.562	567.11	4.08	.99	.0156	-14.66	4.08
4	42.67	1.172	1.194	377.46	6.03	.98	.0234	-14.41	6.03
5	32.00	.428	.410	281.54	7.96	.94	.0313	-14.19	7.96
6	25.60	.265	.256	224.71	11.34	.83	.0391	-16.18	11.34
7	21.33	.434	.470	186.66	12.91	.84	.0469	-15.28	12.91
8	18.29	.816	.874	159.35	10.26	.82	.0547	-10.30	10.26
9	16.00	1.494	1.733	138.76	11.37	.82	.0625	-9.94	11.37
10	14.22	2.877	3.338	122.67	13.05	.87	.0703	-10.08	13.05
11	12.80	3.561	3.593	109.71	16.20	.85	.0781	-11.21	16.20
12	11.64	4.078	4.261	99.03	27.50	.79	.0859	-17.33	27.50
13	10.67	6.144	6.738	89.97	40.73	.79	.0938	-23.63	40.73
14	9.85	10.932	12.024	82.34	51.51	.83	.1016	-27.64	51.51
15	9.14	12.413	14.208	75.76	57.24	.84	.1094	-28.31	57.24
16	8.53	9.356	10.021	69.99	59.36	.82	.1172	-27.02	59.36
17	8.00	6.108	5.937	64.90	64.66	.81	.1250	-27.32	64.66
18	7.53	4.485	4.167	60.37	73.18	.75	.1328	-28.89	73.18
19	7.11	5.119	4.522	56.30	85.99	.77	.1406	-31.97	85.99
20	6.74	5.166	4.881	52.62	93.53	.77	.1484	-32.56	93.53
21	6.40	3.708	3.719	49.23	103.22	.72	.1563	-33.76	103.22
22	6.10	2.607	2.583	46.17	113.85	.61	.1641	-35.09	113.85
23	5.82	1.694	1.811	43.37	128.09	.59	.1719	-37.41	128.09
24	5.57	1.248	1.233	40.78	130.29	.52	.1797	-35.52	130.29
25	5.33	1.194	1.188	38.38	123.96	.55	.1875	-31.35	123.96
26	5.12	1.198	1.208	36.15	127.10	.58	.1953	-30.17	127.10
27	4.92	1.042	1.157	34.08	138.82	.55	.2031	-31.16	138.82
28	4.74	.880	.912	32.15	143.46	.54	.2109	-30.29	143.46
29	4.57	.649	.677	30.33	148.02	.42	.2188	-29.40	148.02
30	4.41	.607	.622	28.64	161.80	.40	.2266	-30.45	161.80
31	4.27	.541	.562	27.06	171.37	.34	.2344	-30.48	171.37
32	4.13	.370	.366	25.59	-160.42	.14	.2422	-33.95	199.58
33	4.00	.225	.238	24.21	-144.37	.11	.2500	-34.81	215.63
34	3.88	.169	.166	22.92	-119.14	.09	.2578	-37.13	240.86
35	3.76	.121	.128	21.71	-97.74	.07	.2656	-38.50	262.26
36	3.66	.092	.086	20.57	-72.94	.08	.2734	-40.23	287.06
37	3.56	.077	.061	19.50	-20.75	.07	.2813	-46.36	339.25
38	3.46	.067	.048	18.52	31.67	.08	.2891	-52.48	391.67
39	3.37	.050	.037	17.60	73.74	.15	.2969	-56.58	433.74
40	3.28	.032	.025	16.73	85.15	.08	.3047	-54.55	445.15
41	3.20	.024	.017	15.93	115.46	.04	.3125	9999.99	9999.99
42	3.12	.018	.013	15.18	97.08	.11	.3203	9999.99	9999.99
43	3.05	.014	.011	14.48	87.56	.09	.3281	9999.99	9999.99
44	2.98	.011	.009	13.82	141.26	.00	.3359	9999.99	9999.99
45	2.91	.009	.009	13.20	-109.73	.00	.3438	9999.99	9999.99
46	2.84	.007	.007	12.62	-8.24	.00	.3516	9999.99	9999.99
47	2.78	.008	.006	12.08	-91.93	.01	.3594	9999.99	9999.99

Table 2.11 TRIAD=cb1 PART=6 PASS=0 02/02/94 04:00 HRS Hmo= [.91; .94; .93] NP= 256
 SAMIN= .5 NDF=160 UNITS=1 WINDOW=4 ICOR=1 CUT= .20 TH=21.40 TL= 1.99 FOR-
 MAT=(8f5.1) FACTOR=1.0 DIST= [29.51; 26.83]

NO	PER	G1	G2	G3	PH1	PH2	COH1	COH2	FREQ	DIR
2	128.00	1.285	1.325	1.265	2.89	6.04	.87	.94	.0078	-69.65
3	64.00	2.292	2.324	2.309	-2.52	4.76	.93	.95	.0156	-117.09
4	42.67	2.132	2.089	2.115	-6.54	8.03	.87	.89	.0234	-132.37
5	32.00	1.759	1.714	1.786	-9.37	7.29	.78	.82	.0313	-151.92
6	25.60	1.413	1.543	1.599	-8.76	3.27	.61	.76	.0391	-177.64
7	21.33	1.425	1.579	1.394	1.21	3.41	.42	.71	.0469	-73.75
8	18.29	2.115	2.300	1.958	31.76	-2.95	.32	.70	.0547	-16.30
9	16.00	2.892	3.340	2.806	65.10	-8.56	.40	.67	.0625	-13.87
10	14.22	5.609	5.271	5.006	77.01	-12.71	.59	.72	.0703	-11.70
11	12.80	10.747	9.985	10.577	89.75	-20.43	.77	.75	.0781	-7.57
12	11.64	21.637	22.459	24.857	103.99	-25.84	.88	.77	.0859	-6.17
13	10.67	63.337	69.610	68.941	115.12	-27.69	.93	.81	.0938	-6.70
14	9.85	132.793	137.724	130.672	123.07	-28.48	.96	.82	.1016	-7.32
15	9.14	125.338	125.599	121.938	129.63	-31.02	.97	.76	.1094	-6.79
16	8.53	75.187	76.562	76.946	140.27	-36.13	.96	.69	.1172	-5.55
17	8.00	59.947	59.899	54.932	151.71	-42.06	.96	.66	.1250	-4.22
18	7.53	45.024	45.330	40.605	159.25	-48.46	.94	.59	.1328	-2.38
19	7.11	25.779	27.402	26.831	170.35	-58.62	.89	.37	.1406	.35
20	6.74	19.805	21.732	21.499	-175.25	-73.53	.87	.36	.1484	138.44
21	6.40	16.130	17.320	13.784	-165.83	-87.97	.87	.29	.1563	134.63
22	6.10	14.575	13.789	14.135	-153.23	-113.90	.82	.27	.1641	128.61
23	5.82	15.898	16.228	15.818	-142.28	-139.92	.80	.26	.1719	123.36
24	5.57	18.271	21.753	24.924	-136.22	-172.83	.76	.33	.1797	118.65
25	5.33	32.301	39.037	41.908	-127.68	176.05	.78	.49	.1875	-127.80
26	5.12	52.163	53.161	48.809	-124.14	146.72	.75	.51	.1953	-133.93
27	4.92	65.249	65.657	63.615	-122.78	123.37	.68	.63	.2031	-140.82
28	4.74	59.645	62.494	59.989	-115.99	109.14	.62	.59	.2109	-143.67
29	4.57	44.391	48.438	55.116	-115.11	87.31	.56	.56	.2188	-153.00
30	4.41	29.389	36.380	37.912	-108.63	69.97	.41	.48	.2266	-159.74
31	4.27	29.948	28.834	30.406	-90.55	50.53	.33	.53	.2344	-165.20
32	4.13	21.060	23.070	23.313	-81.14	35.64	.24	.52	.2422	-173.13
33	4.00	11.375	16.799	14.583	-67.60	16.58	.14	.40	.2500	173.61
34	3.88	9.946	12.302	11.366	-42.65	-1.71	.11	.40	.2578	155.84
35	3.76	8.298	8.568	8.528	-15.78	-16.14	.11	.37	.2656	122.63
36	3.66	6.339	6.551	7.080	-3.99	-33.75	.07	.36	.2734	96.96
37	3.56	4.692	4.754	5.624	16.26	-54.40	.06	.31	.2813	75.93
38	3.46	3.307	3.238	3.618	52.75	-85.90	.04	.28	.2891	58.19
39	3.37	2.448	2.292	2.723	65.28	-107.56	.02	.33	.2969	58.58
40	3.28	1.709	1.636	1.892	21.42	-130.60	.00	.31	.3047	83.28
41	3.20	1.229	1.352	1.412	-162.27	-156.29	.02	.23	.3125	123.75
42	3.12	.983	.964	1.181	-143.70	170.26	.02	.24	.3203	-133.83
43	3.05	.740	.637	.806	-51.37	141.08	.02	.31	.3281	-107.73
44	2.98	.514	.631	.533	-21.09	122.80	.00	.26	.3359	-97.13
45	2.91	.379	.498	.347	47.82	95.87	.01	.29	.3438	-69.03
46	2.84	.275	.281	.245	18.17	74.96	.01	.20	.3516	-77.91
47	2.78	.172	.183	.186	34.84	32.95	.01	.16	.3594	-55.90

Table 2.12 TRIAD=CB1 PART=6 PASS=1 02/02/94 04:00 HRS Hmo= [.91; .94; .93] NP= 256
 SAMIN= .5 NDF=160 UNITS=1 WINDOW=4 ICOR=1 CUT= .20 TH=21.40 TL= 1.99 FOR-
 MAT=(16f5.1) FACTOR=1.0 DIST= [29.51; 26.83]

NO	PER	G1	G2	G3	PH1	PH2	COH1	COH2	FREQ	DIR
2	128.00	1.285	1.325	1.265	2.89	6.04	.87	.94	.0078	-69.65
3	64.00	2.292	2.324	2.309	-2.52	4.76	.93	.95	.0156	-117.09
4	42.67	2.132	2.089	2.115	-6.54	8.03	.87	.89	.0234	-132.37
5	32.00	1.759	1.714	1.786	-9.37	7.29	.78	.82	.0313	-151.92
6	25.60	1.413	1.543	1.599	-8.76	3.27	.61	.76	.0391	-177.64
7	21.33	1.425	1.579	1.394	1.21	3.41	.42	.71	.0469	-73.75
8	18.29	2.115	2.300	1.959	31.76	-2.95	.32	.70	.0547	-16.30
9	16.00	2.892	3.340	2.806	65.10	-8.56	.40	.67	.0625	-13.87
10	14.22	5.609	5.271	5.006	77.01	-12.71	.59	.72	.0703	-11.70
11	12.80	10.747	9.985	10.577	89.75	-20.43	.77	.75	.0781	-7.57
12	11.64	21.637	22.459	24.857	103.99	-25.84	.88	.77	.0859	-6.17
13	10.67	63.338	69.610	68.941	115.12	-27.69	.93	.81	.0938	-6.70
14	9.85	132.794	137.725	130.672	123.07	-28.48	.96	.82	.1016	-7.32
15	9.14	125.339	125.600	121.939	129.63	-31.02	.97	.76	.1094	-6.79
16	8.53	75.187	76.563	76.946	140.27	-36.13	.96	.69	.1172	-5.55
17	8.00	59.947	59.900	54.932	151.71	-42.06	.96	.66	.1250	-4.22
18	7.53	45.024	45.331	40.605	159.25	-48.46	.94	.59	.1328	-2.38
19	7.11	25.779	27.402	26.832	170.35	-58.62	.89	.37	.1406	.35
20	6.74	19.805	21.732	21.499	-175.25	-73.53	.87	.36	.1484	9999.99
21	6.40	16.130	17.320	13.784	-165.83	-87.97	.87	.29	.1563	9999.99
22	6.10	14.575	13.789	14.135	-153.23	-113.90	.82	.27	.1641	9999.99
23	5.82	15.898	16.228	15.818	-142.28	-139.92	.80	.26	.1719	9999.99
24	5.57	18.271	21.753	24.924	-136.22	-172.83	.76	.33	.1797	9999.99
25	5.33	32.301	39.037	41.908	-127.68	176.05	.78	.49	.1875	9999.99
26	5.12	52.164	53.161	48.809	-124.14	146.72	.75	.51	.1953	9999.99
27	4.92	65.249	65.657	63.615	-122.78	123.37	.68	.63	.2031	9999.99
28	4.74	59.646	62.494	59.989	-115.99	109.14	.62	.59	.2109	9999.99
29	4.57	44.391	48.438	55.117	-115.11	87.31	.56	.56	.2188	9999.99
30	4.41	29.389	36.381	37.912	-108.63	69.97	.41	.48	.2266	9999.99
31	4.27	29.948	28.834	30.406	-90.55	50.53	.33	.53	.2344	9999.99
32	4.13	21.060	23.070	23.313	-81.14	35.64	.24	.52	.2422	9999.99
33	4.00	11.375	16.800	14.583	-67.60	16.58	.14	.40	.2500	9999.99
34	3.88	9.946	12.302	11.366	-42.65	-1.71	.11	.40	.2578	9999.99
35	3.76	8.298	8.568	8.528	-15.78	-16.14	.11	.37	.2656	9999.99
36	3.66	6.339	6.552	7.080	-3.99	-33.75	.07	.36	.2734	9999.99
37	3.56	4.692	4.755	5.624	16.26	-54.40	.06	.31	.2813	9999.99
38	3.46	3.307	3.238	3.618	52.75	-85.90	.04	.28	.2891	9999.99
39	3.37	2.448	2.292	2.723	65.28	-107.56	.02	.33	.2969	9999.99
40	3.28	1.709	1.636	1.892	21.42	-130.60	.00	.31	.3047	9999.99
41	3.20	1.229	1.352	1.412	-162.27	-156.29	.02	.23	.3125	9999.99
42	3.12	.983	.964	1.181	-143.70	170.26	.02	.24	.3203	9999.99
43	3.05	.740	.637	.806	-51.37	141.08	.02	.31	.3281	9999.99
44	2.98	.514	.631	.533	-21.09	122.80	.00	.26	.3359	9999.99
45	2.91	.379	.498	.347	47.82	95.87	.01	.29	.3438	9999.99
46	2.84	.275	.281	.245	18.17	74.96	.01	.20	.3516	9999.99
47	2.78	.172	.183	.186	34.84	32.95	.01	.16	.3594	9999.99

Table 2.13 TRIAD=CB1 PART=6 PASS=2 02/02/94 04:00 HRS Hmo= [.91; .94; .93] NP= 256 SAMIN= .5 NDF=160 UNITS=1 WINDOW=4 ICOR=1 CUT= .20 TH=21.40 TL= 1.99 FOR-MAT=(16f5.1) FACTOR=1.0 DIST= [29.51; 26.83]

NO	PER	G1	G2	G3	PH1	PH2	COH1	COH2	FREQ	DIR	QH1	QH2
2	128.00	1.285	1.325	1.265	2.89	6.04	.87	.94	.0078	-69.65	2.89	6.04
3	64.00	2.292	2.324	2.309	-2.52	4.76	.93	.95	.0156	-117.09	-2.52	4.76
4	42.67	2.132	2.089	2.115	-6.54	8.03	.87	.89	.0234	-132.37	-6.54	8.03
5	32.00	1.759	1.714	1.786	-9.37	7.29	.78	.82	.0313	-151.92	-9.37	7.29
6	25.60	1.413	1.543	1.599	-8.76	3.27	.61	.76	.0391	-177.64	-8.76	3.27
7	21.33	1.425	1.579	1.394	1.21	3.41	.42	.71	.0469	-73.75	1.21	3.41
8	18.29	2.115	2.300	1.959	31.76	-2.95	.32	.70	.0547	-16.30	31.76	-2.95
9	16.00	2.892	3.340	2.806	65.10	-8.56	.40	.67	.0625	-13.87	65.10	-8.56
10	14.22	5.609	5.271	5.006	77.01	-12.71	.59	.72	.0703	-11.70	77.01	-12.71
11	12.80	10.747	9.985	10.577	89.75	-20.43	.77	.75	.0781	-7.57	89.75	-20.43
12	11.64	21.637	22.459	24.857	103.99	-25.84	.88	.77	.0859	-6.17	103.99	-25.84
13	10.67	63.338	69.610	68.941	115.12	-27.69	.93	.81	.0938	-6.70	115.12	-27.69
14	9.85	132.794	137.725	130.672	123.07	-28.48	.96	.82	.1016	-7.32	123.07	-28.48
15	9.14	125.339	125.600	121.939	129.63	-31.02	.97	.76	.1094	-6.79	129.63	-31.02
16	8.53	75.187	76.563	76.946	140.27	-36.13	.96	.69	.1172	-5.55	140.27	-36.13
17	8.00	59.947	59.900	54.932	151.71	-42.06	.96	.66	.1250	-4.22	151.71	-42.06
18	7.53	45.024	45.331	40.605	159.25	-48.46	.94	.59	.1328	-2.38	159.25	-48.46
19	7.11	25.779	27.402	26.832	170.35	-58.62	.89	.37	.1406	-.35	170.35	-58.62
20	6.74	19.805	21.732	21.499	-175.25	-73.53	.87	.36	.1484	4.05	184.75	-73.53
21	6.40	16.130	17.320	13.784	-165.83	-87.97	.87	.29	.1563	7.81	194.17	-87.97
22	6.10	14.575	13.789	14.135	-153.23	-113.90	.82	.27	.1641	14.33	206.77	-113.90
23	5.82	15.898	16.228	15.818	-142.28	-139.92	.80	.26	.1719	20.17	217.72	-139.92
24	5.57	18.271	21.753	24.924	-136.22	-172.83	.76	.33	.1797	27.76	223.78	-172.83
25	5.33	32.301	39.037	41.908	-127.68	176.05	.78	.49	.1875	28.83	232.32	-183.95
26	5.12	52.164	53.161	48.809	-124.14	146.72	.75	.51	.1953	34.60	235.86	-213.28
27	4.92	65.249	65.657	63.615	-122.78	123.37	.68	.63	.2031	38.87	237.22	-236.63
28	4.74	59.646	62.494	59.989	-115.99	109.14	.62	.59	.2109	40.17	244.01	-250.86
29	4.57	44.391	48.438	55.117	-115.11	87.31	.56	.56	.2188	43.58	244.89	-272.69
30	4.41	29.389	36.381	37.912	-108.63	69.97	.41	.48	.2266	45.07	251.37	-290.03
31	4.27	29.948	28.834	30.406	-90.55	50.53	.33	.53	.2344	44.88	269.45	-309.47
32	4.13	21.060	23.070	23.313	-81.14	35.64	.24	.52	.2422	45.41	278.86	-324.36
33	4.00	11.375	16.800	14.583	-67.60	16.58	.14	.40	.2500	45.81	292.40	-343.42
34	3.88	9.946	12.302	11.366	-42.65	-1.71	.11	.40	.2578	44.56	317.35	-361.71
35	3.76	8.298	8.568	8.528	-15.78	-16.14	.11	.37	.2656	42.78	344.22	-376.14
36	3.66	6.339	6.552	7.080	-3.99	-33.75	.07	.36	.2734	43.30	356.01	-393.75
37	3.56	4.692	4.755	5.624	16.26	-54.40	.06	.31	.2813	43.12	376.26	-414.40
38	3.46	3.307	3.238	3.618	52.75	-85.90	.04	.28	.2891	9999.99	9999.99	-445.90
39	3.37	2.448	2.292	2.723	65.28	-107.56	.02	.33	.2969	9999.99	9999.99	-467.56
40	3.28	1.709	1.636	1.892	21.42	-130.60	.00	.31	.3047	9999.99	9999.99	-490.60
41	3.20	1.229	1.352	1.412	-162.27	-156.29	.02	.23	.3125	9999.99	9999.99	-516.29
42	3.12	.983	.964	1.181	-143.70	170.26	.02	.24	.3203	9999.99	9999.99	-549.74
43	3.05	.740	.637	.806	-51.37	141.08	.02	.31	.3281	9999.99	9999.99	-578.92
44	2.98	.514	.631	.533	-21.09	122.80	.00	.26	.3359	9999.99	9999.99	-597.20
45	2.91	.379	.498	.347	47.82	95.87	.01	.29	.3438	9999.99	9999.99	-624.13
46	2.84	.275	.281	.245	18.17	74.96	.01	.20	.3516	9999.99	9999.99	-645.04
47	2.78	.172	.183	.186	34.84	32.95	.01	.16	.3594	9999.99	9999.99	-687.05

Table 2.14 TABLE : LINEAR ARRAY - 10 REDUNDANT ESTIMATES OF THE WAVE DIRECTIONAL SPECTRUM PART=6 PASS=2 06/02/94 01:00 HOURS Hmo= .29 m (Hmo and spectral energy are for gauge 4) NP= 256 SAMIN= .5 NDF=160 UNITS=1 WINDOW=4 ICOR=1 CUT=.20 TH=21.40 TL=1.99 FORMAT=(8f5.1) FACTOR=1.0

NO	Period (sec)	Energy (cm**2)	DIRECTION (degrees) for 10 different gauge pairs										Mean dir	Std dev
			43	21	32	42	65	78	89	31	01	54		
2	128.00	.676	-30.94	-29.91	-28.95	-29.17	-26.82	-27.07	-23.01	-29.16	-1.30	-25.79	-25.28	8.27
3	64.00	1.181	-25.24	-19.62	-12.00	-15.46	-15.85	-14.45	-15.30	-14.80	3.89	-15.12	-14.42	7.00
4	42.67	1.233	-19.52	-12.87	-7.37	-10.51	-11.13	-11.53	-12.86	-9.38	10.45	-11.35	-9.64	7.33
5	32.00	.571	-18.93	-12.39	-6.65	-9.97	-9.74	-8.96	-12.22	-8.99	11.83	-12.24	-8.86	7.56
6	25.60	.357	-18.83	-18.97	-11.42	-13.58	-9.48	-9.13	-13.32	-14.62	-.10	-14.67	-12.42	5.18
7	21.33	.445	-17.33	-13.56	-12.06	-13.38	-7.68	-12.53	-14.33	-13.06	-2.39	-11.21	-11.76	3.88
8	18.29	.703	-13.09	-12.85	-11.94	-12.37	-8.68	-11.13	-11.22	-12.93	-2.70	-11.50	-10.84	2.98
9	16.00	1.255	-11.79	-13.49	-10.68	-11.21	-8.27	-10.76	-10.54	-12.41	-5.79	-10.75	-10.57	2.05
10	14.22	2.185	-10.89	-11.92	-9.67	-10.26	-11.49	-9.44	-12.78	-11.17	-5.21	-12.95	-10.58	2.11
11	12.80	3.228	-10.64	-11.29	-9.75	-10.19	-14.65	-10.57	-16.74	-10.80	-4.84	-14.55	-11.40	3.13
12	11.64	3.424	-10.60	-10.96	-10.37	-10.71	-15.55	-13.58	-20.32	-10.98	-6.73	-15.34	-12.51	3.59
13	10.67	4.358	-16.16	-16.96	-16.57	-17.25	-20.44	-20.42	-26.40	-17.83	-11.62	-21.38	-18.50	3.73
14	9.85	6.947	-20.79	-24.33	-22.73	-22.91	-23.23	-25.07	-27.85	-24.64	-19.04	-25.95	-23.65	2.40
15	9.14	8.933	-23.65	-25.97	-24.85	-25.01	-26.34	-29.96	-29.80	-26.10	-21.41	-30.67	-26.38	2.82
16	8.53	8.211	-25.44	-24.66	-25.86	-26.75	-28.45	-30.30	-31.97	-26.84	-19.32	-32.37	-27.20	3.67
17	8.00	8.363	-23.99	-24.04	-25.77	-27.57	-31.80	-31.27	-35.19	-28.83	-18.40	-35.27	-28.21	5.09
18	7.53	8.821	-27.91	-29.77	-29.71	-31.19	-34.50	-35.35	-37.39	-33.47	-25.11	-38.87	-32.33	4.12
19	7.11	10.325	-31.91	-37.50	-35.44	-35.42	-37.03	-37.89	-40.30	-37.99	-34.42	-40.19	-36.81	2.45
20	6.74	9.534	-32.86	-39.55	-36.07	-35.79	-37.96	-38.50	-39.82	-38.49	-35.55	-40.80	-37.54	2.30
21	6.40	6.764	-34.28	-41.78	-37.11	-37.19	-39.50	-40.63	-41.15	-40.30	-37.42	-42.30	-39.16	2.43
22	6.10	4.623	-36.20	-38.72	-37.93	-39.25	-41.06	-41.02	-42.24	-40.52	-33.36	-44.46	-39.48	2.99
23	5.82	3.635	-33.88	-35.20	-37.02	-40.49	-41.78	-43.55	-42.48	-40.53	-28.32	-44.31	-38.76	4.81
24	5.57	2.649	-29.18	-35.48	-33.71	-38.42	-39.55	-46.42	-40.50	-39.97	-29.00	-40.15	-37.24	5.16
25	5.33	1.858	-28.85	-36.10	-34.69	-37.77	-38.33	-41.51	-39.26	-38.30	-30.87	-39.58	-36.53	3.80
26	5.12	1.729	-27.70	-35.46	-36.48	-38.16	-37.46	-38.34	-38.99	-36.82	-31.16	-39.96	-36.05	3.61
27	4.92	1.364	-25.66	-34.27	-37.86	-37.69	-35.72	-37.15	-39.09	-35.23	-29.88	-40.04	-35.26	4.19
28	4.74	.935	-28.90	-39.30	-39.95	-38.95	-34.51	-38.76	-41.29	-40.03	-35.94	-41.31	-37.90	3.63
29	4.57	.631	-30.51	-42.39	-41.32	-41.00	-37.46	-41.31	9999.99	-42.82	-38.40	-42.00	-39.69	3.66
30	4.41	.449	-29.23	-39.23	-42.33	-40.50	-38.08	-41.82	9999.99	-39.59	-35.33	-42.14	-38.70	3.95
31	4.27	.316	-27.53	-42.35	-42.42	-39.18	-36.47	-41.09	9999.99	-40.98	-40.03	-43.25	-39.26	4.57

**Table 2.15 POLYGONAL ARRAY - 15 REDUNDANT ESTIMATES OF THE WAVE DIRECTIONAL SPECTRUM PART=6 PASS=2
01/02/94 01:00 HOURS Hmo=1.07 m (Hmo and spectral energy are for gauge 0) NP= 256 SAMIN= .5 NDF=160 UNITS=1 WIN-
DOW=4 ICOR=1 CUT=20 TH=21.40 TL=1.99 FORMAT=(8f5.1) FACTOR=1.0**

NO	Period (sec)	Energy (cm**2)	DIRECTION (degrees) for 15 different gauge triads															C24	Mean dir	Std dev
			012	34C	D03	D24	C1D	4C5	DOE	CB1	CB2	CB0	D04	DOC	02D	41D				
2	18.00	1.859	-109.46	-92.50	-99.80	-98.33	-100.18	-74.93	-103.11	-120.37	-122.61	-123.34	-96.94	-99.78	-105.23	-96.53	-102.40	12.30		
3	64.00	4.429	-119.10	-106.21	-119.94	-120.00	-117.92	-101.28	-120.34	-129.43	-134.05	-135.17	-119.35	-118.45	-120.11	-117.54	-118.93	9.24		
4	42.67	6.134	-129.20	-107.83	-129.23	-129.96	-128.95	-105.35	-129.39	-142.01	-150.41	-150.64	-129.05	-128.34	-129.53	-128.15	-128.31	13.21		
5	32.00	5.255	-137.09	-118.49	-137.18	-138.98	-138.76	-115.74	-137.09	-154.61	-164.18	-165.79	-137.22	-137.33	-136.78	-133.80	-133.81	14.42		
6	25.60	3.993	-132.38	-104.54	-137.19	-139.78	-133.67	-92.12	-136.86	-154.66	-167.09	-170.93	-137.39	-137.23	-136.73	-124.88	-133.81	21.37		
7	21.33	3.720	-84.39	-40.11	-57.09	-43.72	-61.42	-37.15	-69.77	-77.60	-74.94	-74.87	-45.67	-43.85	-84.88	-49.54	-60.16	15.99		
8	18.29	6.587	-12.78	-10.76	-7.57	-8.96	-13.31	-16.11	-9.87	-13.08	-15.33	-17.94	-6.39	-4.09	-18.52	-11.89	-11.40	5.35		
9	16.00	17.082	-6.94	-6.28	-5.30	-6.39	-7.64	-15.30	-5.73	-6.70	-7.53	-7.76	-4.99	-2.6	-10.23	-6.65	-6.76	2.75		
10	14.22	28.523	-5.90	-5.06	-6.23	-6.41	-5.91	-9.95	-1.46	-5.96	-7.07	-8.53	-5.79	-2.26	-10.30	-5.62	-5.21	2.42		
11	12.80	26.181	-7.80	-6.55	-8.61	-8.61	-7.38	-10.78	-1.86	-7.76	-8.79	-10.83	-8.16	-5.08	-12.50	-7.39	-6.92	2.28		
12	11.64	41.125	-10.13	-6.88	-9.25	-8.95	-8.77	-11.13	-5.59	-8.57	-8.03	-8.61	-8.62	-6.46	-11.36	-9.05	-8.39	1.51		
13	10.67	100.914	-9.17	-6.56	-8.90	-7.08	-7.28	-10.44	-6.50	-6.93	-6.14	-6.31	-8.37	-6.73	-9.72	-8.18	-7.49	1.29		
14	9.85	170.327	-7.49	-6.14	-7.56	-7.08	-6.11	-10.35	-7.35	-5.31	-4.46	-4.07	-7.22	-6.33	-8.41	-6.83	-6.44	1.49		
15	9.14	190.153	-6.70	-5.45	-6.53	-6.05	-5.06	-9.08	-7.99	-4.49	-3.53	-2.73	-6.22	-5.76	-7.54	-6.03	-5.76	1.56		
16	8.53	153.843	-5.69	-5.50	-6.31	-5.38	-4.34	-8.83	-6.93	-3.94	-3.14	-2.07	-6.13	-5.28	-6.83	-5.76	-5.74	1.58		
17	8.00	96.541	-4.30	-4.70	-5.21	-5.38	-4.34	-8.83	-5.61	-3.09	-2.46	-1.07	-5.07	-4.32	-5.99	-5.11	-4.71	1.67		
18	7.53	69.287	3.44	1.61	1.99	1.51	4.35	-1.97	1.93	6.16	5.60	7.15	2.01	2.75	1.90	3.62	2.11	2.94	2.17	
19	7.11	79.713	7.67	5.91	6.39	6.24	9.86	4.46	6.59	12.05	11.44	12.61	6.44	7.28	6.57	9.11	6.99	7.97	2.38	
20	6.74	76.729	8.81	8.78	8.68	8.81	11.56	9.07	8.32	13.97	13.86	14.89	8.79	9.32	8.27	11.92	9.46	10.30	2.22	
21	6.40	64.330	9.79	12.53	11.75	11.96	13.33	12.98	11.00	15.57	16.07	17.07	12.01	12.27	11.07	14.54	12.35	12.95	1.96	
22	6.10	57.727	11.96	14.14	13.78	13.81	14.72	15.41	13.05	16.68	18.12	18.12	14.02	14.41	13.41	15.57	13.68	14.67	1.61	
23	5.82	54.983	15.42	16.64	16.91	16.54	18.31	19.38	16.17	20.30	20.34	21.31	17.01	17.41	16.87	19.23	16.68	17.89	1.73	
24	5.57	42.309	17.31	16.64	18.68	18.04	20.57	21.71	18.18	22.63	21.93	23.08	18.60	19.03	19.20	21.24	17.72	19.64	1.99	
25	5.33	30.758	17.39	15.25	18.69	17.31	20.08	19.73	18.28	22.41	21.23	22.70	18.37	19.21	19.55	21.23	16.47	19.19	2.06	
26	5.12	28.902	19.55	17.37	19.13	18.30	21.76	21.46	18.89	24.25	22.91	24.03	18.92	19.74	19.40	24.13	18.22	20.54	2.28	
27	4.92	24.668	21.45	19.72	19.39	19.67	23.67	23.02	18.95	26.01	24.12	24.67	19.51	19.88	18.93	25.55	20.11	21.64	2.49	
28	4.74	17.462	25.82	21.11	22.18	22.11	27.97	25.30	21.75	31.11	27.96	28.34	22.17	22.71	21.16	30.56	22.37	24.84	3.41	
29	4.57	13.202	27.55	24.07	24.38	24.1	29.02	23.87	23.87	32.44	28.70	29.11	24.45	24.97	23.50	33.52	23.88	26.76	3.13	
30	4.41	9.299	25.18	24.05	25.16	24.99	29.51	27.37	24.64	32.88	27.08	27.91	24.99	25.70	25.11	37.95	23.33	27.20	3.83	
31	4.27	6.144	23.63	24.30	29.48	29.99	32.03	30.08	29.40	33.90	29.16	29.64	29.01	29.73	30.07	38.82	25.60	29.63	5.68	

Table 2.7 gives the wave directional spectrum ($PASS = 0$) for the computer simulated swell of $\approx 10s$ using gauge triad 41D. We note that the wave directions are correctly computed for the swell of $\approx 10s$ as the swell frequencies satisfy the criterion of Barber and Doyle (1956) for the gauges 41 and 4D.

In the spectrum and cross-spectrum analyses of the measured data at North Carolina we used 80 ensembles of 256 points sampled at $2Hz$, i.e. $0.5s$ sampling interval, thus yielding 160 degrees of freedom. Blackman window was used. Spectral densities were scaled up by a factor of $1/0.303$ to compensate for loss of energy due to windowing. Spectral densities were further scaled upto compensate for attenuation of wave amplitude. Attenuation correction for frequencies above $0.2Hz$ was assumed to be the same as for $0.2Hz$ to prevent amplification of noise at higher frequencies. A similar strategy was used by Fernandes et al. [1981] to correct for attenuation of waves measured with a shipborne wave recorder. For computation of significant wave height H , spectral densities corresponding to periods between 21.40 and 1.99 sec were summed up. Spectral densities are given in units of cm^2 . To convert to m^2/Hz the spectral densities must be multiplied by (0.0064). Values of coherence squared above 0.057 are significant at 0.01 significance level.

Table 2.8 gives the observed wave directional spectra ($PASS = 0$) at North Carolina for gauge pair 78 at 16 hours on 5 February 1994. We note that the gauges 78 are coherent at 0.01 significance level (coherence squared ≥ 0.057) upto spectral line No. 40 corresponding to 0.3047 Hz frequency. We note that for gauges 78 there exists a positive jump across the $-180^\circ / +180^\circ$ pseudo discontinuity at spectral line number 32. Therefore the wave directions in this $PASS=0$ Table 2.8 are correct upto spectral line number 31. Above spectral line number 31 the wave directions are incorrect and are flagged as 9999.99 in Table 2.9, which is $PASS=1$ for the same record. In the $PASS=2$ Table 2.10 for the same record wave directions are flagged as 9999.99 for spectral lines above and including number 41. Thus $PASS=2$ extends the range of frequencies over which wave directions can be correctly estimated by $PASS=1$ analysis. For the same record Figure 2.12 shows the spectral densities, coherence squared, “apparent” and “true” phase differences and wave direction estimates ($PASS=1$ and $PASS=2$), as a function of frequency. Figure 2.13 gives an example of a negative jump in case of gauge pair 65 for the record on 2 February at 13 hours.

Table 2.11 gives the observed wave directional spectra ($PASS = 0$) at North Carolina for gauge triad CB1 at 04 hours on 2 February 1994. We note that the gauges CB are coherent at 0.01 significance level (coherence squared ≥ 0.057) upto spectral line No. 37 corresponding to 0.2813 Hz frequency. Gauges C1 are coherent at 0.01 significance level upto spectral line No. 52, which is beyond range of the above table. We note that for gauges CB there exists a positive jump across the $-180^\circ / +180^\circ$ pseudo discontinuity at spectral line number 20. For gauges C1 there exist negative jumps across the $-180^\circ / +180^\circ$ pseudo discontinuity at spectral line numbers 25 and 42. Thus the lowest spectral line at which either gauges CB or C1 are incoherent or a phase

jump across the $-180^\circ / +180^\circ$ pseudo discontinuity occurs is spectral line number 20. Therefore the wave directions in this PASS=0 Table 2.11 are correct upto spectral line number 19. Above spectral line number 19 the wave directions are incorrect and are flagged as 9999.99 in Table 2.12, which is PASS=1 for the same record. The lowest spectral spectral line at which either gauges CB or C1 are incoherent is number 38. Therefore in the PASS=2 Table 2.13 for the same record wave directions are flagged as 9999.99 for spectral lines above and including number 38. Thus PASS=2 extends the range of frequencies over which wave directions can be correctly estimated by PASS=1 analysis. Figure 2.14 shows the spectral densities, coherence squared, “apparent” and “true” phase differences and wave direction estimates (PASS=1 and PASS=2), as a function of frequency. Figure 2.15 to Figure 2.18 are more examples of jumps in case of gauge triads.

As already mentioned in Chapter 2.4 10 redundant estimates of wave direction using the ‘Modified Borgman method’ (i.e. PASS=2 or “true” phase and “coherence”) for each of the 47 records of *measured* data at Duck, North Carolina, USA during 1-6 February 1994, using the following 10 gauge pairs: 43, 21, 32, 42, 65, 78, 89, 31,01 and 54, were made. Table 2.14 presents the wave direction estimates PASS=2 for each of the 10 redundant gauge pairs for central wave periods $\geq 4.27s$ – for the record on 6 February 1994 at 01 hours. The vector mean wave direction as well as the standard deviation over the 10 redundant estimates of wave direction are also given. Similar tables for each of the 47 records are given in Appendix A.

As already mentioned in Chapter 2.5 15 redundant estimates of wave direction using the ‘Modified Esteva method’ (i.e. PASS=2 or “true” phase and “coherence”) for each of the 47 records of *measured* data at Duck during 1-6 February 1994, using the following 15 gauge triads: 012, 34C, D03, D24, C1D, 4C5, D0E, CB1, CB2, CB0, D04, D0C, 02D, 41D and C24, were made. Table 2.15 presents the wave direction estimates PASS=2 for each of the 15 redundant gauge triads for central wave periods $\geq 4.27s$ – for the record on 1 February 1994 at 01 hours. The vector mean wave direction as well as the standard deviation over the 15 redundant estimates of wave direction are also given. Similar tables for each of the 47 records are given in Appendix B. For a gauge triad 123, estimates of wave direction are not available for frequencies $> f_o$, where f_o is the smallest frequency at which the coherence squared for either gauges 12 or 13 falls below the threshold of 0.057. Therefore the number of available redundant estimates of wave direction using Esteva’s method is ≤ 15 , and this number decreases with increasing frequency. Table 2.16 gives the number of redundant estimates actually available for the 47 records in case of spectral period 4.27 s. Table 2.16 shows that in case of 12 of the 47 records, all the 15 redundant estimates of wave direction were available at 4.27 s and that the number of available redundant estimates were ≥ 4 . In case of all the 47 records, all the 15 redundant estimates were available for spectral periods $\geq 8.00s$ (not shown).

Table 2.16 Number of available redundant estimates of wave direction at 4.27 s, using Esteva's method. For spectral periods > 4.27 s, the number of available redundant estimates is larger than that indicated in this table

No.	Hours	February 1994					
		1	2	3	4	5	6
1	01	14	5	7	15	8	15
2	04	13	15	7	15	14	14
3	07	13	7	7	15	15	11
4	10	–	6	5	4	15	10
5	13	12	7	14	13	15	6
6	16	14	14	15	8	15	8
7	19	11	8	15	11	9	11
8	22	8	8	15	7	8	14

Figure 2.12 Wave direction estimation using gauge pair 78 on 5 February 1994 at 16 hours using the modified Borgman method (a) Spectral densities for gauges 78 (b) Coherence squared for gauges 78 (c) Wave direction estimates (PASS=1, solid; PASS=2, dashed) (d) Phase difference for gauges 78, *apparent* phase (solid) and *true* phase (dashed)

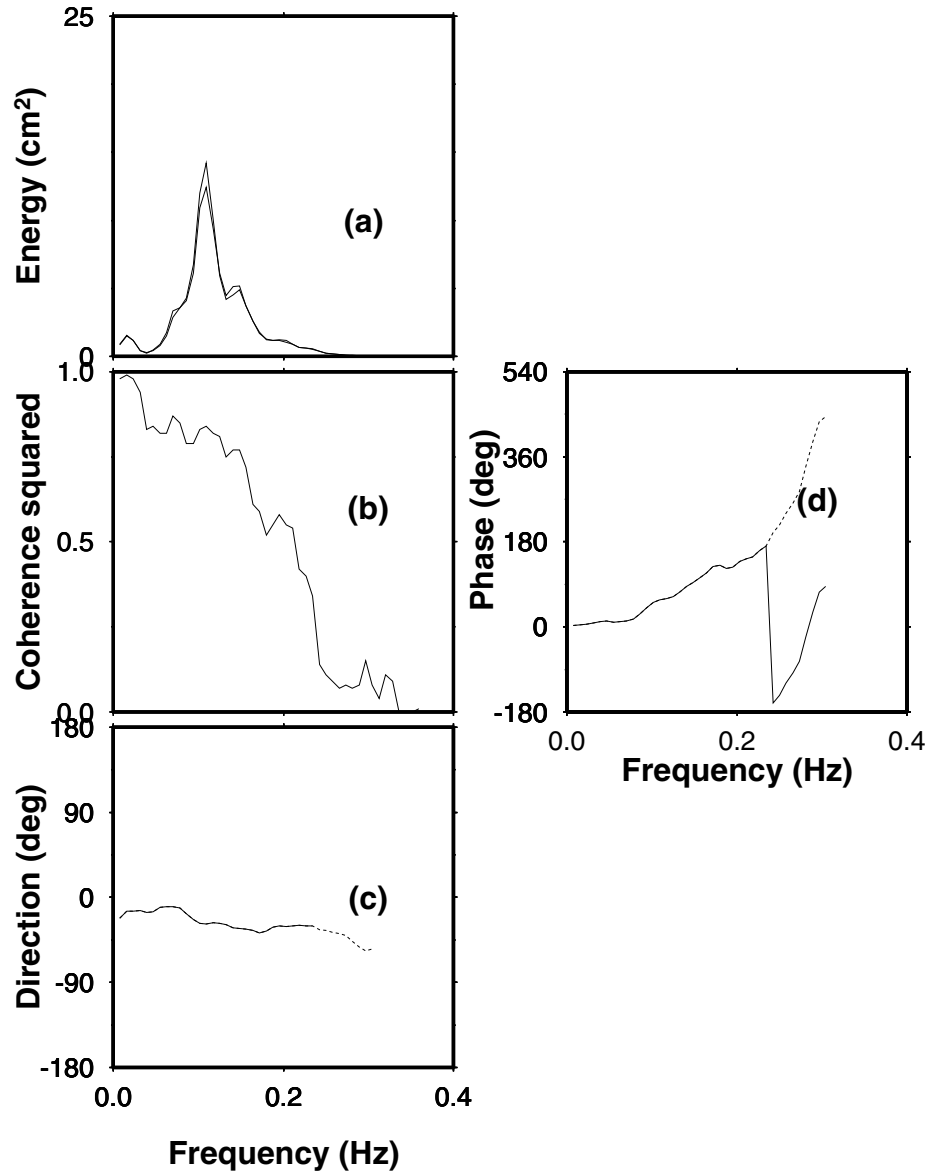


Figure 2.13 Wave direction estimation using gauge pair 65 on 2 February 1994 at 13 hours using the modified Borgman method (a) Spectral densities for gauges 65 (b) Coherence squared for gauges 65 (c) Wave direction estimates (PASS=1, solid; PASS=2, dashed) (d) Phase difference for gauges 65, *apparent* phase (solid) and *true* phase (dashed)

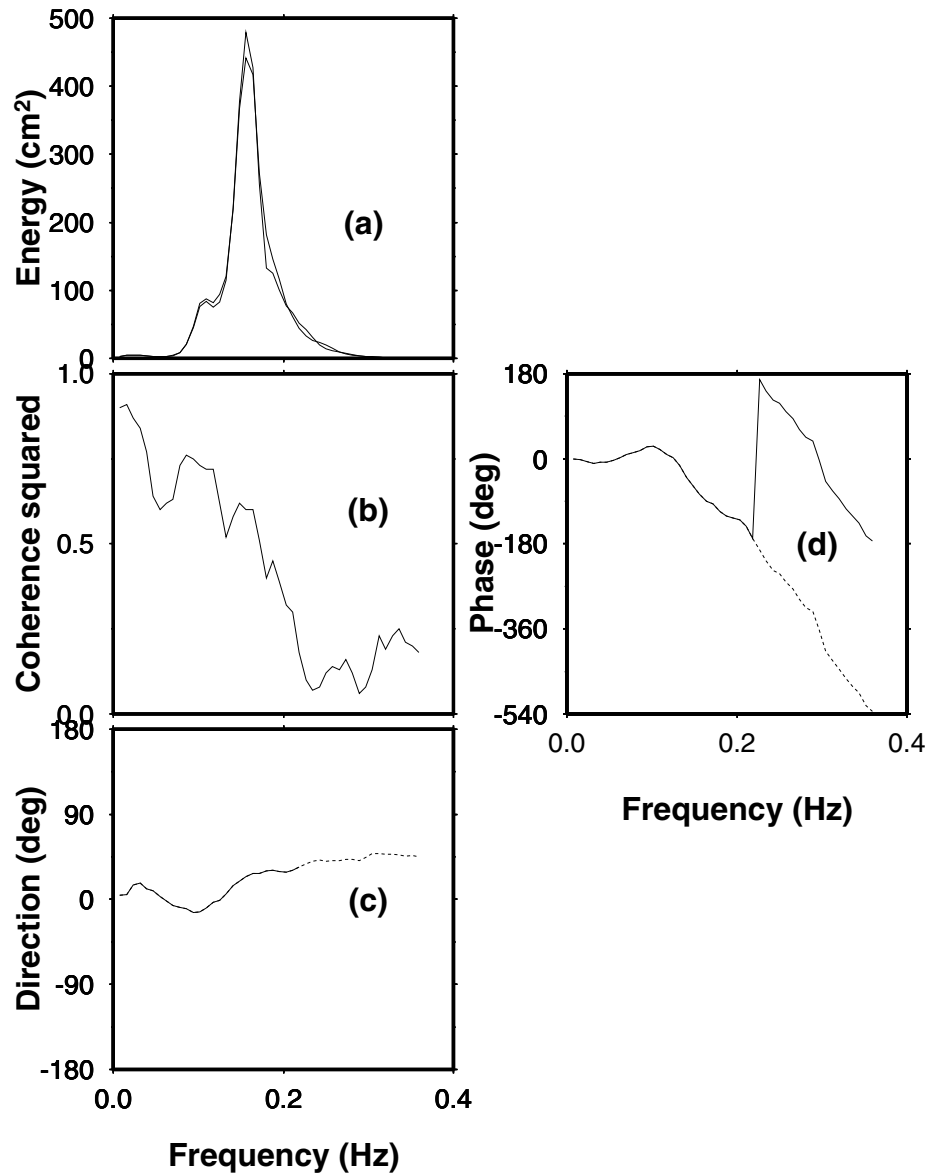


Figure 2.14 Wave direction estimation using gauge triad CB1 on 2 February 1994 at 04 hours using the method of Esteva [1977] as modified by us (a) Spectral densities for gauges CB1 (b) Coherence squared for gauges CB (solid) and gauges C1 (dashed) (c) Wave direction estimates (PASS=1, solid; PASS=2, dashed) (d) Phase difference for gauges CB, *apparent* phase (solid) and *true* phase (dashed), and (e) Phase difference for gauges C1, *apparent* phase (solid) and *true* phase (dashed)

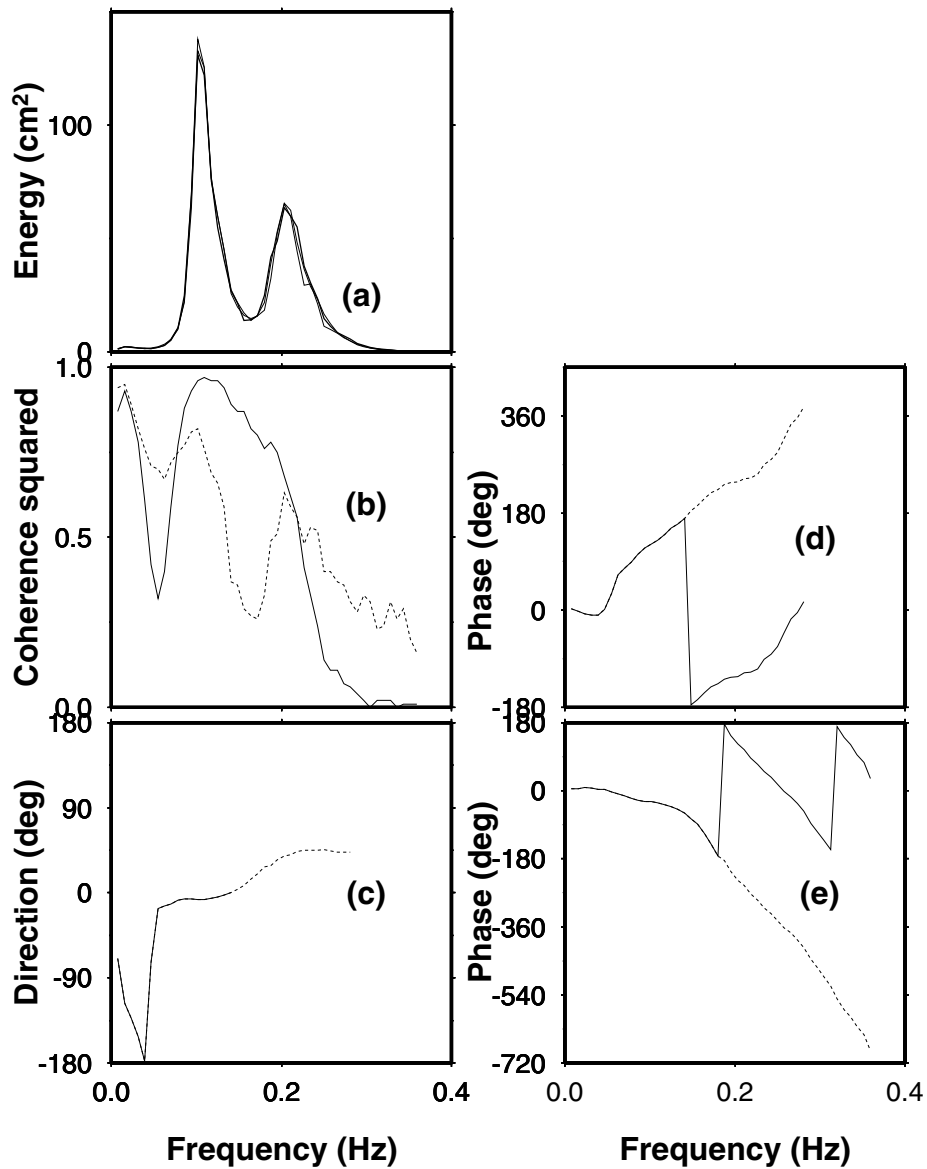


Figure 2.15 Wave direction estimation using gauge triad CB1 on 4 February at 10 hours using the method of Esteva [1977] as modified by us (a) Spectral densities for gauges CB1 (b) Coherence squared for gauges CB (solid) and gauges C1 (dashed) (c) Wave direction estimates (PASS=1, solid; PASS=2, dashed) (d) Phase difference for gauges CB, *apparent* phase (solid) and *true* phase (dashed), and (e) Phase difference for gauges C1, *apparent* phase (solid) and *true* phase (dashed)

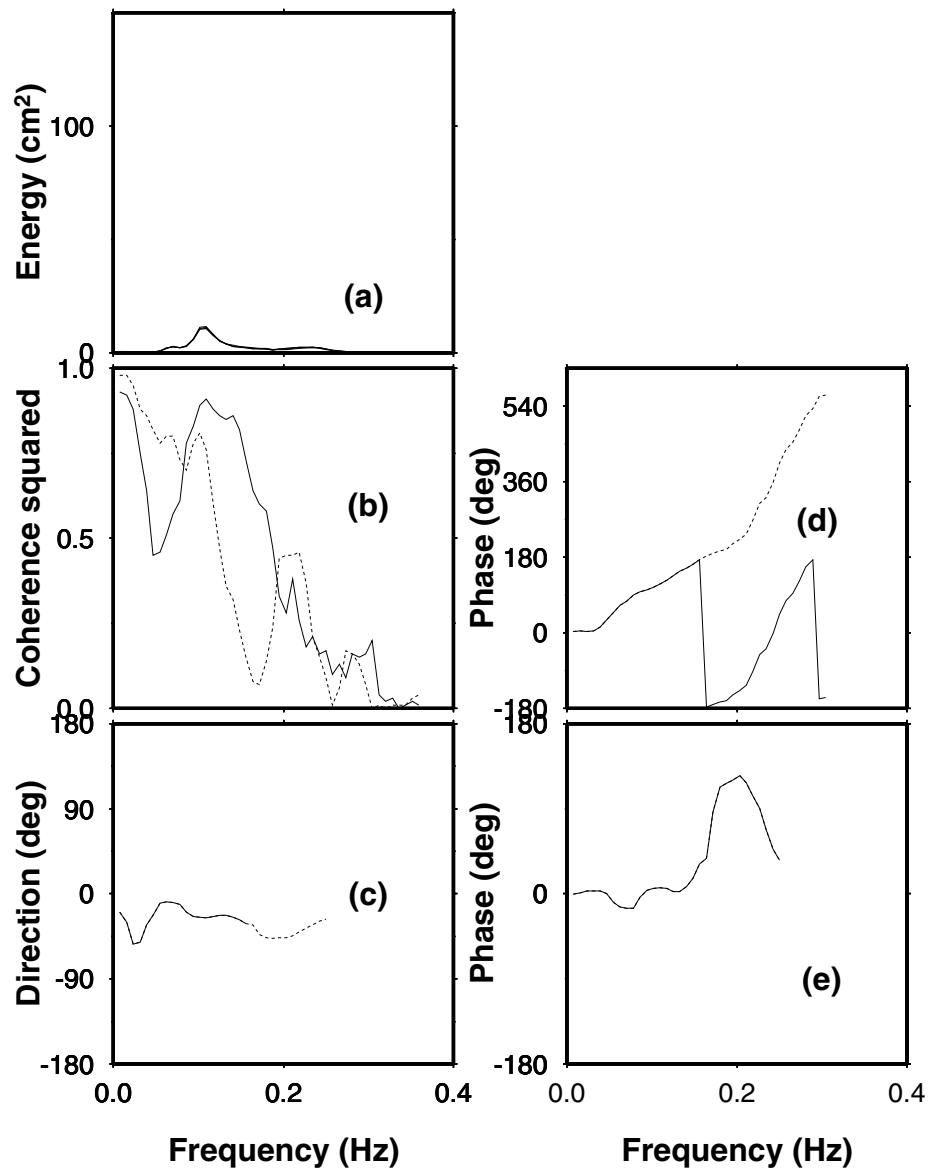


Figure 2.16 Wave direction estimation using gauge triad C1D on 2 February at 10 hours using the method of Esteva [1977] as modified by us (a) Spectral densities for gauges C1D (b) Coherence squared for gauges C1 (solid) and gauges CD (dashed) (c) Wave direction estimates (PASS=1, solid; PASS=2, dashed) (d) Phase difference for gauges C1, *apparent* phase (solid) and *true* phase (dashed), and (e) Phase difference for gauges CD, *apparent* phase (solid) and *true* phase (dashed)

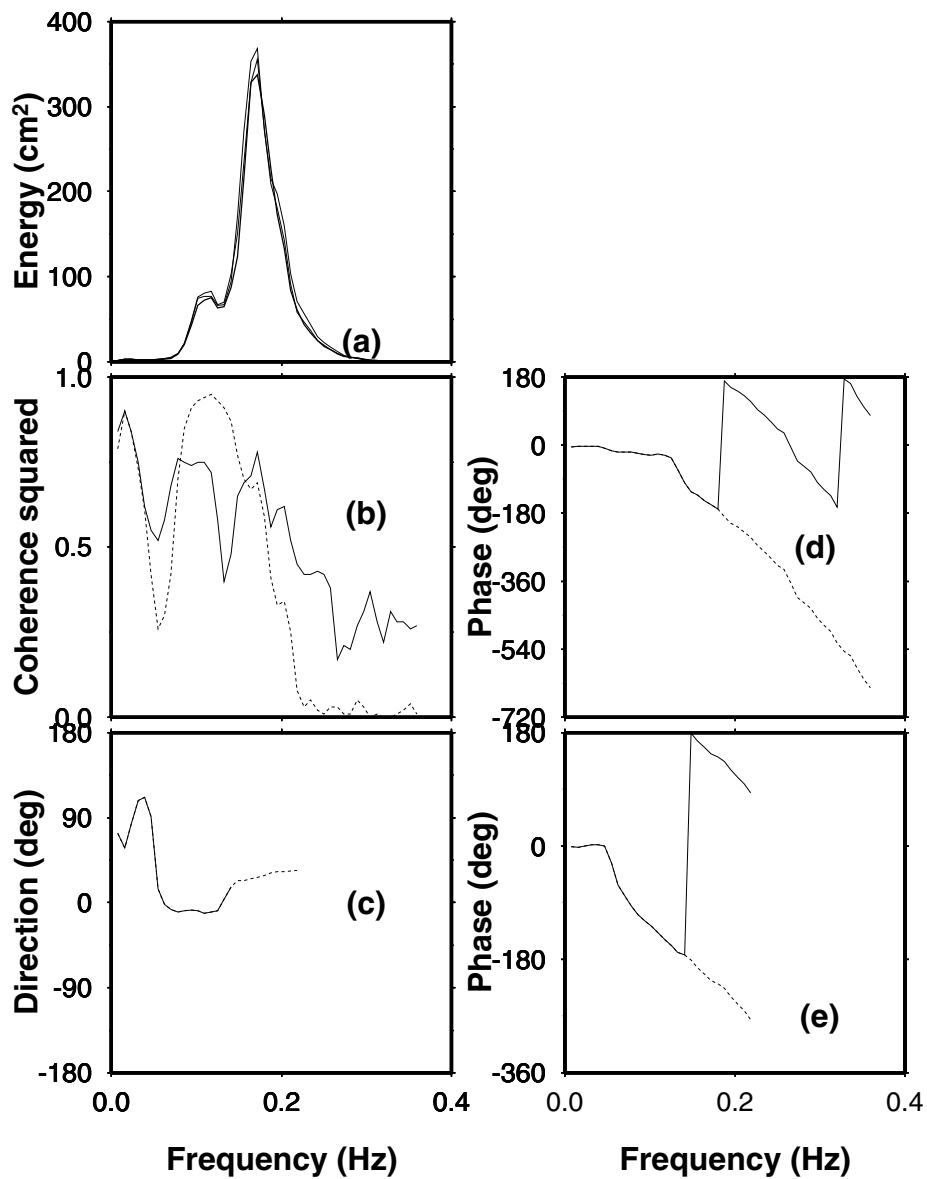


Figure 2.17 Wave direction estimation using gauge triad C1D on 1 February at 01 hours using the method of Esteva [1977] as modified by us (a) Spectral densities for gauges C1D (b) Coherence squared for gauges C1 (solid) and gauges CD (dashed) (c) Wave direction estimates (PASS=1, solid; PASS=2, dashed) (d) Phase difference for gauges C1, *apparent* phase (solid) and *true* phase (dashed), and (e) Phase difference for gauges CD, *apparent* phase (solid) and *true* phase (dashed)

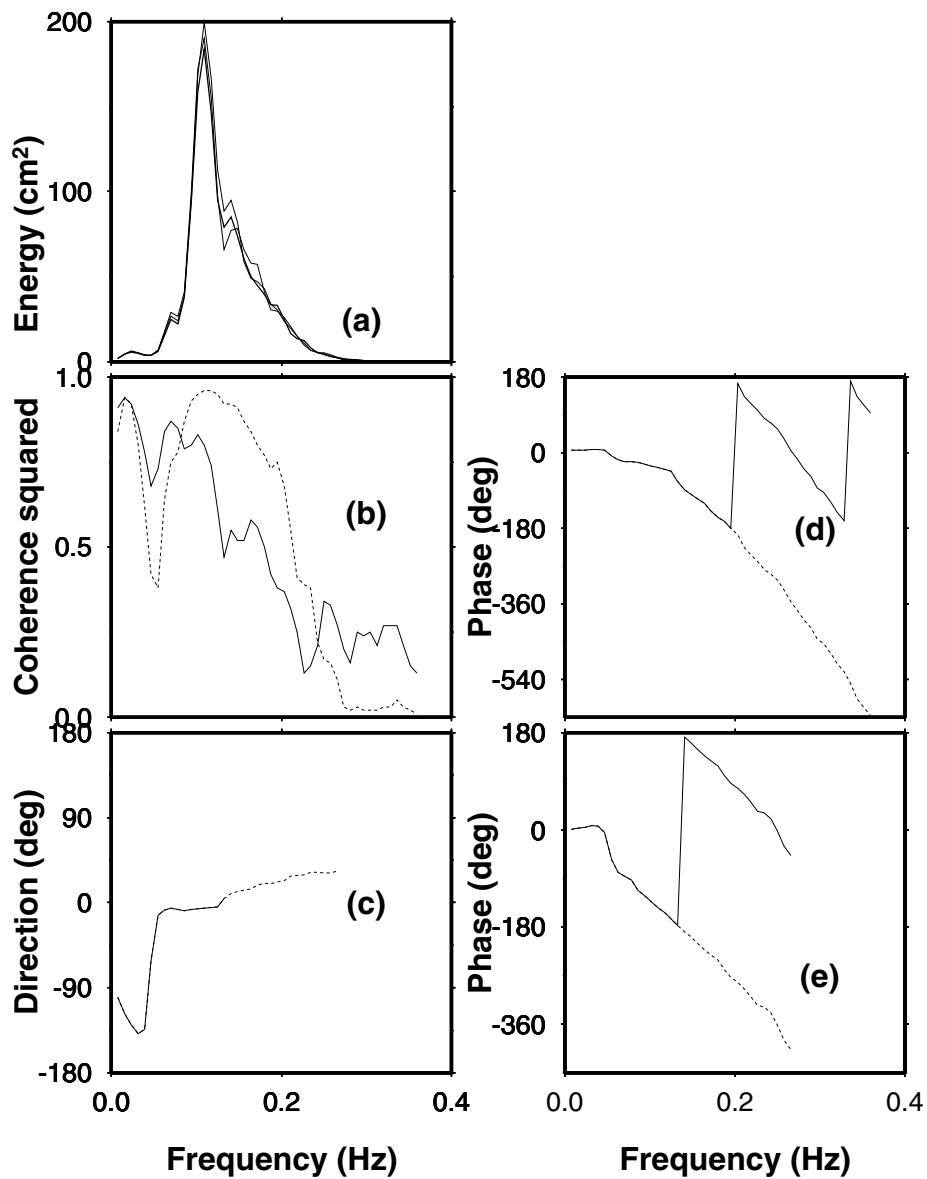


Figure 2.18 Wave direction estimation using gauge triad 012 on 5 February at 16 hours using the method of Esteva [1977] as modified by us (a) Spectral densities for gauges 012 (b) Coherence squared for gauges 01 (solid) and gauges 02 (dashed) (c) Wave direction estimates (PASS=1, solid; PASS=2, dashed) (d) Phase difference for gauges 01, *apparent* phase (solid) and *true* phase (dashed), and (e) Phase difference for gauges 02, *apparent* phase (solid) and *true* phase (dashed)

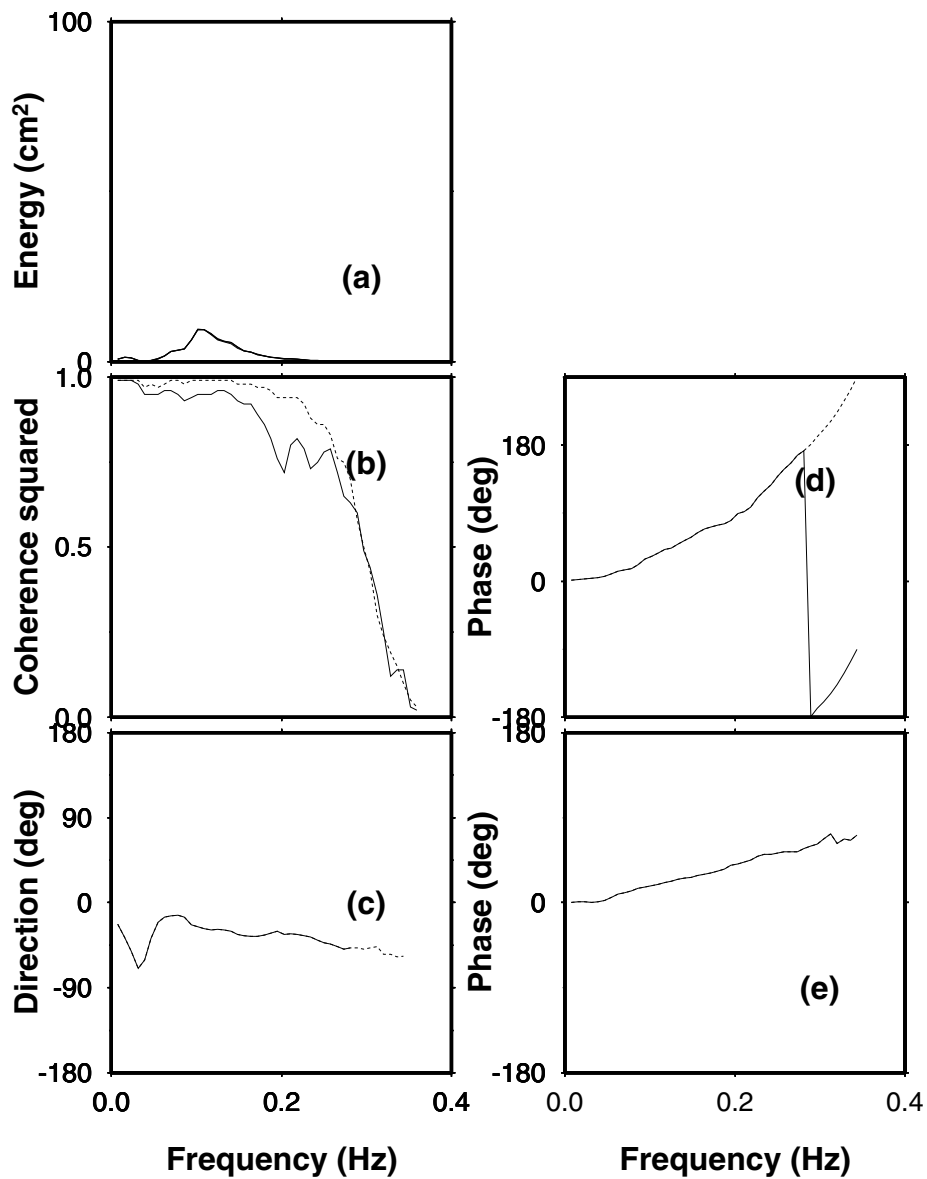


Figure 2.19 to Figure 2.24 show the spectral densities for gauge 0 on a uniform scale for the period 1-6 February 1994, one figure for each day. The wave spectra show three peaks, one centred at 64.00 or 42.67s (this peak which is due to surf beat is not perceptible in the figures); the second peak is centred at 9.85s (this peak is due to swell, i.e., waves generated by distant storms); and the third peak which is centred at 3.28s at 22 hours on 1 February and gradually shifts with increasing time to 6.40s at 13 hours on 2 February, is due to a growing sea, which subsequently decays. The trough between the peak due to surf beat and the peak due to swell generally occurs at spectral period 25.60 or 21.33s. The peaks due to surf beat, swell and sea occur at the same respective frequencies for all the 15 gauges in the array. The significant wave heights for each record measured using the 15 wave gauges (gauge A was not analyzed as it, unfortunately was not part of any of the 15 redundant gauge triads or 10 redundant gauge pairs!) differed by $\pm 0.01m$. On 1 February 1994, energetic swell of $\approx 10s$ period is present.

Figure 2.25 to Figure 2.30 based on tables in Appendix A and Appendix B gives the mean wave direction (PASS=2) as a function of frequency by considering a maximum of 15 gauge triads and a maximum of 10 gauge pairs, one figure for each day. It may be noted that the mean wave direction computed by using linear (Borgman's 2-gauge) arrays and polygonal (Esteva's 3-gauge) arrays are nearly identical for central wave periods $\leq 14.22s$, as by providence the waves for these wave periods are directed *towards* shore, even when the wind is directed away from the shore (as we shall shortly see), so that there is no ambiguity in the Borgman determination. We found from the analysis of all the 47 records, that the difference between the mean of 10 redundant estimates using Borgman's method and the 15 redundant estimates using Esteva's method, had a mean of 0.33° and a standard deviation of 2.89° for spectral periods between $14.22 - 4.27s$ ($47 * 22 = 1034$ points). On 1 February 1994, when energetic swell propagating up the coast, towards the shore is present, surf beat is locally generated and travels up the coast, away from the shore, so that surf beat directions reported by linear arrays are incorrect.

During 4-6 February 1994, when low wave conditions occur (significant wave height, $H_{1/10} < 0.41m$), the surf beat propagates up the coast, towards shore, i.e., is of remote origin, so that surf beat directions estimated by linear arrays and polygonal arrays should be identical – Figure 2.28 to Figure 2.30 show that the direction estimates of surf beat using the 'Modified Borgman Method' are closer to the shore normal than the estimates obtained using the 'Modified Esteva Method' by about 25° . However experiments with computer simulated wave trains with surf beat direction -75° with respect to the shore normal showed that both the Esteva and Borgman determinations yielded correct and accurate surf beat directions. The large departure in case of the observed data is probably due to the fact that both the gauge triads as well as the gauge pairs with small gauge separations (distances) have been selected, i.e., the analysis scheme is tuned to study *wind* wave directionality. It is worth mentioning that initially, we analyzed only nine records, viz., the eight

Figure 2.19 Spectral density for gauge 0 on 1 February 1994 at 01, 04, 07, 10, 13, 16, 19 and 22 hours. Record for 10 hours was not available. The values in metres represent the significant wave height, H_{mo}

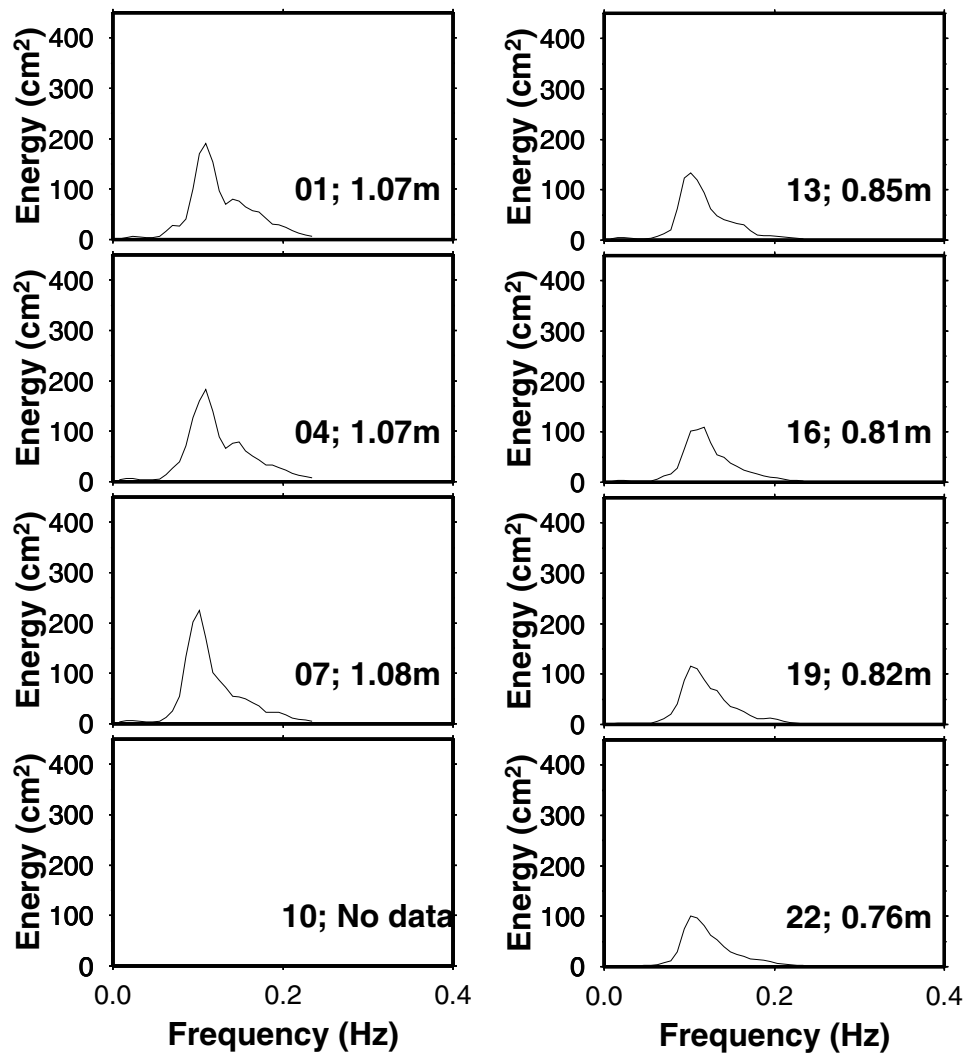


Figure 2.20 Spectral density for gauge 0 on 2 February 1994 at 01, 04, 07, 10, 13, 16, 19 and 22 hours. The values in metres represent the significant wave height, H_{m0}

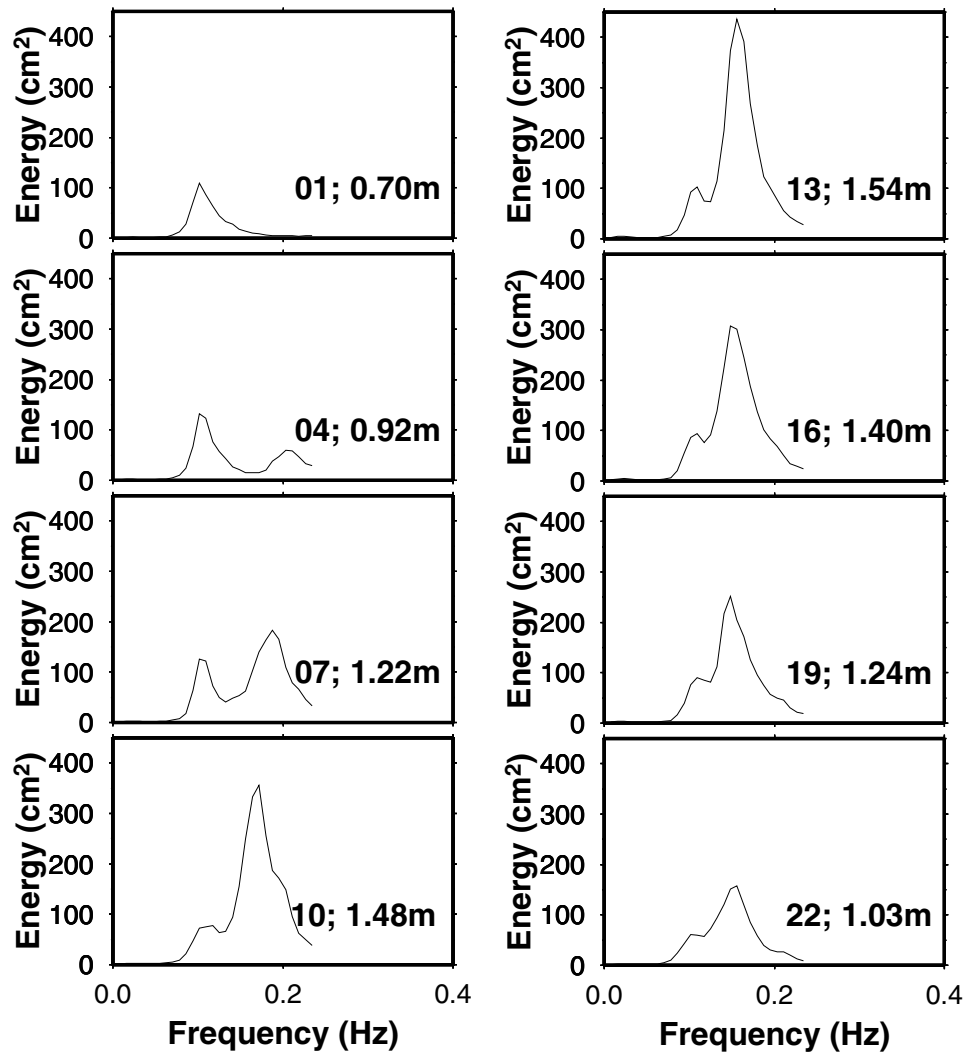


Figure 2.21 Spectral density for gauge 0 on 3 February 1994 at 01, 04, 07, 10, 13, 16, 19 and 22 hours. The values in metres represent the significant wave height, H_{m0}

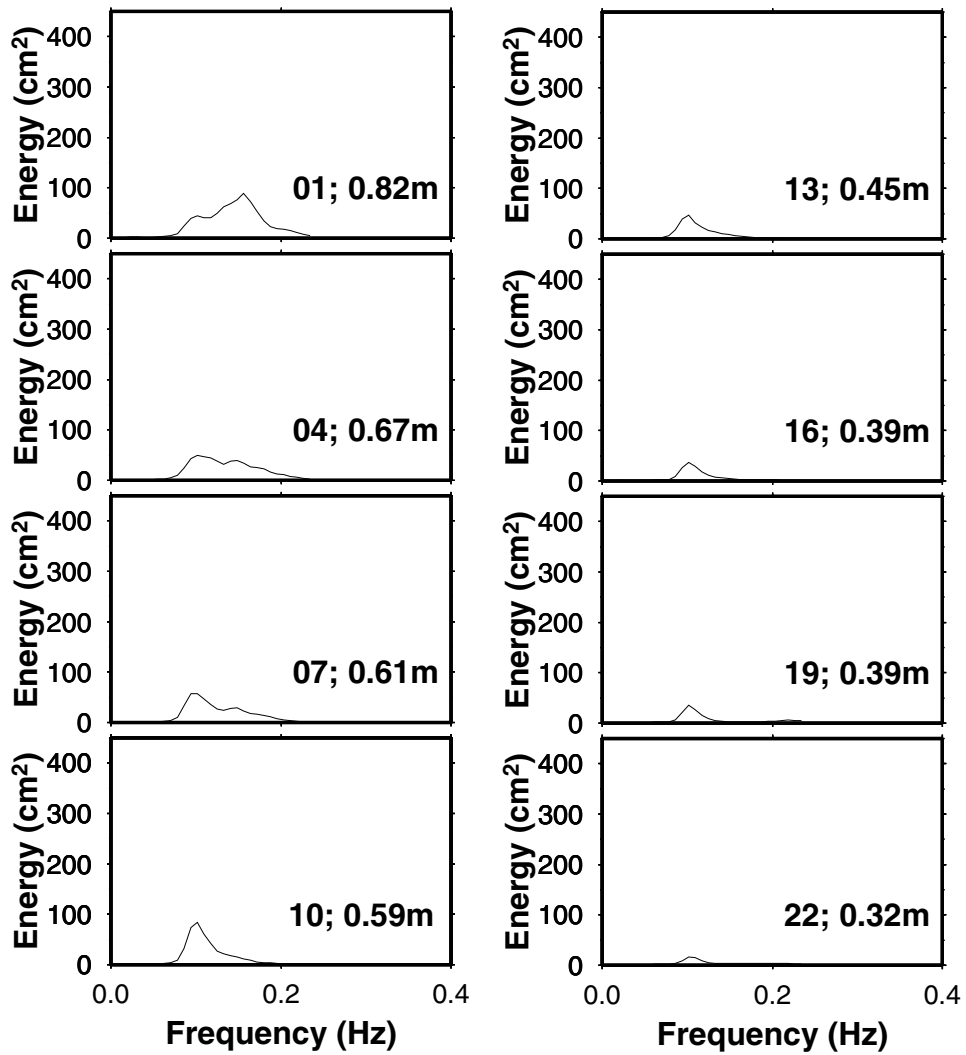


Figure 2.22 Spectral density for gauge 0 on 4 February 1994 at 01, 04, 07, 10, 13, 16, 19 and 22 hours. The values in metres represent the significant wave height, H_{m0}

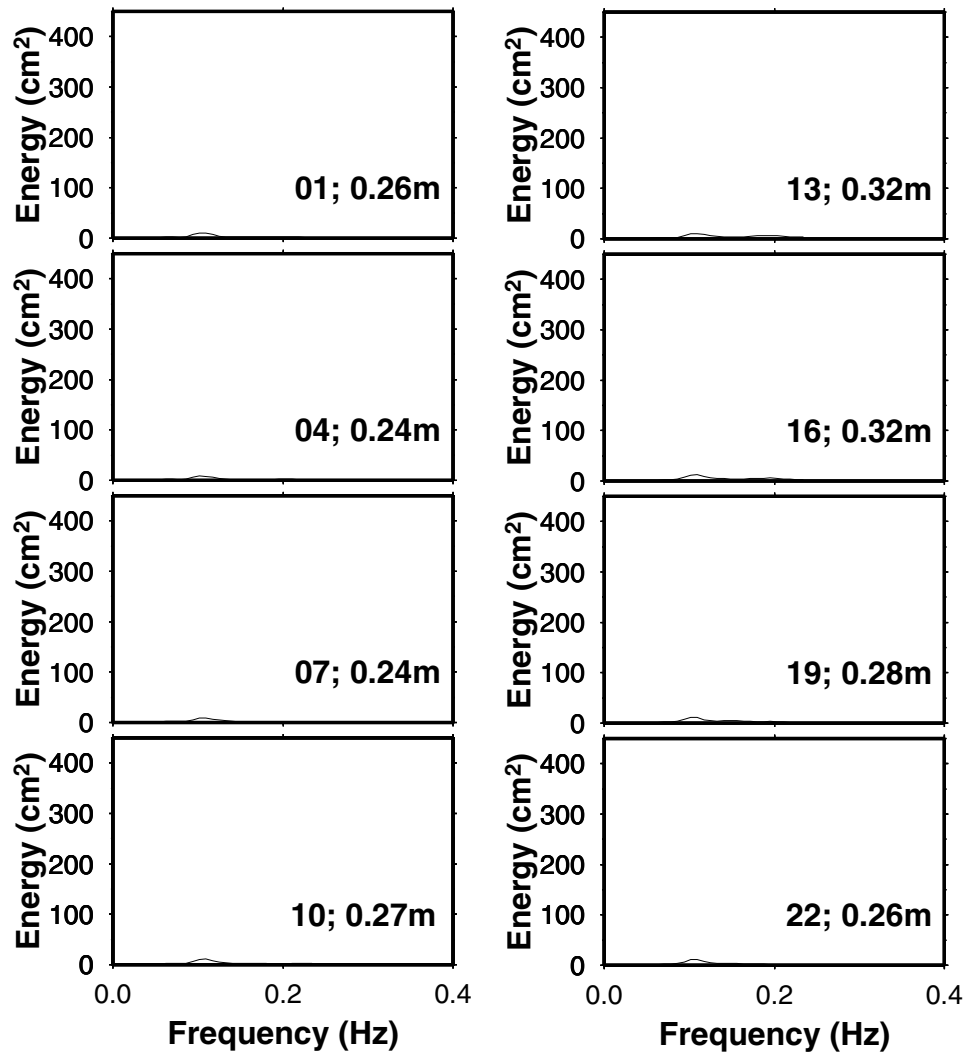


Figure 2.23 Spectral density for gauge 0 on 5 February 1994 at 01, 04, 07, 10, 13, 16, 19 and 22 hours. The values in metres represent the significant wave height, H_{m0}

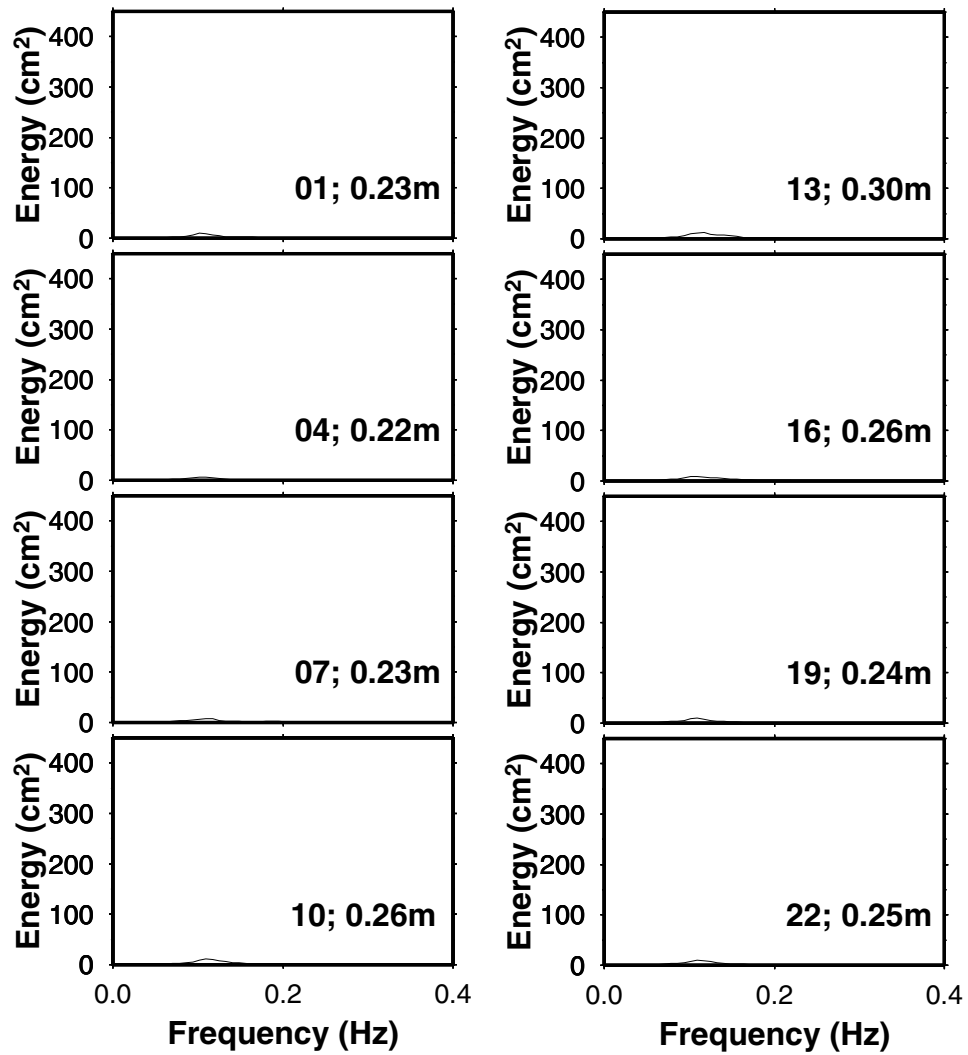


Figure 2.24 Spectral density for gauge 0 on 6 February 1994 at 01, 04, 07, 10, 13, 16, 19 and 22 hours. The values in metres represent the significant wave height, H_{m0}

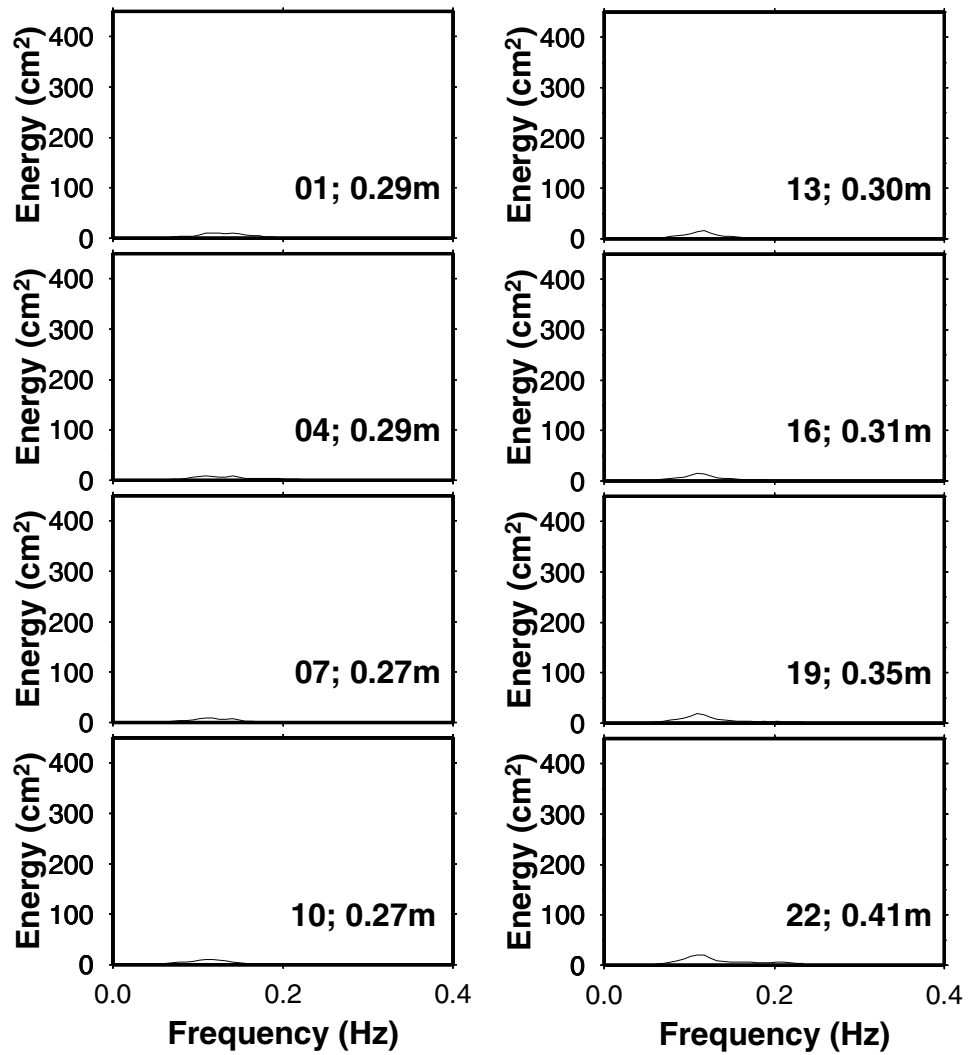


Figure 2.25 Mean of maximum 15 redundant gauge triad wave direction estimates (solid), and mean of maximum of 10 redundant gauge pair wave direction estimates (dashed); determined using *true* phase, i.e. PASS=2, on 1 February 1994

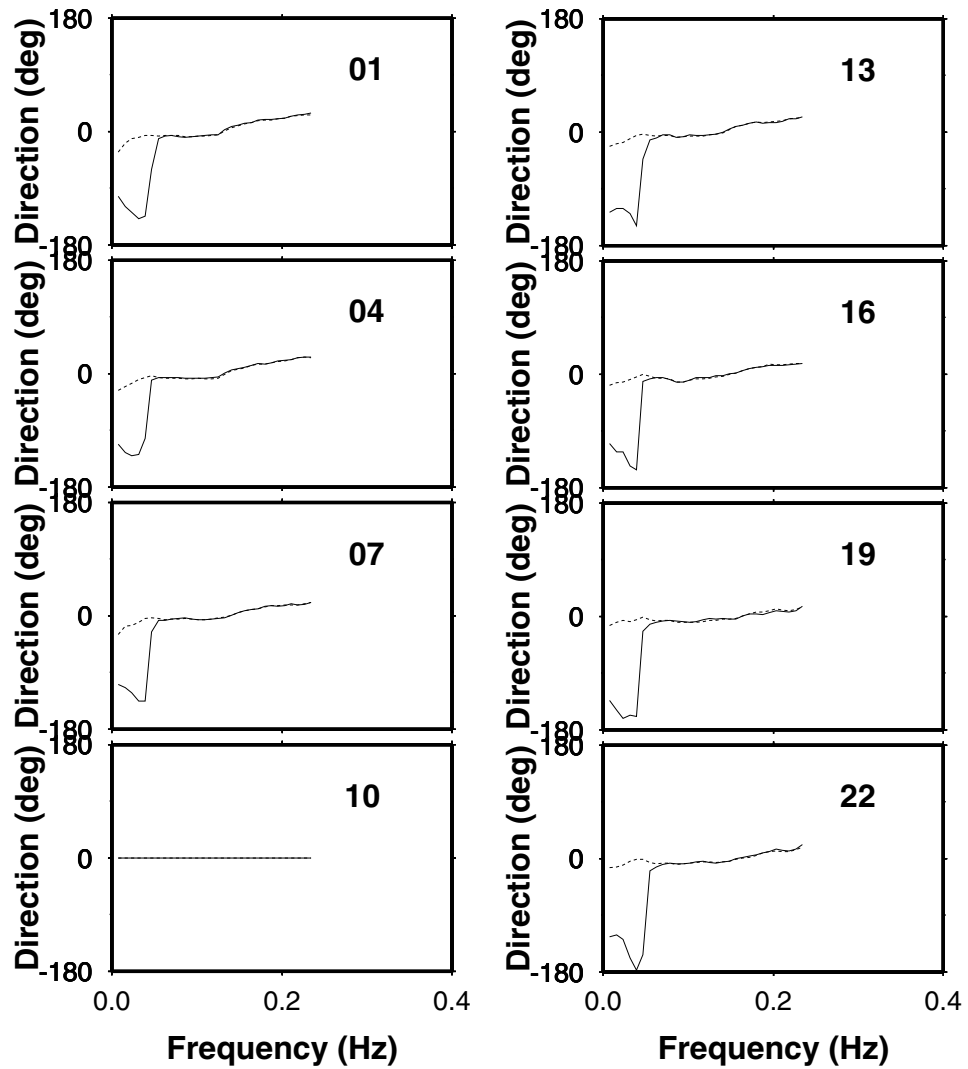


Figure 2.26 Mean of maximum 15 redundant gauge triad wave direction estimates (solid), and mean of maximum of 10 redundant gauge pair wave direction estimates (dashed); determined using *true* phase, i.e. PASS=2, on 2 February 1994

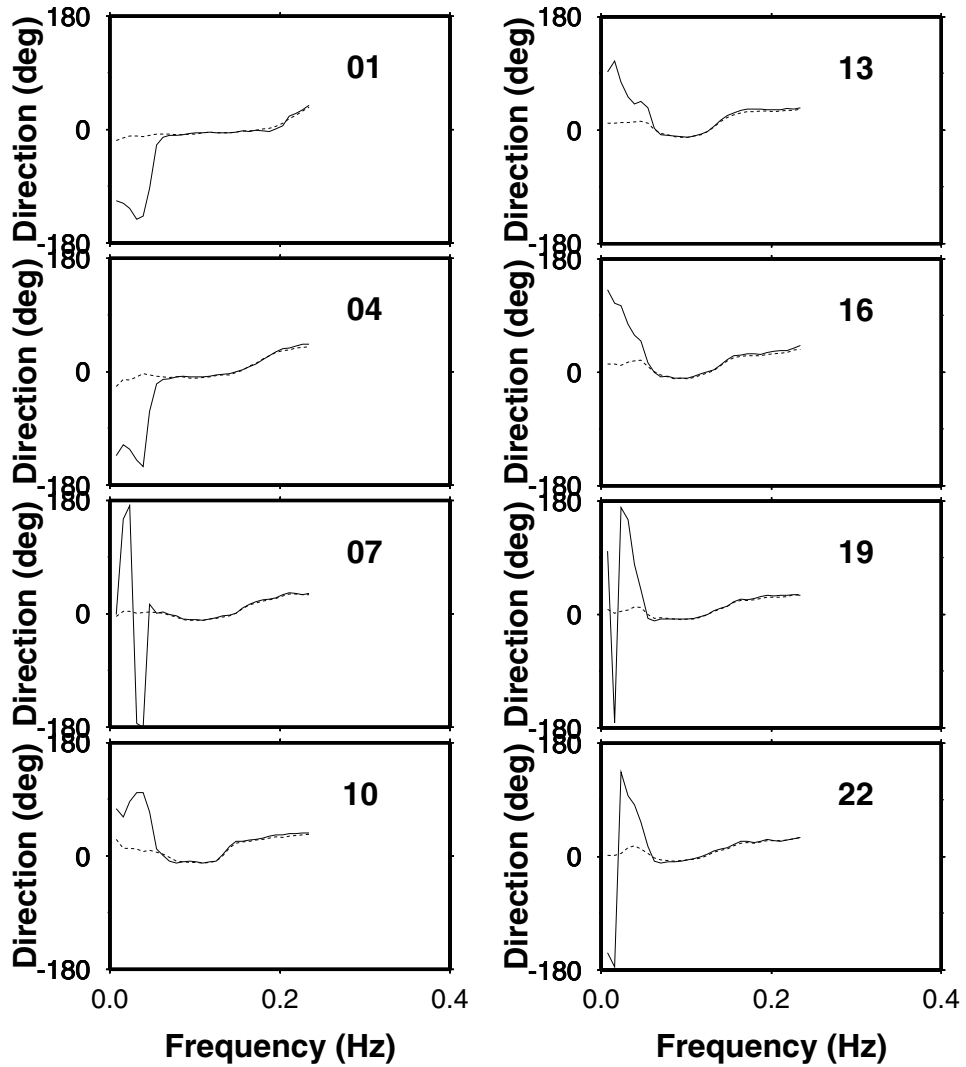


Figure 2.27 Mean of maximum 15 redundant gauge triad wave direction estimates (solid), and mean of maximum of 10 redundant gauge pair wave direction estimates (dashed); determined using *true* phase, i.e. PASS=2, on 3 February 1994

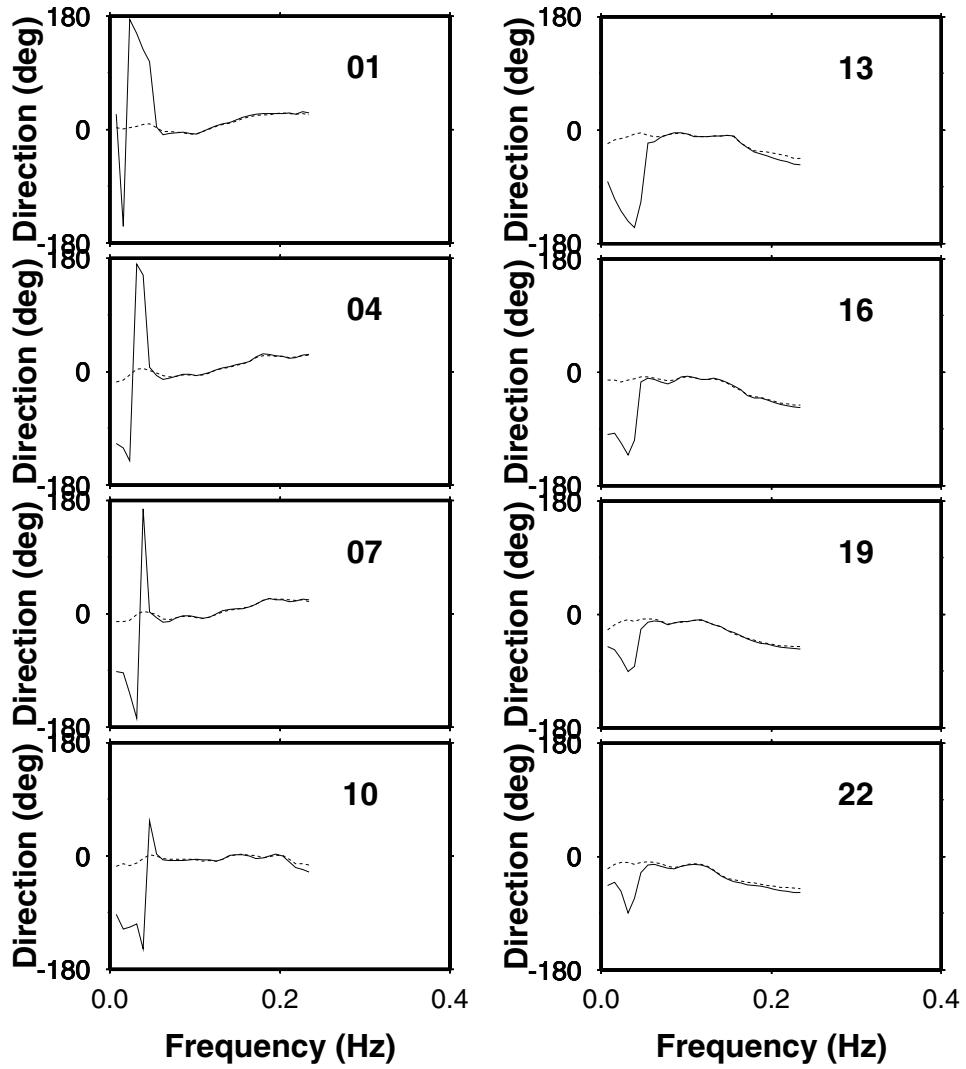


Figure 2.28 Mean of maximum 15 redundant gauge triad wave direction estimates (solid), and mean of maximum of 10 redundant gauge pair wave direction estimates (dashed); determined using *true* phase, i.e. PASS=2, on 4 February 1994

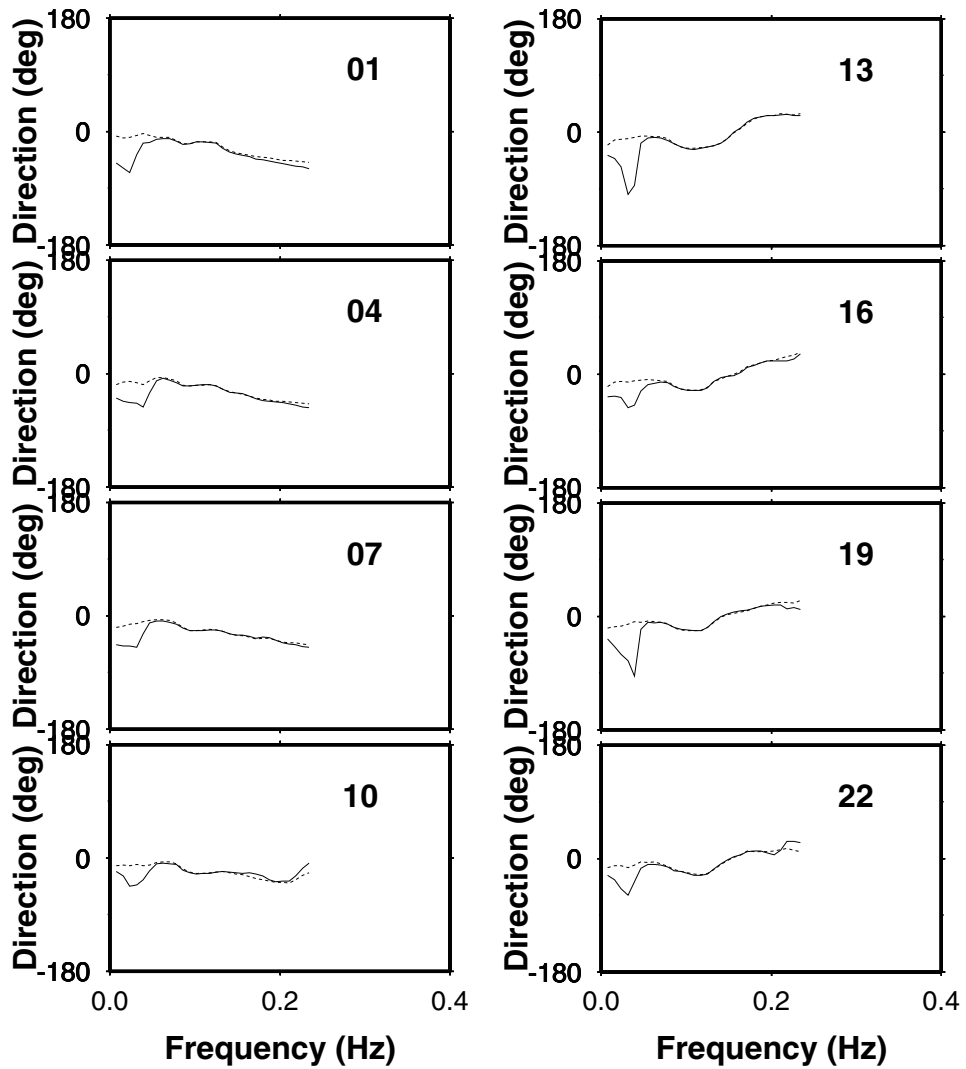


Figure 2.29 Mean of maximum 15 redundant gauge triad wave direction estimates (solid), and mean of maximum of 10 redundant gauge pair wave direction estimates (dashed); determined using *true* phase, i.e. PASS=2, on 5 February 1994

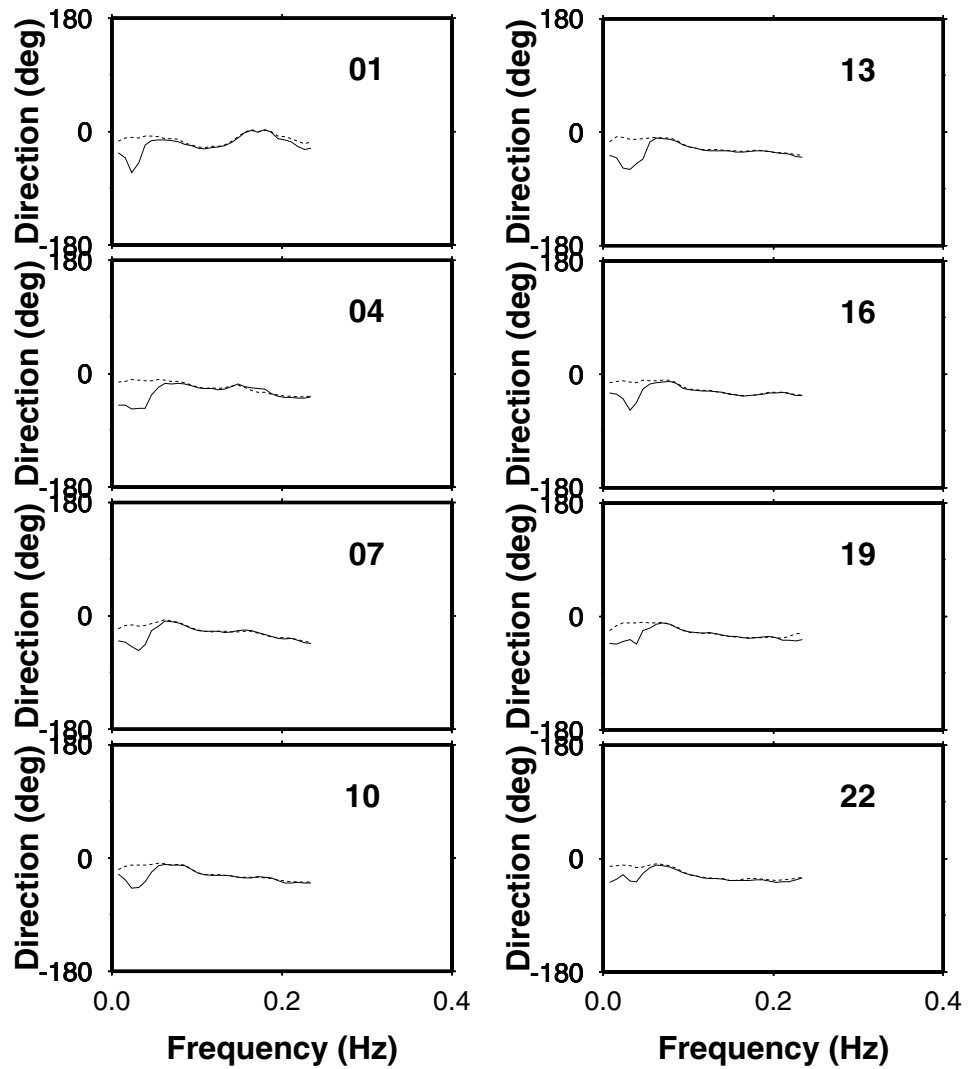
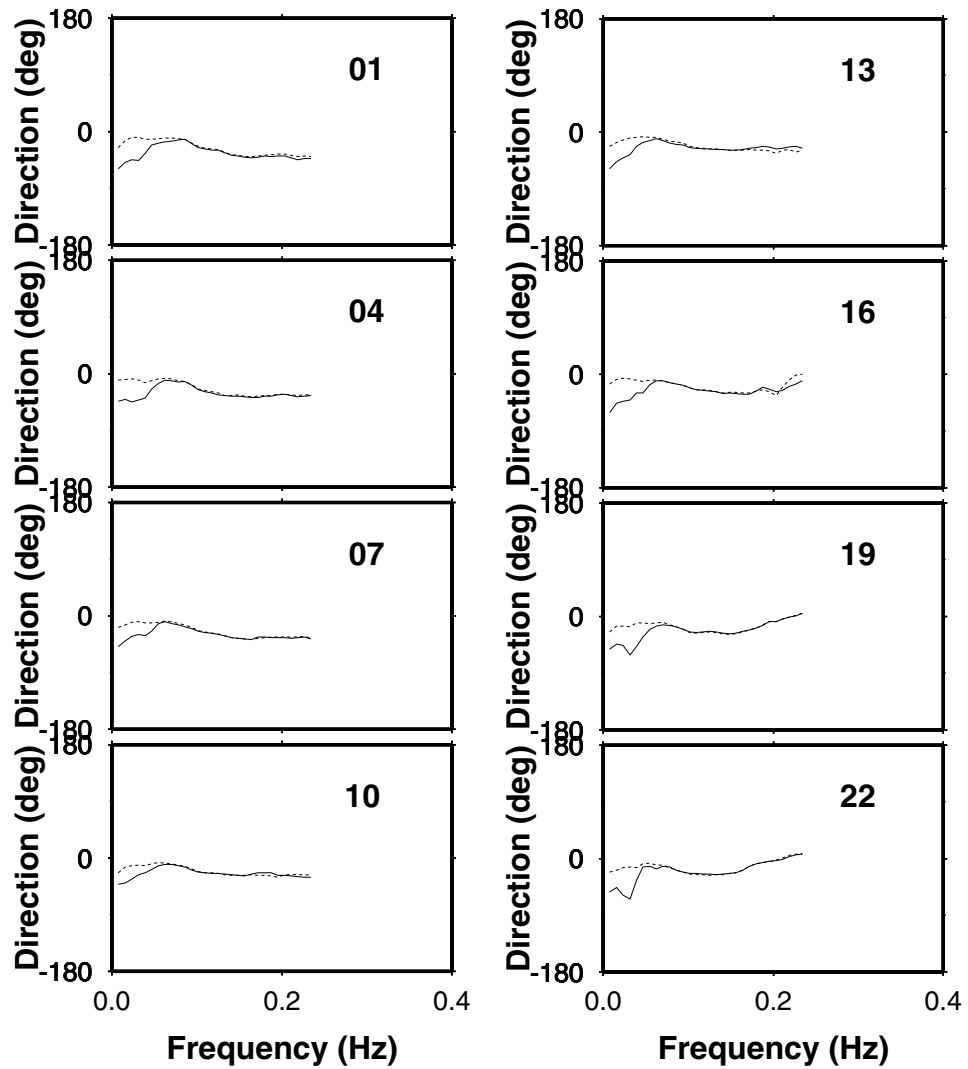


Figure 2.30 Mean of maximum 15 redundant gauge triad wave direction estimates (solid), and mean of maximum of 10 redundant gauge pair wave direction estimates (dashed); determined using *true* phase, i.e. PASS=2, on 6 February 1994



records on 2 February 1994 and one record on 3 February 1994 at 01 hours, during which we made a number of computer runs with gauge triads having large separations, with the intention of studying surf beat directionality, but unfortunately, these records included cases of wind wave generation directed down the coast, towards shore, which in turn generates surf propagating down the coast away from shore. We may recollect that the surf beat generated by the energetic swell, propagates up the coast, away from the shore, as a result of which, our simple model of one frequency, one direction was not satisfied, and therefore even the gauge triad analysis gave garbage results, in case of surf beat in presence of locally generated wind waves.

Figure 2.31 based on the tables in Appendix B shows the standard deviation of wave direction over a maximum of 15 redundant estimates of wave direction using the modified Esteva method (PASS=2) during 1-6 February 1994, while Figure 2.32 shows the mean of a maximum of 15 redundant estimates of wave direction. Both the figures include representations of the significant wave height as well as the vector mean wind speed and direction. From the energy contours in Figure 2.32, it is seen that the swell centred at spectral period 9.85s, which is present throughout the observation period, is dominant (energy $> 10^{2.0} \text{ cm}^2$) from the beginning upto 2 February 04 hours, after which the sea gains dominance, reaching its peak at 13 hours on the same day (energy $> 10^{2.4} \text{ cm}^2$). It is also seen that the sea decays completely by 3 February 22 hours, after which only very low swell (energy $\approx 10^{0.8} \text{ cm}^2$) is present, the significant wave height being less than 0.41m. The energy values given above are for the particular spectral frequencies, i.e., they do not indicate the total energy (variance) for swell, surf beat and sea components, each of which spreads over several spectral frequencies. Figure 2.31 shows that during 1-6 February 1994, a maximum of 15 redundant estimates of wave direction has a standard deviation of $< 4^\circ$ in the range 14.22 – 6.40s. During this time swell of $\approx 10\text{s}$ propagated towards shore, up the coast at an angle of $\approx 7^\circ$ with the seaward shore normal during the successive dominance of both swell and sea, with the angle increasing to and steadying at $\approx 23^\circ$ during the period of incidence of very low swell on 4, 5 and 6 February. The above standard deviation is also $< 4^\circ$ for periods between 6.40 – 4.27s during 01-13 hours on 2 February, when waves are locally generated (note the energy contour ridge line is oriented in such a way that the frequency decreases with increasing time) by a *Northeaster* of $\approx 10\text{m/s}$, owing to which the wave direction in the period range 6.40 – 4.27s aligned itself with the wind direction, and the significant wave height increased from 0.70 to 1.54m. The low value of the standard deviation indicates that the directional spread in case of sea as well as as swell is unimodal and very narrow. In general the standard deviation $< 12^\circ$ in the range 21.33 – 4.27s, so that our estimates are reliable. It is curious to note that during 3 and 5 February the wind is blowing *away* from shore, but the high frequency waves generated by this wind are all directed *towards* shore, almost at a right angle to the wind. When I brought this apparent anomaly of offshore winds generating onshore waves to the attention of Dr. C. E.

Long, in a personal communication he informed me, that he very frequently sees the phenomenon of wind from the southwest generating high frequency waves from the south east (our case!) and he sees high frequency waves from the northeast during much rarer occasions when the observed wind is from the northwest. An explanation for this anomaly may be that at Duck, the cross-shore component of the wind is fetch limited and the waves generated by the longshore component of the wind are refracted towards shore.

The standard deviation of 15 redundant estimates of wave direction $< 12^\circ$ even for surf beat when low wave conditions ($H_{mo} < 0.41m$) prevailed on 4, 5 and 6 February indicating that the directional spread is unimodal and narrow. This surf beat (the lowest three rows of wave vectors in Figure 2.32 representing 32.00, 42.67 and 64.00s) propagates up the coast towards shore at angles in excess of 45° with the shore normal. It may be noted that this surf beat of remote origin does not get refractively straightened as it approaches the coast as much as the swell centred at 9.85s, probably because the 150m depth contour makes an angle of $\approx 30^\circ$ with the shore normal. Based on a 24-gauge polygonal array at 13m depth at Duck installed by the Scripps Institution of Oceanography, using a variational method, Herbers et al. [1995] found that surf beat of remote, possibly trans-oceanic origin propagates at normal incidence towards the shore when very low swell energies (variance in the range $0.04 - 0.14Hz < 100 cm^2$) are present. Our results therefore introduce an element of doubt whether the direction polarization parameter, on the basis of which Herbers et al. [1995] inferred normal incidence, is properly constructed. The standard deviation of a maximum of 15 redundant estimates of wave direction $< 16^\circ$ also in case of surf beat when energetic swell was propagating from the beginning upto 2 February 04 hours, the surf beat propagating up the coast away from the shore at an angle of about 45° with the shore normal. The direction of surf beat generated by the energetic swell conforms to the schematic diagram of surf beat generation given by Herbers et al. [1995] (their Fig 2). During the period 2 February 07 hours to 3 February 04 hours, the period when locally generated wind waves are predominant, the standard deviation of a maximum of 15 redundant estimates of wave direction in case of surf beat is very large, indicating that our assumption of unimodal directional spread is incorrect so that our estimates of surf beat direction are not correct in this particular case. It may be speculated that since the swell and the sea both propagate towards shore, the upcoast and downcoast directions of the swell and the sea respectively give rise to a bimodal directional spread for this surf beat.

The histogram in Table 2.17 shows that 61 out of 72 estimates of direction of surf beat observed during 4-6 February 1994 indicate that the surf beat propagates towards the shore, up the coast at angles of $30 - 60^\circ$ with respect to the shore normal. Table 2.17 in conjunction with Figure 2.33, which depicts geodesic paths of the surf beat incident at Duck — show that the surf beat of remote origin is largely trans-oceanic in origin. Geodesic is the shortest distance on an elliptical earth is the geodesic, and this differs considerably from the great circle path when the range is close to

Figure 2.31 Frequency – time plot: (a) Significant wave height, H_{mo} , (b) Vector mean wind, and (c) Standard deviation of a maximum of 15 redundant estimates of wave direction during the period 1-6 February 1994, using the method of Esteva [1977] as modified by us

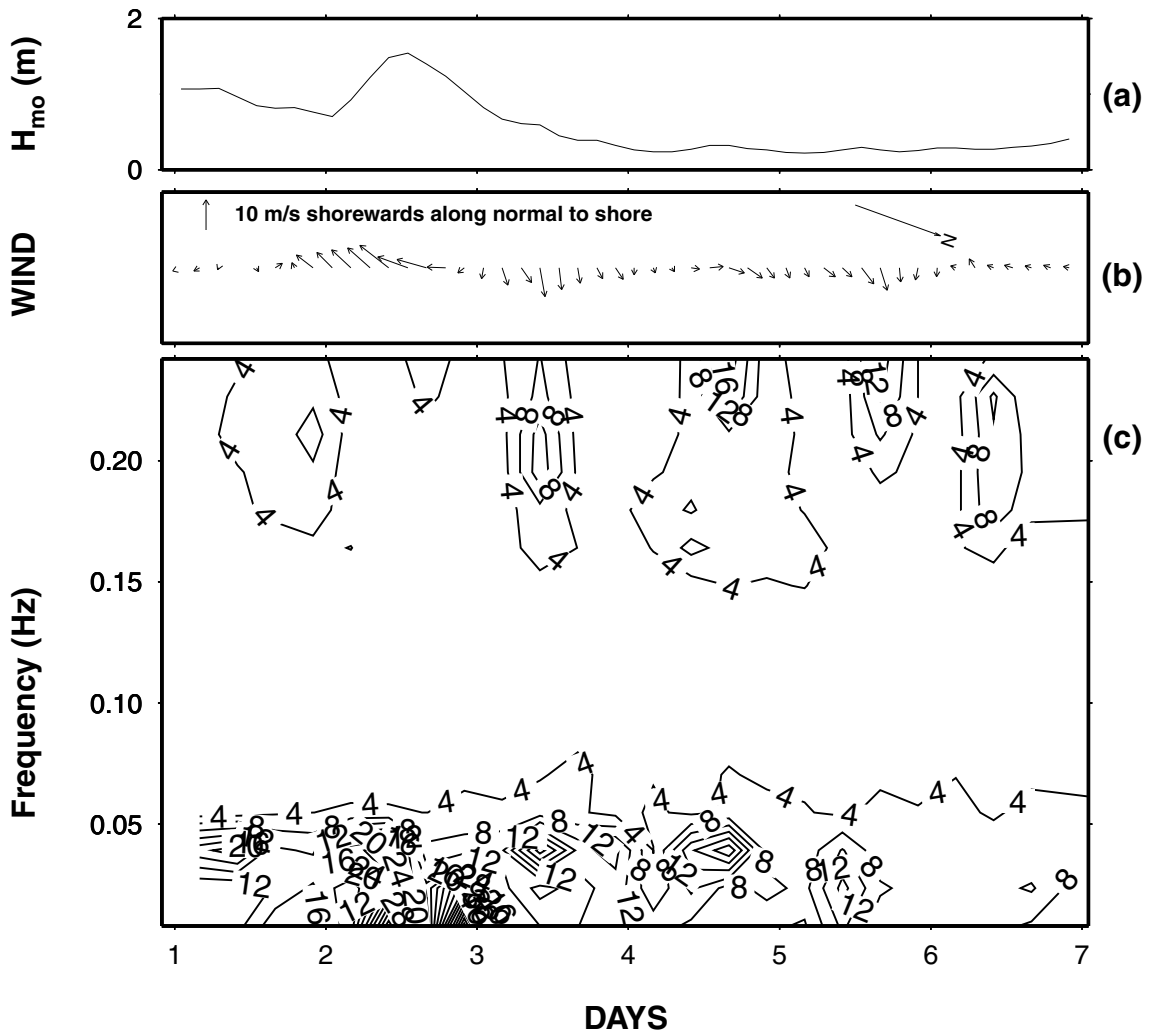
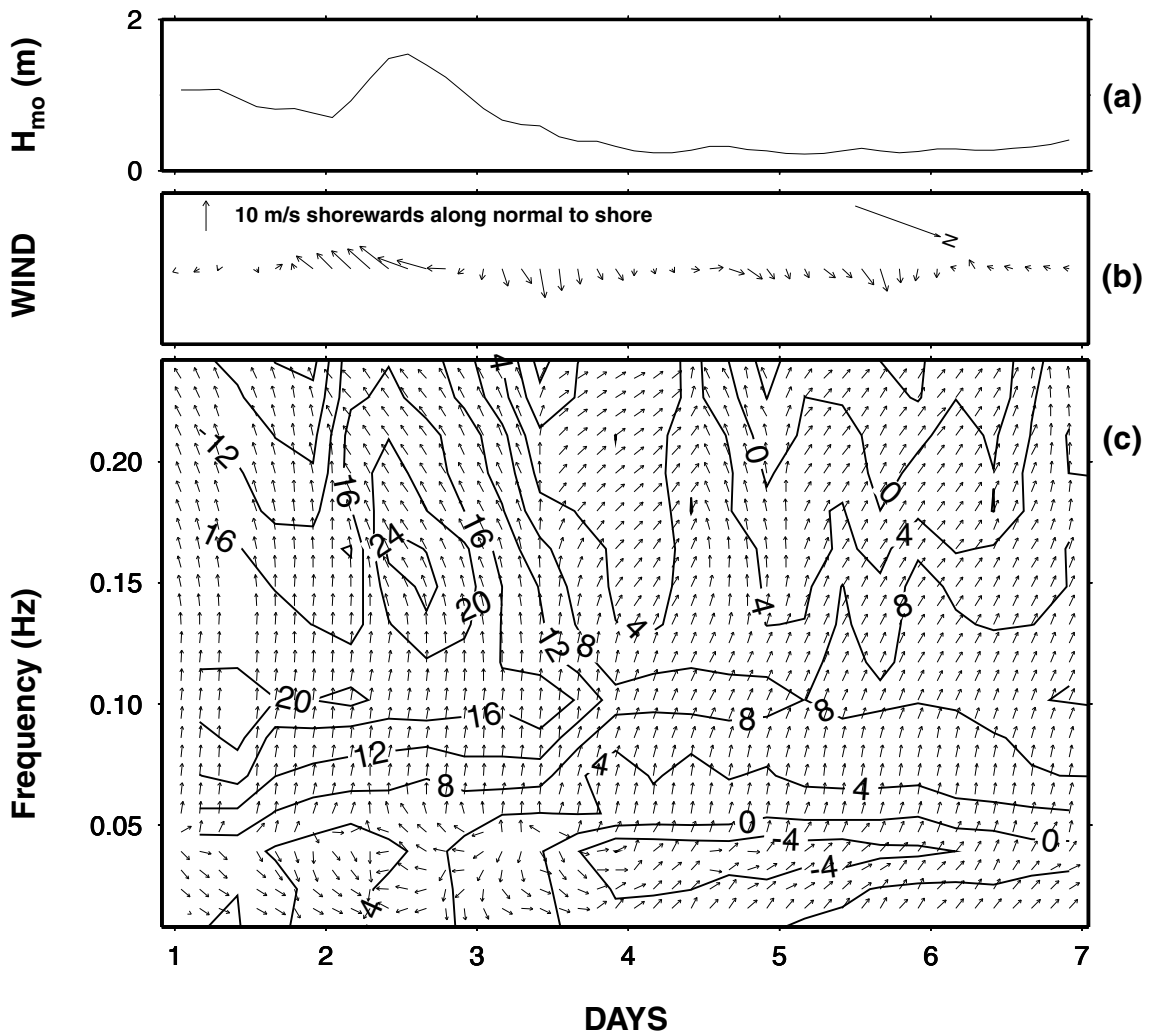


Figure 2.32 Frequency – time plot: (a) Significant wave height, H_{mo} , (b) Vector mean wind, and (c) Mean of a maximum of 15 redundant estimates of wave direction during the period 1-6 February 1994, using the method of Esteva [1977] as modified by us. Energy contours are in decibels ($10 * \log_{10}$ Energy). Energy is measured in cm^2



antipodal. The fact that the 30 – 60° geodesic represent the boundaries of a narrow window into the South Atlantic and the Indian Ocean to the West of Australia, suggest that the surf beat of remote origin does propagate along geodesics just like sound propagation in the deep ocean in the SOFAR (Sound frequency and ranging) channel. It may be worth mentioning that Munk and Forbes [1989] report that in 1960, 300 lbs of high explosives were detonated near the sound axis off Perth, on the West coast of Australia, and these were clearly recorded on axial hydrophones off Bermuda off the East coast of USA. In one case the surf beat of remote origin appears to have been generated as close as the West Indies.

Table 2.17 Histogram of surf beat of remote origin (spectral periods 64.00, 42.67 and 32.00s) occurring during 4-6 february 1994 (8 observations per day) giving a total of 72 estimates of surf beat direction. Surf beat directions are up the coast, towards shore measured with respect to the seaward shore normal. The uniform negative sign of surf beat direction has been dropped for convenience

Range (degrees)	Frequency
25-30	4
30-35	7
35-40	9
40-45	14
45-50	19
50-55	4
55-60	8
60-65	3
65-70	3
.	.
.	.
95-100	1
25-100	72

Figure 2.34 shows the energy spectrum for gauge C at 01 hours on 3 February 1994 with both axes in logarithmic scale. It is seen that on the forward face of the spectrum the energy falls faster than f^{-5} as the surface elevation is measured with a bottom mounted pressure gauge.

We shall now show that, in the wind wave regime (0.04-0.32 Hz), our estimates of wave direction as a function of frequency using Esteva’s method as modified by us, are consistent with the results of frequency-direction spectra obtained by the Coastal Engineering Reseach Center (CERC) using the sophisticated Iterative Maximum Likelihood Estimation (IMLE) method described by Pawka [1983], which assumes that at a given frequency waves can approach from all

Figure 2.33 Great circle paths indicating origin of surf beat incident at Duck during 4-6 February 1994, when low wave conditions (significant wave height, $H_{mo} < 0.41m$) occur. The gure in conjunction with Table 2.17 suggests that the surf beat of remote origin is largely trans-oceanic in origin

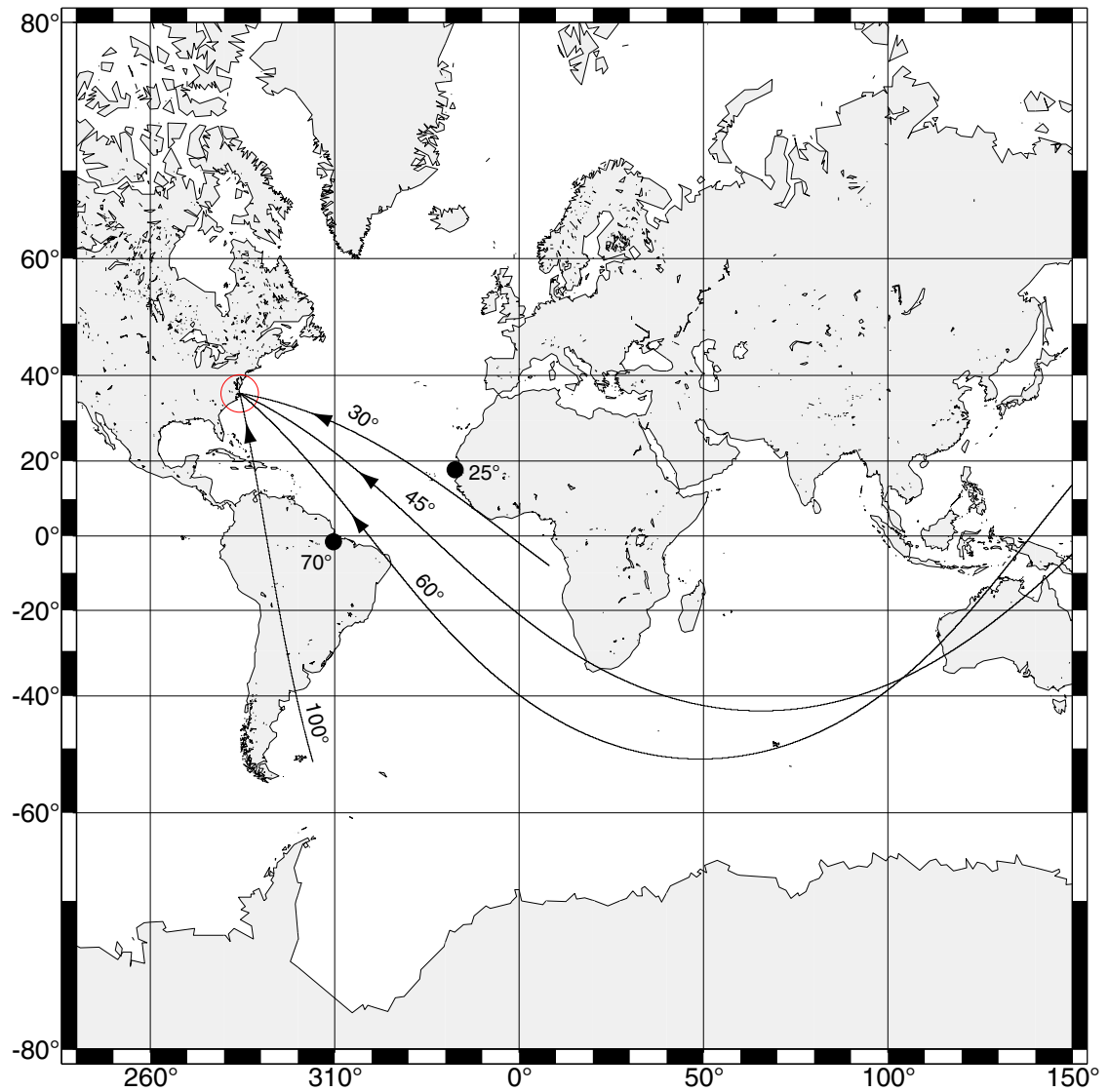
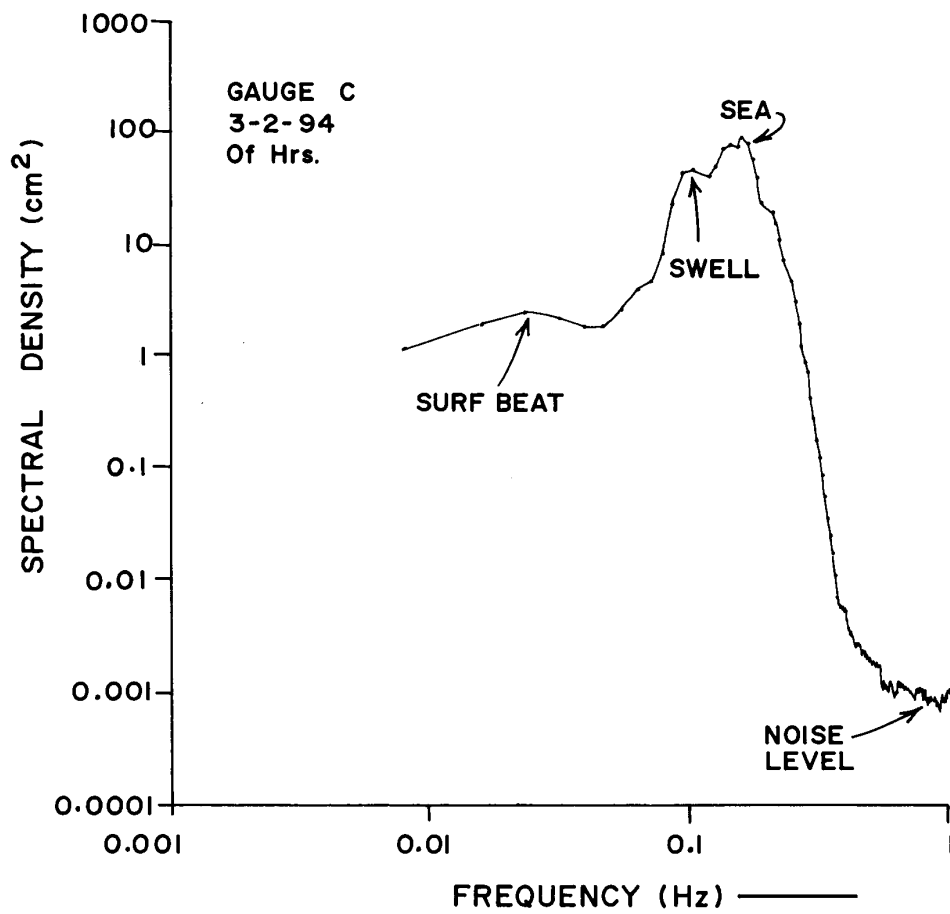


Figure 2.34 Wave spectrum at Duck for gauge C on 3 February 1994 at 01 hours in logarithmic scales



directions. The frequency-direction spectrum for the record on 3 February 1994 at 22 hours (i.e., when locally generated waves have nearly decayed) using IMLE method for the full 15-gauge array is shown in Figure 2.35(a,b). Superimposed on the IMLE contour plot of energy shown in Figure 2.35(b) is a plot (the thick curve down the page!) of wave direction (mean of a maximum of 15 redundant estimates) as a function of frequency using Esteva's method as modified by us, which shows that the results of IMLE and Esteva's method are consistent with each other. In Figure 2.36, which is similar to Figure 2.35 and is for the record on 2 February 1994 at 13 hours (i.e., at the peak of wave generation) for the full array, we note that the curve showing Esteva's method surprisingly does not exactly follow the ridge on the IMLE contour plot at the high frequency end of the spectrum. Since the wave direction in Figure 2.36 varies within the range $(-90^\circ, +90^\circ)$ there will be no ambiguity in the IMLE analysis even if it is restricted to the linear part, i.e., the longshore part of the array – this is given in Figure 2.37, which shows that the curve depicting Esteva's method lies exactly along the ridge of the IMLE contour plot even at the high frequency end of the spectrum. Thus the results of Esteva's method as modified by us are consistent with that of the IMLE method. These methods were found to be consistent with each other not only for just the above two records, but also for all the 16 records on 2 and 3 February 1994 for which the CERC IMLE plots were available, and which as we have seen include instances of predominant swell, a developing sea and a decaying sea. Our estimates of wave direction using Esteva's method Figure 2.31 and Figure 2.32 are also consistent with the CERC IMLE derived bulk parameters, viz., peak period, peak direction, etc., given in Figure 2.38, which is reproduced from Long and Roughton [1995]. We note that our representation explains the singularities in the peak period and peak direction (bulk parameters) as given by the CERC publication. Also the unchanging direction of swell as shown by our representation appears to be realistic.

. . .

Figure 2.35 CERC computed frequency-direction spectrum on 3 February 1994 at 22 hours for full array using the IMLE method. In part (b) the thick curve down the page gives the wave direction (mean of 15 redundant estimates) computed using the Modified Esteva Method

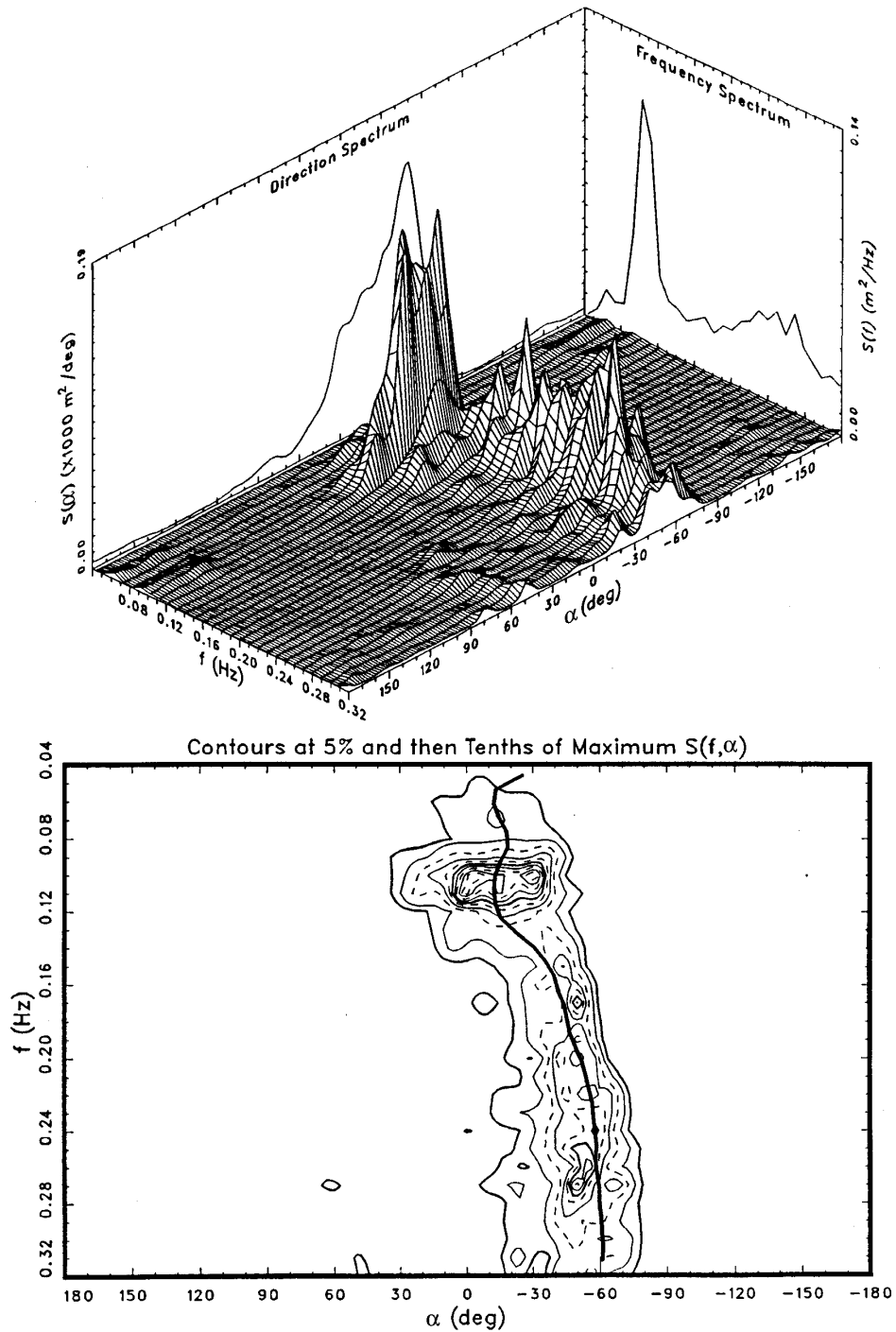


Figure 2.36 CERC computed frequency-direction spectrum on 2 February 1994 at 13 hours for full array using the IMLE method. In part (b) the thick curve down the page gives the wave direction (mean of 15 redundant estimates) computed using the Modified Esteva Method

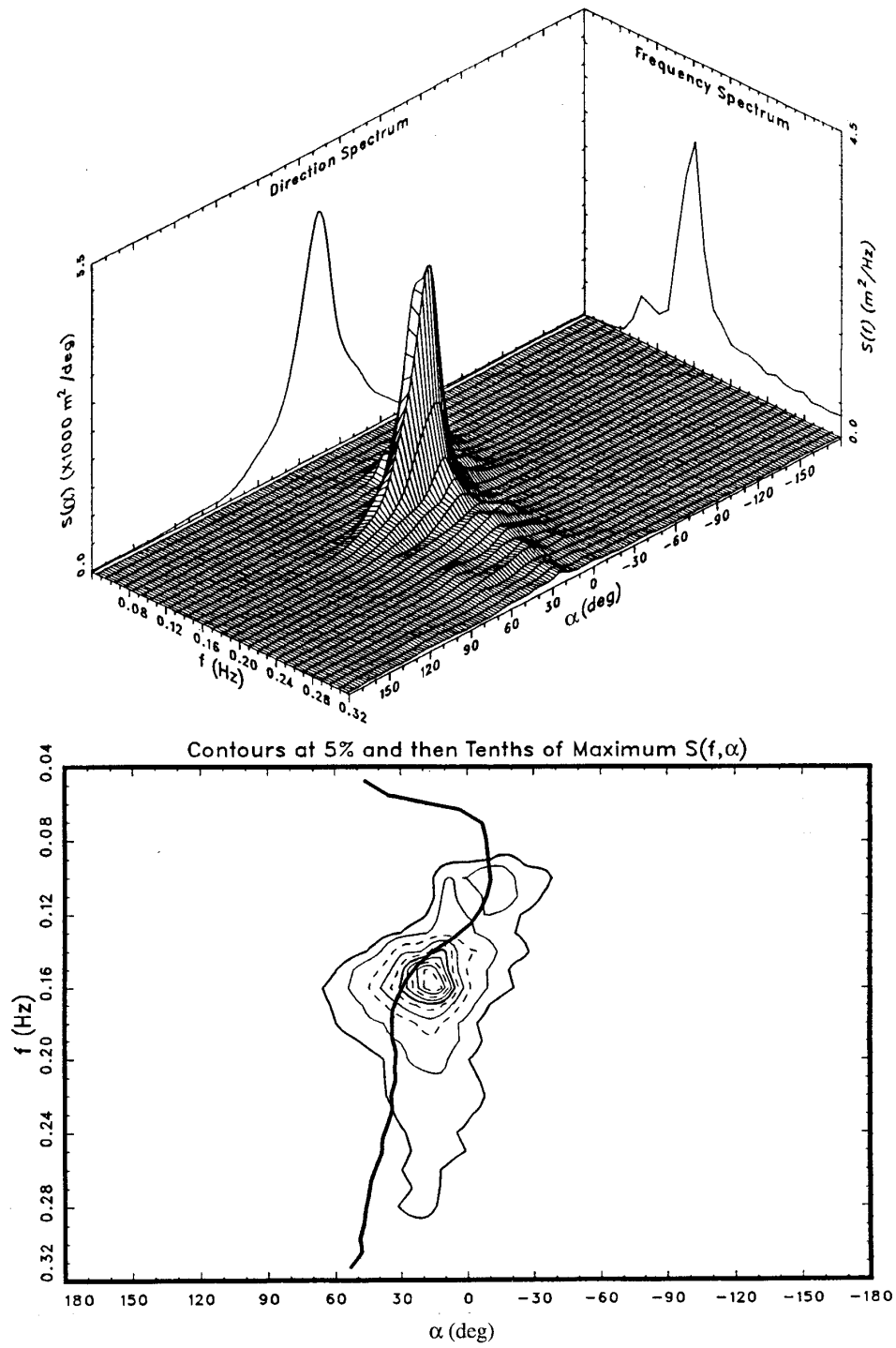


Figure 2.37 CERC computed frequency-direction spectrum on 2 February 1994 at 13 hours for linear part of the array using the IMLE method. In part (b) the thick curve down the page gives the wave direction (mean of 15 redundant estimates) computed using the Modified Esteva Method

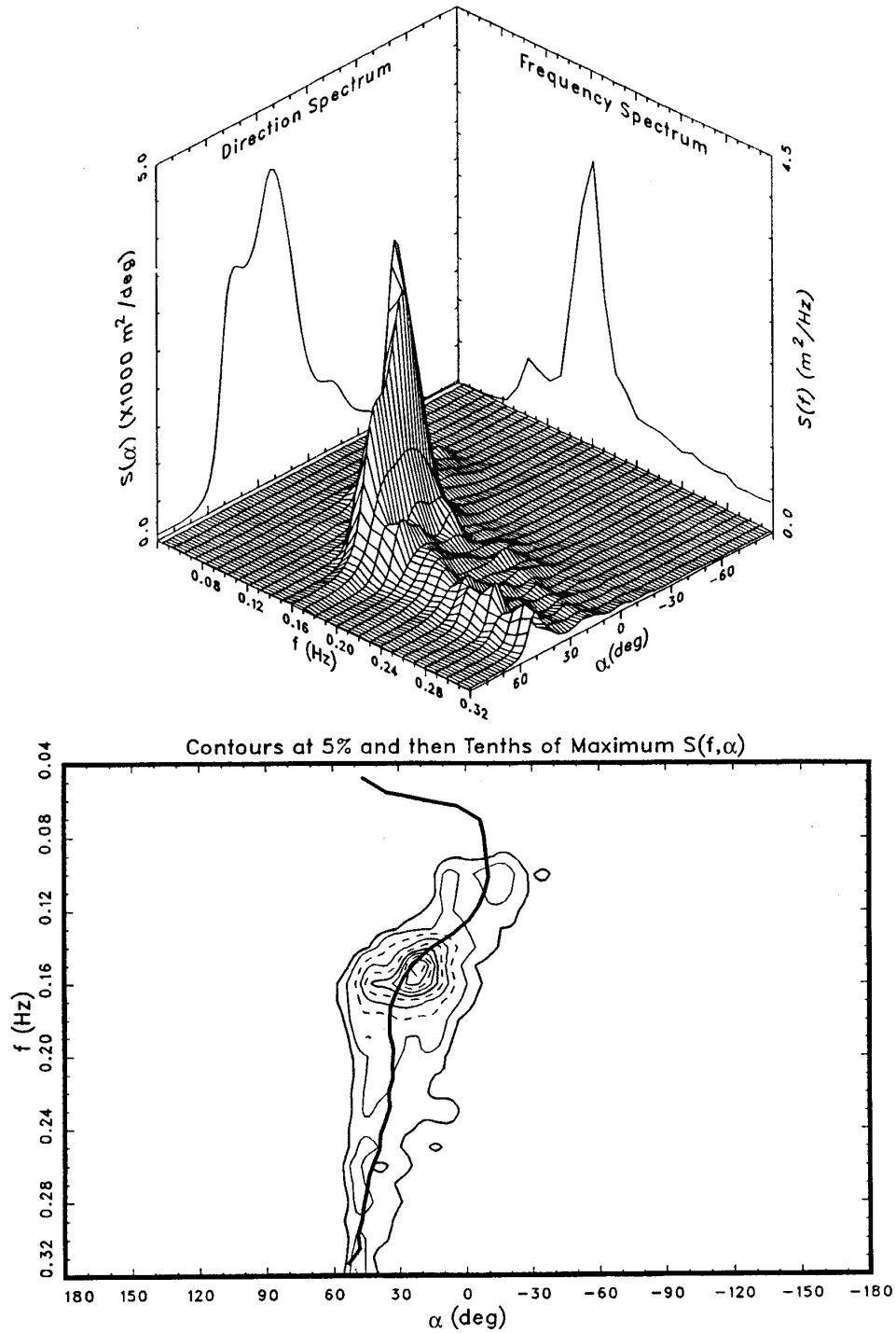


Figure 2.38 Bulk parameters derived by the CERC using IMLE method for the month of February 1994. For comparison with the results using Esteva's method as modified by us, the period of interest is 1-6 February 1994. H_{mo} is the significant wave height, $T_{p,IFS}$ is the peak period from the integrated frequency spectrum, $\alpha_{p,IDS}$ is the peak wave direction of the integrated direction spectrum, $\Delta\alpha_{IDS}$ is the directional spread parameter of the integrated direction spectrum. (Figure reproduced from Long and Roughton [1995])

